TURUN
YLIOPISTO
UNIVERSITY
OF TURKU

BIOACTIVE GLASSES

In Air Particle Abrasion Treatment of Contaminated Implant Surfaces

Faleh Abushahba

TURUN YLIOPISTON JULKAISUJA – ANNALES UNIVERSITATIS TURKUENSIS
SARJA – SER. D OSA – TOM. 1582 | MEDICA – ODONTOLOGICA | TURKU 2021

TURUN
YLIOPISTO
UNIVERSITY
OF TURKU

BIOACTIVE GLASSES

In Air Particle Abrasion Treatment of Contaminated Implant Surfaces

Faleh Abushahba

TURUN YLIOPISTON JULKAISUJA – ANNALES UNIVERSITATIS TURKUENSIS
SARJA – SER. D OSA – TOM. 1582 | MEDICA – ODONTOLOGICA | TURKU 2021

University of Turku

Faculty of Medicine
Institute of Dentistry
Department of Prosthetic Dentistry and Stomatognathic Physiology
Finnish Doctoral Program in Oral Sciences (FINDOS-Turku)

Supervised by

Professor Timo Närhi, DDS, PhD
Department of Prosthetic Dentistry and Stomatognathic Physiology
Institute of Dentistry
University of Turku
Turku, Finland

Reviewed by

Docent, Patricia Stoor, DDS, PhD
Helsinki University Central Hospital,
University of Helsinki
Helsinki, Finland

Docent, Pirkko Pussinen, PhD
Department of Oral and Maxillofacial Diseases,
University of Helsinki,
Helsinki, Finland

Opponent

Professor, Andreas Stavropoulos, DDS. PhD, odont. Dr.
Regenerative Dentistry & Periodontology,
CUMD, University of Geneva, Switzerland

ISBN 978-951-29-8613-2 (PRINT)
ISBN 978-951-29-8614-9 (PDF)
ISSN 0355-9483 (Print)
ISSN 2343-3213 (Online)
Painosalama, Turku, Finland 2021

“In the name of God, the Most Gracious, the Most Merciful”

To the soul of my mother,
my father,
my dear wife Nagat,
my beloved kids, Rahaf, Roua, Ahmed, and Mohamed.

UNIVERSITY OF TURKU
Faculty of Medicine
Institute of Dentistry
Department of Prosthetic Dentistry and Stomatognathic Physiology
FALEH ABUSHAHBA: Bioactive Glasses in Air Particle Abrasion Treatment of Contaminated Implant Surfaces
Doctoral Dissertation, 128 pp.
Finnish Doctoral Program in Oral Science (FINDOS-Turku)
September 2021

ABSTRACT

The use of dental implants has become an established treatment modality with a predictable survival rate. However, inflammation of peri-implant tissue, peri-implant mucositis, may occur over time due to the establishment of bacterial biofilm on the implant surfaces. If left untreated, the inflammation can extend apically, resulting in a condition called peri-implantitis (PI), which is characterized by submucosal infection and peri-implant bone resorption. Therefore, one of the main objectives of PI therapy is the removal of bacterial biofilm from the implant surface.

This study series aimed to evaluate the effect of bioactive glass (BAG) powder in air particle abrasion treatment of titanium alloy surfaces. A further aim was to study the antibacterial properties of BAG abraded surfaces and to examine the effect of BAG air-abrasion on bacterial biofilm removal on sandblasted and acid-etched (SA) titanium alloy surfaces. An additional aim was to study the attachment, viability, and proliferation of human osteoblast-like MC3T3-E1 cells on SA surfaces subjected to BAG air particle abrasion.

The effect of BAG air-abrasion on the antibacterial properties of smooth titanium disc surfaces was evaluated for 45S5 BAG and three novel zinc oxide doped BAGs: Zn4, Zn6, and Zn4Sr8. SA titanium discs were used to assess the BAG air-abrasion effect on surface chemistry, roughness, wettability, and surface free energy. *Streptococcus mutans,* as well as *Fusobacterium nucleatum* and *Porphyromonas gingivalis* dual biofilms, were formed on SA titanium discs. SA discs with biofilms were subjected to BAG air-abrasion and then cultured in an anaerobic chamber for 5 hours for *S. mutans* and 21 hours for *F. nucleatum* and *P. gingivalis* dual biofilms. The efficiency of biofilm removal was evaluated using scanning electron microscopy (SEM) imaging and culturing techniques. The thrombogenicity of the BAG air-abraded discs was assessed spectrophotometrically using whole blood clotting measurement at predetermined time points. The viability and proliferation of pre-osteoblastic MC3T3-E1 cells were evaluated on SA surfaces with and without BAG air-abrasion. The air-abrasion procedures were similar for all experiments. Each titanium alloy disc was air-abraded for 20 seconds, at a 90 ° angle, 3 mm distance, and 4 bars air pressure.

A statistically significant decrease in the viability and biofilm formation of *S. mutans* was observed for BAG air-abraded titanium discs. Air particle abrasion with BAG effectively eradicated *S. mutans* and *F. nucleatum* and *P. gingivalis* dual biofilms formed on SA surfaces compared with inert glass air-abrasion. No significant difference was seen in the speed of blood clot formation since complete blood clotting was achieved in 40 minutes on all substrates. Air-abrasion of SA titanium discs with BAG or inert glass significantly reduced surface roughness, enhanced the wettability and surface free energy of the SA surfaces. MC3T3-E1 cell number was higher for SA surfaces air-abraded with Zn4 BAG or 45S5 BAG than inert glass. Confocal laser scanning microscope images showed that the pre-osteoblast cells did not spread as well on the SA and BAG abraded surfaces as they did on control cover glass discs. However, for 45S5 and Zn4 BAG abraded substrates, cells spread the most within 24 hours and changed their morphology to more spindle-like when cultured further.

It can be concluded that air particle abrasion with BAG has good potential for the treatment of peri-implantitis. However, their effectiveness needs to be evaluated *in vivo* before any definitive conclusion can be made.

KEYWORDS: Acid-etching, air-abrasion, bioactive glass, biofilm, contact angle, dental implant, *F. nucleatum,* osteoblast, *P. gingivalis*, peri-implant infection, *S. mutans*, sandblasting, titanium.

TURUN YLIOPISTO
Lääketieteellinen tiedekunta
Hammaslääketieteen laitos
Hammasprotetiikka ja purentafysiologia
FALEH ABUSHSHBA: Bioaktiiviset lasit kontaminoituneiden implanttipintojen ilma-abraasio käsittelyssä
Väitöskirja, 128 s.
Kansallinen suun terveystieteiden tohtoriohjelma (FINDOS-Turku)
Syyskuu 2021

TIIVISTELMÄ

Hammasimplanttien käytöstä on tullut vakiintunut ja hyväennusteinen hoitomuoto. Hammasimplantteja ympäröivien pehmytkudosten tulehdus, peri-implantti mukosiitti, voi kuitenkin ilmetä implanttien ympärillä bakteereiden muodostaman biofilmin aiheuttamana. Hoitamattomana infektio voi levitä syvemmälle pehmytkudoksiin johtaen peri-implantiitiksi kutsuttuun tilaan, jota karakterisoi ikenen alainen tulehdusreaktio ja implanttia ympäröivän luun resorboituminen. Peri-implantiittihoidon tärkein tavoite on bakteerien muodostaman biofilmin eliminoiminen implantin pinnalta. Tämän tutkimussarjan tavoitteena oli selvittää bioaktiivisella lasijauheella tehdyn ilma-abraasio-käsittelyn vaikutus titaaniyhdisteen pintaan. Tarkoituksena oli myös tutkia bioaktiivisella lasilla hiekkapuhallettujen pintojen antimikrobisia ominaisuuksia sekä selvittää bioaktiivisella lasilla tehdyn hiekkapuhalluksen vaikutus biofilmien poistoon hiekkapuhalletuilta ja happoetsatuilta (SA; sand blasted acid etched) titaanipinnoilta. Tämän lisäksi tarkoituksena oli tutkia ihmisen osteoblastin kaltaisten MC3T3-E1 solujen tarttuminen, elinkyky ja jakautuminen SA -pintaisilla titaaninäytteillä bioaktiivisella lasilla tehdyn hiekkapuhalluskäsittelyn jälkeen.

Bioaktiivisella lasilla tehdyn hiekkapuhalluksen vaikutuksia tasaisen titaanikiekon pinnan antimikrobisiin ominaisuuksiin selvitettiin 45S5 bioaktiivisella lasilla ja kolmella uudella sinkkipitoisella lasilla: Zn4, Zn6, ja Zn4Sr8. SA -pintaisia titaanikiekkoja käytettiin tutkittaessa bioaktiivisella lasilla tehdyn hiekkapuhalluksen vaikutusta pinnan kemialliseen koostumukseen, karheuteen, kostutusominaisuuksiin ja vapaaseen pintaenergiaan. SA -pintaisille titaanikiekoille kasvatettiin sekä *S. mutans* biofilmi että *F. nucleatum* ja *P. gingivalis* kaksoisbiofilmit. Titaanikiekot hiekkapuhallettiin bioaktiivisella lasijauheella, minkä jälkeen kiekot siirrettiin anaerobiseen viljelykammioon 5 tunniksi *S. mutans* biofilmiä ja 21 tunniksi *F. nucleatum* ja *P. gingivalis* kaksoisbiofilmiä tutkittaessa. Biofilmien eliminoituminen selvitettiin pyyhkäisyelektronimikroskooppikuvista ja viljelytekniikoita käyttäen. Bioaktiivisella lasilla hiekkapuhallettujen SA -pintaisten titaanikiekkojen vaikutus veren hyytymiseen selvitettiin tutkimalla veren adsorbanssia spektrofotometrisesti useissa eri aikapisteissä. MC3T3-E1 pre-osteoblastisolujen elinkyky ja jakautuminen SA -pintaisilla titaaninäytteillä selvitettiin ennen ja jälkeen bioaktiivisella lasilla tehtyä ilma-abraasiokäsittelyä. Ilma-abraasiokäsittelyt tehtiin samalla tavalla kaikissa kokeissa. Titaanikiekot hiekkapuhallettiin 20 sekunnin ajan 90º kulmassa 3 mm etäisyydellä 4 baarin ilmanpainetta käyttäen.

Bioktiivisella lasilla käsitellyillä pinnoilla todettiin tilastollisesti merkitsevä *S. mutans* bakteerien elinkykyä ja biofilmin muodostumista heikentävä vaikutus. Bioaktiivisella lasilla tehty ilma-abraasio käsittely poisti tehokkaammin sekä *S. mutans* että *F. nucleatum* ja *P. gingivalis* kaksoisbiofilmit SA -pintaisilta titaanikiekoilta inertillä lasilla tehtyyn ilma-abraasio käsittelyyn verrattuna. Käsitellyillä pinnoilla ei havaittu merkitseviä eroja veren hyytymisnopeudessa, sillä veri hyytyi kaikilla testikappaleilla 40 minuutissa. Ilma-abraasio käsittely tasoitti SA -pintaisten titaanikiekkojen pinnan, paransi pintojen kosteutusta ja lisäsi vapaan pintaenergian määrää kaikilla käsittelyillä. MC3T3-E1 solujen määrä oli suurempi Zn4 tai 45S5 bioaktiivisilla laseilla hiekkapuhalletuilla SA -pintaisilla titaanikiekoilla verrattuna inertillä lasilla hiekkapuhallettuihin titaanikiekkoihin

Laserkonfokaalipyyhkäisymikroskooppikuvat osoittivat, että pre-osteoblastit eivät levinneet SA -pintaisilla tai bioaktiivisella lasilla hiekkapuhalletuilla titaanipinnoilla yhtä hyvin kuin kontrollina toimineilla peitelaseilla. Bioaktiivisilla 45S5 ja Zn4 laseilla hiekkapuhalletuilla pinnoilla pre-osteoblastisolut kuitenkin jakautuivat parhaiten 24 tunnin aikana ja muuttuivat viljelyperiodin pidentyessä morfologialtaan kehrämäisiksi.

Tulosten perusteella voidaan todeta, että bioaktiivisella lasilla tehtävä ilma-abraasiokäsittely on potentiaalinen peri-implantiitin hoitomenetelmä. Hoitomenetelmän teho on kuitenkin vielä osoitettava *in vivo* olosuhteissa ennen lopullisten johtopäätösten tekoa.

AVAINSANAT: Happoetsaus, ilma-abraasio, bioaktiivinen lasi, biofilmi, kontaktikulma, hammasimplantti, *F. nucleatum*, osteoblasti, *P. gingivalis*, peri-implantiitti, *S. mutans*, hiekkapuhallus, titaani.

Table of Contents

Abbreviations

ADSA	axisymmetric drop shape analysis
ANOVA	analysis of variance
BAG	bioactive glass
BHI	brain heart infusion
BIC	bone to implant contact
°C	degree Celsius
CA	contact angle
Ca^{2+}	calcium ion
CFU	colony-forming unit
EDS	energy-dispersive X-ray spectroscopy
EPS	extracellular polysaccharide
FBS	fetal bovine serum
GTF	glucosyltransferase
HA	hydroxyapatite
LPS	libopolysaccharide
α-MEM	alpha minimum essential medium
MMPs	matrix metalloproteinases
Na	sodium
OD	optical density
OI	osseointegration
PBS	phosphate-buffered saline
PFA	paraformaldehyde
PI	peri-implantitis
PO_4^{3-}	phosphate ion
Ra	arithmetical mean deviation
ROS	reactive oxygen species
SA	sandblasted and acid-etched
SBF	simulated body fluid
SEM	scanning electron microscope
SFE	surface free energy
Si	silicon
SPSS	statistical package for social science
TSB	tryptic soy broth

List of Original Publications

This dissertation is based on the following original publications, which are referred to in the text by their Roman numerals:

I **Abushahba F**, Söderling E, Aalto-Setälä L, Sangder J, Hupa L, Närhi T. (2018). Antibacterial properties of bioactive glass particle abraded titanium against *Streptococcus mutans*. *Biomedical Physics & Engineering Express.* **4**: 045002.

II **Abushahba F**, Söderling E, Aalto-Setälä L, Hupa L, Närhi T. (2019). Air abrasion with bioactive glass eradicates *Streptococcus mutans* biofilm from a sandblasted and acid-etched titanium surface. *J Oral Implantol*. **45**: 444-450.

III **Abushahba F**, Tuukkanen J, Aalto-Setälä L, Miinalainen I, Hupa L, & Närhi T. (2020). Effect of bioactive glass air-abrasion on the wettability and osteoblast proliferation on sandblasted and acid-etched titanium surfaces. *Eur J Oral Sci*. **128:** 160-9.

IV **Abushahba F**, Gürsoy M, Hupa L, & Närhi T. (2021). Effect of bioactive glass air-abrasion on *Fusobacterium nucleatum* and *Porphyromonas gingivalis* biofilm formed on moderately rough titanium surface. *Eur J Oral Sci*, **129** (3) e12783.

1 Introduction

Peri-implantitis (PI) is an infectious disease associated with complex bacterial biofilm structures that induce an inflammatory reaction, leading to connective tissue destruction (Berglundh et al., 2018). It refers to an inflammation of the implant mucosa with progressive peri-implant bone loss (Schwarz et al., 2018). The prevalence of PI varies significantly in the literature due to the discrepancies in its definition and ranges from 4-45 % (Atieh et al., 2013; Salvi et al., 2017). Exposure of the rough implant surface to the oral environment results in developing a high-affinity biofilm that is difficult to eliminate using the current therapeutic approaches, such as using manual instruments, plastic or carbon tips, ultrasonic/sonic instruments, and air powder abrasion combined with systemic or local antimicrobial agents (Estefanía-Fresco et al., 2019; Heitz-Mayfield & Mombelli, 2014; Suarez et al., 2013; Teughels et al., 2006). Furthermore, the use of various bone augmentation materials has been shown to result in unsatisfactory outcomes, disease recurrence, and further progression of PI (Froum et al., 2015; Khoury & Buchmann, 2001; Ramanauskaite et al., 2019; Wohlfahrt et al., 2012).

One of the primary objectives of PI therapy is removing bacterial biofilm from the implant surface, followed by possible bone regeneration. Nevertheless, management of PI is complicated as the implant design and various surface treatments of titanium may enable plaque accumulation. Furthermore, the rough implant surfaces limit the effectiveness of mechanical debridement, resulting in incomplete removal of biofilm (Suarez et al., 2013; Teughels et al., 2006). Additionally, due to the lack of periodontal ligament and less blood supply, the regenerative capacity of peri-implant tissues is weaker than the regeneration ability of periodontal tissues around natural teeth (Larsson et al., 2016).

Findings from earlier studies indicated that bioactive glasses (BAG) possess broad-spectrum antimicrobial properties and biofilm preventing activities against wide varsities of clinically important microorganisms (Allan et al., 2001; Allan et al., 2002; Stoor et al., 1998). Particulate 45S5 BAG has demonstrated significance antibacterial and antibiofilm effects against a wide range of supra- and sub-gingival bacterial species (Allan et al., 2001). These effects are mainly due to the rise in the pH and osmolarity caused by releasing alkali ions from 45S5 BAG such as Na and

Ca^{2+}, making the local environment unfavorable for bacterial growth and adhesion (Allan et al., 2001). BAG S53P4 also shows a broad antibacterial effect against several oral bacterial species (Stoor et al., 1998) and demonstrates a better balance between the pH increase and antimicrobial effect compared to 45S5 BAG (Vallittu et al., 2015). Also, BAG doped with zinc oxide (ZnO) can still yield antimicrobial properties against a wide range of bacteria in the absence of pH elevation (Kapoor et al., 2014). Therefore, they may be well tolerated by cells and tissues and thus benefit the healing process (Kogan et al., 2017). The antimicrobial activity of ZnO may be explained by several mechanisms. One mechanism is releasing Zn^{2+} from the dissolved BAG that penetrates the bacterial cell membrane and generates reactive oxygen species (ROS), leading to bacterial death (Sawai et al., 1998). However, the exact mechanism of antibacterial activity of Zn^{2+} is yet to be fully understood. Also, it is not known whether the small amount of Zn^{2+} released from Zn-containing BAG can lead to an antibacterial effect.

This study series aimed to study the effect of BAG air-abrasion on the surface characteristics, antibacterial properties, and biofilm eradication from titanium surfaces. The effects of three novel zinc-containing BAG formulae were compared with the effects of the commercially available 45S5 glass. Furthermore, the aim was to study the impact of BAG air-abrasion on the attachment, viability, and proliferation of human osteoblast-like cells on those surfaces.

2 Review of the Literature

2.1 Peri-implant vs periodontal tissue

The soft tissue structures, including the epithelial and connective tissue parts surrounding dental implants, are to a large extent similar to those surrounding the natural teeth. The peri-implant mucosa, which is established during wound healing after the implant/abutment placement, consists of an outer well-keratinized oral epithelium that is in continuation with a sulcular epithelium lining the gingival sulcus (Listgarten et al., 1991). The sulcus at the implant–mucosa interface mimics that linked to teeth as the supra-alveolar transmucosal parts compromise a sulcus, junctional epithelium, and connective tissue attachment.

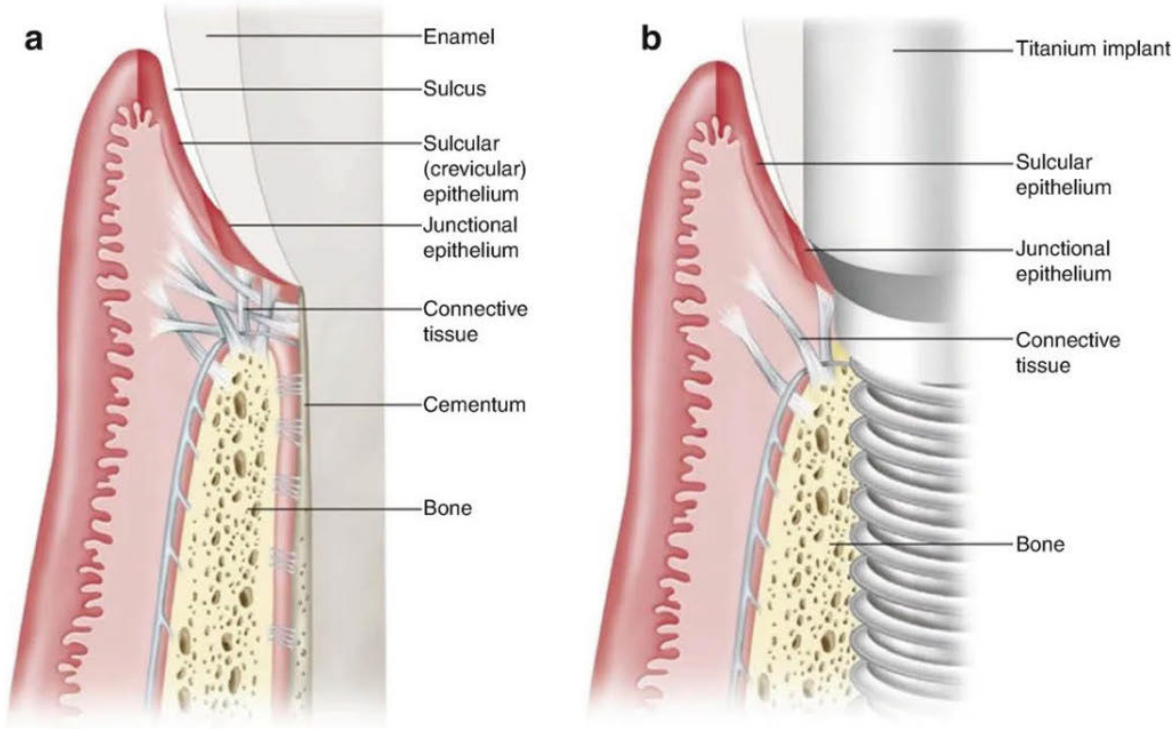

Figure 1. Schematic illustration of periodontal vs peri-implant tissues. (**a**) Periodontal tissue around a natural tooth. (**b**) Peri-implant tissue around an implant. (From Rose LF, Mealey BL: Periodontics: Medicine, surgery, and implants, St. Louis, 2004, Mosby).

The mucosal connective tissue attachment around dental implants has rather similar clinical and histological characteristics to natural teeth. Nevertheless, the principal dissimilarity is noticed in the fiber orientation and cellular composition. The dental implant is surrounded by connective tissue that is in direct contact with the implant material. The connective tissue contains a network of collagen fibers that emerge from the periosteum of the alveolar bone, directed to the margin of the mucosa. These fibers orientation is parallel to the implant/abutment surface (Araujo & Lindhe, 2018; Berglundh et al., 1991; Ivanovski & Lee, 2018). In contrast, the connective tissue attachment to teeth is organized so that the collagen fibers enter in a perpendicular or oblique direction into the root cementum (Berglundh et al., 1991).

Analogous to teeth, implants also have an intraosseous part established within alveolar bone and provides structural anchorage. Even though the periodontal and peri-implant tissues share comparable histologic and clinical characteristics, a few fundamental dissimilarities exist between dental implants and teeth. A principal distinction is that dental implants lack periodontal ligament and cementum. Accordingly, the alveolar bone is in direct contact with the endosseous implant part (Albrektsson & Sennerby, 1991; Berglundh et al., 2007). Due to the lack of periodontal ligament, peri-implant mucosa also has less vascular supply.

2.2 Osseointegration

Brånemark and his co-workers introduced the term osseointegration (OI). It has been originally defined as “a direct functional and structural connection between living bone and the surface of load-carrying implant” (Brånemark et al., 1977). Later, a more clinically oriented definition has been formulated, defining the OI as “a process whereby clinical asymptomatic rigid fixation of alloplastic materials is achieved and maintained in bone during functional loading” (Brånemark et al., 1983).

Process of bone healing following implant placement

Preparation of the osteotomy site for implant placement results in vascular trauma to the mature bone. After 2 hours of the implant installation, the chambers adjacent to the implant surface are occupied with blood clots, and then the cellular and plasmatic hemostasis mechanisms are initiated (Abrahamsson et al., 2004). This leads to the formation of a fibrin network containing erythrocytes, neutrophils, and monocytes which serves as a matrix for the bone-forming cells. Four days later, the coagulum is partly replaced with granulation tissue that contains innumerable mesenchymal cells, immature connective tissue, and newly formed vascular structures. A cell-rich immature woven bone is seen in the immature connective tissue after a 1-week

healing period. The formation of woven bone is more apparent after 2 weeks healing period (Abrahamsson et al., 2004; Berglundh et al., 2003).

Bone mineralization starts at week 4; bone generates from the osteotomy site borders (distance osteogenesis) or the bone-forming cells located on the implant's surface (contact osteogenesis). The osteogenic cells migrate to the surface of the implant and start the new bone formation in distance osteogenesis. While in contact osteogenesis, osteoblast cells move right onto the implant's surface and give rise to de novo bone. Six to twelve weeks later, mineralized bone fills most wound sites, and primary and secondary osteons can be observed (Abrahamsson et al., 2004; Berglundh et al., 2003; Junker et al., 2009). At the end of the remodeling phase, bone-to-implant contact (BIC) is approximately 60–70 %. BIC is commonly used in dental implant research to estimate the degree of OI (Schenk & Buser, 1998; von Wilmowsky et al., 2014).

2.3 Influence of material's characteristics on osseointegration

2.3.1 Implant surface topography

The topography of the implant refers to its macroscopic and microscopic surface characteristics that result from various surface modifications. The implant surface modifications are primarily carried out to enhance cellular activity, improve bone apposition, and encourage OI for rapid and robust bone formation (Ponsonnet et al., 2003; Rosales-Leal et al., 2010; Smeets et al., 2016). These will have a remarkable effect on clinical stability, especially in poor bone quality and quantity. The implant surface roughness may be produced either by additive or subtractive techniques. They can also be classified as mechanical, chemical, thermal, electrochemical, and laser techniques (Ellingsen et al., 2006).

Implant surface roughness is classified according to the measured surface's dimension into macro-, micro-, and nano-scale levels ranged from few millimeters to nanometers roughness. Macroroughness is linked to the geometry of implants and can enhance the implant's primary and long-term stability (Wennerberg et al., 1995). Microroughness modifications can maximize the mechanical interlocking between the implant surface and newly formed bone. Nanoscale roughness is associated with protein adsorption and osteoblast cell adhesion and thus plays a vital role in enhancing the rate of OI (Brett et al., 2004).

Implant surface macro topography

Implant surface modifications are typically performed to modify the surface topography and the properties of the substrate materials. The surface area of the implant can be significantly increased using appropriate modification processes, either using addition or subtraction techniques (Gupta et al., 2014; Jemat et al., 2015). The macro-topography of the implant surface is determined by visible geometry such as tapered design, threads, and microporous and can range from microns to millimeters. Proper macro roughness can substantially enhance implant stability (Shalabi et al., 2006; Wennerberg et al., 1996). In addition, BIC, primary stability, and implant surface area are significantly increased by implant threads that also demonstrate better stress distribution in the bone (Carlsson et al., 1988; Wong et al., 1995).

Implant surface microtopography

The implant surface micro-topography is linked to a micrometer scale and frequently ranged from 1-100 μm. Machining, sandblasting, acid-etching, and various coating techniques have been used in manufacturing implant surface micro-roughness (Dohan Ehrenfest et al., 2010). The surface micro-roughness can be described by the arithmetical mean deviation (Ra), which indicates the 2-dimensional profile roughness average, and the arithmetical mean height (Sa), which indicates the 3-dimensional area roughness average (Dohan Ehrenfest et al., 2010). Most commercially available dental implants have an Ra value of 1-2 μm. This scale appears to allow an ideal degree of surface roughness and improve OI (Albrektsson & Wennerberg, 2004a).

The rationale for implant surface micro-roughness is to speed up the bone healing process and secure the primary stability that can make early loading of the implant possible (Albrektsson & Wennerberg, 2019). It can also have an apparent impact on the biological response of bone as implants with micro roughened surfaces have proven to be superior compared to smooth implants (Wennerberg & Albrektsson, 2009). Moreover, appropriate micro-roughness helps to enhance osteoblast differentiation, provide better biomechanical interlocking, and increase the BIC ratio (Albrektsson & Wennerberg, 2019; Olivares-Navarrete et al., 2010; Vlacic-Zischke et al., 2011; Wennerberg & Albrektsson, 2009). However, the increased implant surface roughness might aggravate bacterial colonization. Therefore, the balance between the desired biological response and plaque biofilm removal around the implant must be considered (Wassmann et al., 2017; Wennerberg & Albrektsson, 2009).

2.3.2 Surface chemistry

The interactions of a material with the tissues or biological fluids are guided mainly through its surface properties and chemical composition. These properties may differ from that of the bulk properties of the material because of surface reactivity and favored presentation of certain elements (Rompen et al., 2006). Implant surface chemistry plays a critical role in protein adsorption, cell adhesion, and the interaction between cells and tissues at the implant/tissue interface (Buser et al., 2004). Moreover, the surface chemistry of dental implants is considered one of the parameters that enhances the BIC and improves OI (Ellingsen et al., 2006). Chemical modifications of the titanium implant surface have also been shown to enhance the surface's hydrophilicity and initial stages of wound healing, therefore facilitating bone integration (Buser et al. 2004).

2.3.3 Surface wettability

The wettability can be significantly affected by the roughness of the material surface. It can be determined by the surface contact angle (CA) value, which Thomas Young introduced in 1805 (Young, 1805). As a rule, a CA value less than 90° is considered a hydrophilic surface. CA values close or equal to 0° are regarded as a super-hydrophilic surface. The hydrophobic surface is determined when its CA value is above 90°, and the super-hydrophobic surface has a CA value above 150°. The surface CA of pure titanium is about 70–90° irrespective of their surface roughness. Nevertheless, after these surfaces have been subjected to serial surface roughening processes, including sandblasting and acid-etching, the surface CA's value could be increased up to 150° (Gittens et al., 2013; Velasco-Ortega et al., 2019).

Results from earlier studies demonstrate that hydrophilic surfaces significantly encourage the early stages of cell adhesion, proliferation, differentiation, as well as bone mineralization compared to their hydrophobic counterparts (Bornstein et al., 2008; Eriksson et al., 2004). In a systematic review, Wennerberg et al. (2011) reported that the more hydrophilic SLA-active implant surfaces demonstrated a more robust early cell and bone tissue response than the less hydrophilic SLA surface. Additionally, the SLA-active surface demonstrated collagen fiber formation as early as after the first 4 days following the implant placement. Furthermore, bone formation has been much denser after 2 weeks of implantation than on the SLA control surface. However, following 6 to 8 weeks post-implant placement, the differences between the SLA-active and the control groups have been diminished (Junker et al., 2009; Schwartz et al., 2008).

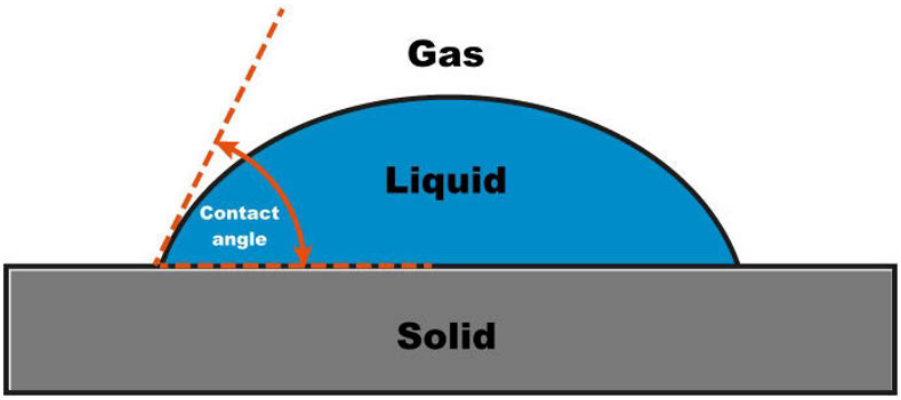

Figure 2. An illustration of the sessile drop method with liquid droplet.

2.4 Implant surface modifications

Treatment on implant surfaces is usually carried out to modify their surface properties. Proper surface modification can increase the surface area, improve wettability, increase cell proliferation, and enhance the OI process (Lacefield, 1999; Ponsonnet et al., 2003; Rosales-Leal et al., 2010). Surface modification is classified into mechanical, chemical, and physical methods. They can also be broadly classified into subtractive and additive procedures.

2.4.1 Subtractive surface modifications

Subtractive modification techniques are produced by deforming the material's surface or removing a layer of core material to increase its roughness (Jemat et al., 2015; Ting et al., 2017). These techniques can be divided into mechanical and chemical methods. Mechanical modification methods include machining, grinding, sandblasting, or grit blasting using physical force. Chemical processes involve utilizing either alkaline or acid solutions to increase the roughness, improve the wettability and surface energy, as well as modifying the surface composition (Liu et al., 2004a).

The macro roughness of the sandblasted and acid-etched (SA) surface is created by sandblasting with large grit (0.25–0.5 mm) corundum particles at 5 bars (Wennerberg et al., 2011). A subsequent acid-etching process produces the micro-roughness surface structure using a strong combination of hydrochloric and sulphuric acids (HCl/H_2SO_4) at high temperatures (Jemat et al., 2015). A positive association has been suggested between the degree of surface roughness and attachment and proliferation of osteoblast-like cells (Anselme et al., 2000). Also, the surface roughness is associated with selective protein adsorption, collagen synthesis, and chondrocyte maturation, which subsequently affect the implant OI (Schwartz et al., 2001).

Better OI has been reported for SA implant surfaces during the healing phase because of the increased surface area, which maximizes the surface available for new bone

formation, and consequently, better mechanical fixation (Blatt et al., 2018). In a minipig model, Li et al. (2002) found that SA implants showed a higher BIC than machined or acid-etched implants and demonstrated considerably increased torque removal values. In a 10-year follow-up study of 24 patients, Fischer & Stenberg (2012) showed that SA titanium implants demonstrated satisfactory long-term outcomes with an implant survival rate of 95 % and average bone loss of 1.07 mm. Buser et al. (2012) have also evaluated a total of 511 implants in 303 patients with SA implants over 10 years. Their study showed a 97.0 % implant success rate and 98.8 % survival rate over the study period.

Grit blasting is a frequently used implant surface modification in which ceramic particles (Al_2O_3, TiO_2, or $Ca_2P_2O_7$) are used for the air-abrasion process (Guéhennec et al., 2007). The particle's shape, hardness, velocity, and titanium tearing strength can highly influence the degree of titanium surface infliction. (Barriuso et al., 2014). Wennerberg and Albrektsson (2009) reported that the ideal implant surface roughness induced by grit blasting has Sa values on a scale of 0.6-2.1 mm.

2.4.2 Additive surface modifications

In these procedures, various additive techniques are used on implant surfaces to improve their biological and biomechanical properties. These techniques include plasma spraying, calcium phosphate coatings, ion deposition, fluoride coating, sol-gel coating, and sputter deposition (Wennerberg & Albrektsson, 2009).

The plasma spray method includes spraying a thermally melted material such as hydroxyapatite (HA) and titanium particles onto the titanium implant surfaces that substantially increases the surface roughness and implant surface area (Ong et al., 2004). Le Guéhennec et al. (2007) reported that plasma-sprayed coatings deposited on the implant surface must reach 40-50 µm to form a uniform layer. Results from animal studies and *in vitro* research reveal that the HA coatings promote the healing process and encourage cell proliferation (Fouda et al., 2009; Xie et al., 2006). Furthermore, findings from *in vivo* studies indicated that implant coating using calcium phosphate ($Ca_3(PO_4)_2$) plasma spray demonstrated faster bone apposition compared to the uncoated implants (Gottlander et al., 1997; Meirelles et al., 2008). However, the resultant coating has several drawbacks, including porosity and high residual stresses at the implant-coating interface due to the increased processing temperature involved (Filiaggi et al., 1991). Coating delamination from the titanium implant surface is another concern that may lead to failure at the implant-coating interface (Ong et al., 2004). Moreover, several studies reported that the bonding and coating strength of HA on titanium surface decreases, leading to bonding degradation (Liu et al., 2004b; Ong et al., 2004). Besides, more marginal bone resorption has been demonstrated around plasma sprayed titanium surfaces compared to minimally or moderately rough surfaces (Åstrand et al., 2000; Becker et al., 2000).

The radio frequency (RF) magnetron sputtering method is also used to obtain HA coating on titanium surfaces (Surmenev et al., 2017; Wolke et al., 1998). This method allows for the deposition of calcium phosphate coatings with uniform thickness and good adhesion to the substrate (Hung et al., 2017). This technique utilizes a low processing temperature, and the thicknesses of the coating films can be controlled more precisely (Wan et al., 2007).

2.5 Peri-implant diseases

Peri-implant diseases are defined as plaque-induced inflammatory diseases affecting soft and hard tissues surrounding the dental implants (Berglundh et al., 2018). They are broadly classified into peri-implant mucositis and peri-implantitis (PI). Peri-implant mucositis can be determined as an inflammatory lesion confined to the soft tissue around the implant, with no indication of peri-implant marginal bone loss beyond the initial bone remodelling that happened after the implant installation (Heitz-Mayfield et al., 2018). Clinically peri-implant mucositis is characterized by bleeding on probing, redness and swelling in peri-implant mucosa, suppuration, and increased pocket depth (Renvert et al., 2018; Schwarz et al., 2018).

PI refers to inflammation of the mucosa surrounding a dental implant and combined with progressive peri-implant bone loss (Schwarz et al., 2018). It usually shares comparable clinical features with peri-implant mucositis yet with a progressive bone loss after the initial bone remodelling, which is considered the main clinical feature distinguishing PI from peri-implant mucositis (Heitz-Mayfield et al., 2018; Renvert et al., 2018; Schwarz et al., 2018). However, it is accepted that both peri-implant disease entities have an infectious etiology caused by the formation of biofilm composed of an excessive number of bacteria with known pathogenicity (Lafaurie et al., 2017; Persson & Renvert, 2014). Many studies have demonstrated a strong association between history of periodontitis and an increased risk for PI (Renvert & Persson, 2009; Schou et al., 2006).

The prevalence of PI varies significantly in the literature and ranges from 4-45 % (Atieh et al., 2013; Salvi et al., 2017). In a systematic review, Derks and Tomasi (2015) reported that PI and peri-implant mucositis prevalence has been around 22 % and 43 %, respectively. In another systematic review by Lee et al. (2017), the prevalence of PI and peri-implant mucositis at the implant level is about 9.25% and 29.48 %, respectively. While at a patient level, the reported prevalence has been 19.8 % and 46.83 %, respectively. The wide range of prevalence reported in the literature is owing to discrepancies in the definition of PI instead of actual differences in prevalence between studied populations.

The definition of PI is complicated by various factors such as implant design, surface characterization, and the surgical protocol used for implant surgery

(Berglundh et al., 2018). Froum and Rosen (2012) suggested a classification of PI. They categorized the disease entity into early, moderate, and advanced. The early PI is defined as less than 25 % bone loss of the implant length and 4 mm or greater probing depth. Moderate PI is determined with 25-50 % bone loss and 6 mm or greater probing depth. In comparison, advanced PI has a bone loss of more than 50 % and probing depth greater than 8 mm.

The anatomy of bone defects due to PI may depend on many factors, such as the location of the dental implant, the thickness of keratinized mucosa, and the alveolar bone configuration. Schwarz et al. (2007) classified peri-implant bone defects according to the pattern of bone loss around implants. Class I defect is described by the presence of buccal dehiscence, an intrabony defect, or a combination of both. Class I bone defects are sub-classified based on the presence or absence of bone walls into classes Ia to Ie (Figure 3). Class II bone defect is described by horizontal and vertical bone loss. Findings from their study indicate that circumferential bone defect (class Ie) is the most frequent defect configurations, representing 55% of all defects compared to 5.5%, 15%, 13%, and 10% for class Ia, Ib, Ic, and Id, respectively (Schwarz et al., 2007). However, a recent clinical study by Wehner et al. (2021) evaluated a total of 193 PI defects in 100 patients subjected to surgical treatment. According to their study, class Ic and Id (intrabony defect and buccal/oral dehiscence) are more common compared to Ie (circumferential bone defect). However, 18.7% of the examined bone defects did not fit Schwarz et al. classification (Wehner et al. 2021).

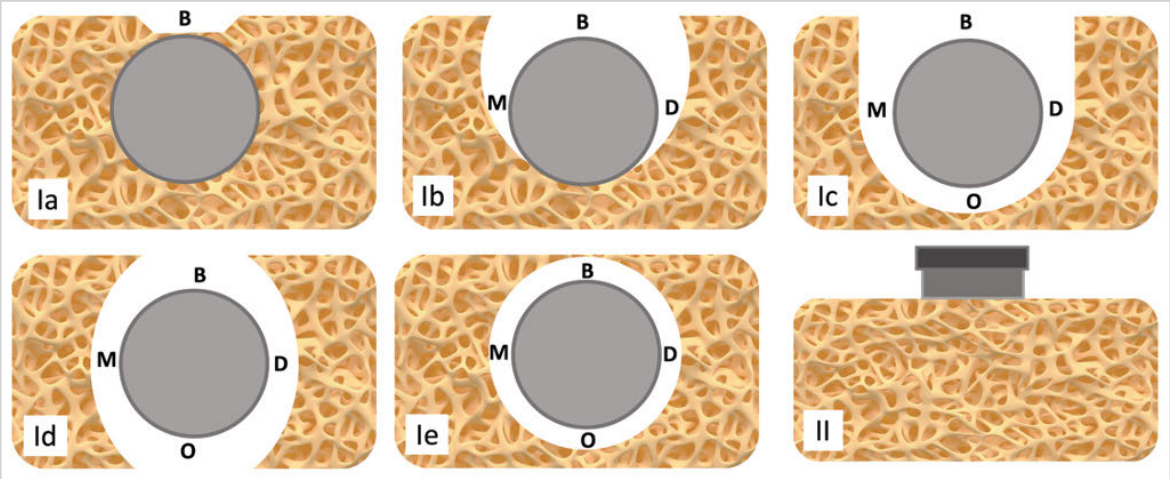

Figure 3. Schematic drawing illustrating the classification of peri-implant bone defects. Class **Ia**- occlusal view represents buccal dehiscence; class **Ib**- occlusal view represents buccal dehiscence combined with semicircular bone resorption; class **Ic**- occlusal view represents buccal dehiscence combined by circular bone resorption; class **Id**- occlusal view represents buccal and oral dehiscence combined with circular bone resorption and class **Ie**- occlusal view represents circular bone resorption with maintained peri-implant boney walls. Class **II**-vestibular/oral view shows vertical and horizontal bone resorption. (B = buccal, M = mesial, D = distal and O = oral). Modified from Schwarz et al. 2007.

Even though PI has many clinical signs and etiologic factors in common with periodontitis (Berglundh et al., 2011), Carcuac et al. (2013) demonstrated in an experimental animal study that the PI progression rate has been faster than periodontitis and resulted in rapid bone loss. The structural differences between the periodontium and the peri-implant tissue are believed to be the reason for this faster progression. Peri-implant tissue is characterized by lacking cementum and periodontal ligaments, poor peri-implant epithelium attachment, reduced blood flow, and parallel direction of the collagen fibers (Berglundh et al., 2011; Larjava et al., 2011). Accordingly, several animal studies have demonstrated more marked clinical and radiographic signs of tissue destruction around dental implants compared to natural teeth (Lindhe et al., 1992; Zitzmann et al., 2004).

In an *in vivo* animal study, Lindhe et al. (1992) studied experimentally induced periodontal and peri-implant lesions in beagle dogs. Their study showed that, due to the parallel direction of collagen fibers around the dental implant, the connective tissue infiltration is more significant and extends to the peri-implant bone level compared to periodontal tissue, which is protected by a band of non-infiltrated connective tissue. Similarly, in a clinical study, Carcuac & Berglundh (2014) demonstrated that more inflammatory cells infiltrate, including plasma cells and lymphocytes, along with neutrophils and macrophages, are observed in the peri-implant mucosa compared to periodontal tissue. PI inflammatory infiltrates contain, for the most part, plasma cells that resemble plasm cell lesions of periodontitis. Furthermore, the infiltrated connective tissues around dental implants lack collagen, which is substantially replaced by increased vascularity and inflammatory cells (Berglundh et al., 2004).

Both B and T lymphocytes are markedly noticed at PI sites. Results from immunohistochemistry analysis reveal that T cells overcount the B cells in PI sites (Bullon et al., 2004). However, findings from Gualini & Berglundh (2003) demonstrated an increased number of B lymphocytes compared to T lymphocytes. Cytokines such as IL-1 β, IL-6, and TNF-α are inflammatory biomarkers produced by many cells, especially T cells and macrophages (Ghassib et al., 2019). Their concentration differs remarkably in normal biologic and pathologic conditions (Bhardwaj & Prabhuji, 2013). Increased levels of these mediators have been reported in PI and periodontitis sites compared to their healthy counterparts (Gundoğar & Uzunkaya, 2021). The presence of the inflammatory mediators at a higher level has been shown to evoke tissue destruction and bone resorption (Pan et al., 2019; Seymour & Gemmell, 2001).

2.5.1 Treatment of peri-implantitis

The rough dental implant surfaces have questioned the feasibility of a complete infection resolution. Exposure of rough implant surface microstructures to the oral

environment leads to developing a high-affinity biofilm that is robust, retentive, and difficult to eliminate and maintain plaque-free. Owing to the similar pathophysiology of periodontal and peri-implant diseases, therapeutic approaches proposed for treating PI seem to stand mainly on the evidence available to treat periodontitis (Renvert et al., 2008). Surface debridement to eliminate the biofilm is an essential part of treating both periodontal and peri-implant infections. However, the implant design and different surface treatments may enable the accumulation of bacterial plaque and limit the effect of mechanical debridement resulting in incomplete removal of biofilm (Suarez et al., 2013; Teughels et al., 2006).

Despite multiple treatment protocols tested, there is no generally accepted protocol on the best course of treatment for peri-implant diseases (Esposito et al., 2012; Periodontitis. Current care recommendation, 2019). Various devices are used for implant biofilms mechanical debridement such as manual instruments, plastic or carbon tips, ultrasonic/sonic instruments, and air powder abrasion combined with systemic or local antimicrobial agents (Estefanía-Fresco et al., 2019; Heitz-Mayfield & Mombelli, 2014). However, the outcomes of current non-surgical treatments failed to demonstrate a significant improvement and showed limited success and low predictability (Lang et al., 2019; Valderrama & Wilson, 2013). Keim et al. (2019) evaluated the efficiency of mechanical debridement using a single device. Findings from their study showed that air powder abrasion has been superior to the sonic scaler and demonstrated no implant surface damage. While using a sonic scaler has been more efficient than using a curette despite causing damage to the implant surface.

Autogenous bone and various bone replacement materials, including xenograft, alloplastic bone fillers, and titanium granules, have been used to augment intrabony peri-implant defects. Statistically significant improvement in bleeding on probing and probing depth values have been observed post-operatively (Froum et al., 2015). Regardless of the successful clinical and radiographic outcome of augmentative therapies, recurrence, disease progression, and implant loss have also been reported (Froum et al., 2015; Khoury & Buchmann, 2001; Ramanauskaite et al., 2019; Wohlfahrt et al., 2012).

It is noteworthy that the treatment choice of PI and the outcome of surgical therapy are primarily affected by the morphology of the bone defects (Aghazadeh et al., 2020; Schwarz et al., 2010). Narrow, circumferential bone defects will more likely result in defect fill compared to their wide counterparts (Schwarz et al., 2010). The number of the remaining bone walls is another crucial factor that has been reported to be associated with successful bone defect healing (Isehed et al., 2016). Aghazadeh et al. (2020) evaluated the influence of bone defect configuration on treatment outcome after 1 year. In addition to the shape of the bone defect, the number of remaining walls has an impact on the post-operative results. Bone defects with 4-walls have better reconstruction potential than 2- and 3-wall bone defects

(Aghazadeh et al., 2020). Regenerative surgical therapy using grafting and collagen membranes demonstrates a better treatment outcome in circumferential bone defect (class Ie) compared to intrabony defect and buccal/oral dehiscence (class Ib, Ic, and Id) (Schwarz et al., 2010).

2.5.2 Oral bacterial biofilm

Microbial biofilm formation in the oral cavity is a dynamic complex multistage process (Dhir, 2013; Kumar et al., 2012; Shibli et al., 2008). The initial bacterial adhesion on the implant surface is considered the first and an essential step in forming the peri-implant biofilms, which sequentially may result in PI and subsequent loss of the supporting tissue (Abrahamsson et al., 1998). The surface properties, chemical composition, roughness, surface topography, and surface free energy (SFE) remarkably affect the bacterial adhesion and biofilm formation on the implant surface (Abrahamsson et al., 1996; Busscher et al., 2010; Subramani et al., 2009). Therefore, recent implant surface modifications are focused on reducing biofilm formation after exposure to the oral environment.

Dental implant biofilm formation follows similar stages of microbial adhesion and colonization on natural teeth. It starts with forming the salivary protein-derived acquired pellicle as early as 30 minutes after the implant surface is exposed to the oral environment (Fürst et al., 2007; Lee et al., 2010). The bacteria adhere to the pellicle proteins and glycoproteins by their adhesins presented on their surfaces. Oral streptococci are considered the early species to attach to the teeth/materials surfaces, and they represent the vast majority of the early colonizers (Diaz et al., 2006; Dige et al., 2007). These early bacterial species serve as anchors for the successive bacterial colonizers, such as anaerobic bacteria. *Fusobacterium nucleatum* is a crucial species in dental plaque formation and maturation and can bind to several oral bacterial species. It serves as a bridge between early and late bacterial colonizers such as *Porphyromonas gingivalis*, *Tannerella forsythia*, and *Treponema denticol*a, leading to the formation of a mature, complex biofilm (Diaz et al., 2002; Lee & Wang, 2010; Socranskyet al., 1998).

Microbial studies suggest that microorganisms exist within polymicrobial communities and typically interact synergistically to enhance the colonization capability and pathogenicity of the entire biofilm community (Hajishengallis & Lamont, 2016; Lamont et al., 2018). This microbial synergy resulted from the interaction between the primary bacterial colonizers, such as oral streptococci, with the late colonizers. The primary colonizers facilitate the attachment and colonization on the substrate surfaces and provide nutrition to the late bacterial colonizers (Nobbs et al., 2009; Wright et al., 2013). Increased consumption of carbohydrate diet or alteration in the competence of the host immunity can alter the microbial community

and result in the production of virulence factors, which in turn may cause the transition of the local bacterial environment to a dysbiotic state (Dabdoub et al., 2016). The polymicrobial synergy and dysbiosis model may explain periodontal disease pathogenicity. Interaction between *P. gingivalis* and other commensal microorganisms can facilitate synergy and the transition to pathogenicity, leading to the development of a dysbiotic community. Development of dysbiosis in periodontitis occurs over time, turning the symbiotic association of host and microbial community to pathogenic, which can stimulate the inflammatory response in the susceptible hosts (Hajishengallis, 2014; Lamont et al., 2015). On disease progression, orange-complex bacteria such as *F. nucleatum, Prevotella intermedia, Prevotella nigrescens* shift toward red-complex bacteria comprise *P. gingivalis, T, forsythia, and T. denticola* (Nath & Raveendran, 2013).

Streptococcus mutans

Oral streptococci, including *S. mutans*, are considered the first bacterial species essential to the early phase of oral biofilm formation (Koo et al., 2010; Marsh, 2005). *Streptococcus species* represent the vast majority of all primary bacterial colonizers that adhere to the acquired pellicle formed on dental implants (Donlan, 2002; Elter et al., 2008).

The initial bacterial colonizers are assumed to facilitate the colonization of the later bacterial colonizers, resulting in an anaerobic Gram-negative biofilm formation. *S. mutans* is facultatively anaerobic, Gram-positive cocci that possess multiple virulence factors. The virulence of *S. mutans* is referred to its ability to synthesizing potent extracellular polysaccharides (EPS) called glucans that adhere to tooth/material surfaces and form intercellular nests within dental plaques. EPS serves as an energy supplier during any extraneous carbohydrate deficiency (Decker et al., 2011). Besides, *S. mutans* can metabolize carbohydrates to generate an acidic environment (acidogenicity), which causes enamel demineralization. Moreover, *S. mutans* isolates demonstrated a high ability to survive at low pH values, which is considered toxic to most other bacterial species (Forssten et al., 2010; Lemos & Burne, 2008).

Glucosyltransferase (GTF) is a key enzyme that catalyzes sucrose to form the adhesive glucans, contributing significantly to dental plaque formation. *S. mutans* expresses three GTF enzymes with distinct roles and locations. Two enzymes, GtfB and GtfC, are located on the bacterial cell wall and synthesize primarily insoluble glucan. In contrast, GtfD is secreted by the bacterial cell and synthesizes exclusively water-soluble glucan (Hanada & Kuramitsu, 1988; Hanada & Kuramitsu, 1989). Findings from Guo et al. (2017) showed that the adhesin SpaP protein located on *S. mutans* is used by the bacterial cell to bind and interact with other proteins on other

bacteria such as RadD of *F. nucleatum,* which enhances the ability of both species to efficaciously colonize the oral surfaces. The elimination of *S. mutans* from the oral biofilm ecosystem considerably influences its formation, causing a significant decrease in the biofilm volume and slowing its development (Krzyściak et al., 2014). The insoluble glucans produced by *S. mutans* allow binding locations for the late bacterial colonizers, which cannot attach to the oral surfaces. The percentage of *S. mutans* cells decreases as the biofilm maturates, and consequently, the environment shifts to late bacterial colonizer (Koo et al., 2010; Koo et al., 2013; Tamura et al., 2009).

Fusobacterium nucleatum and *Porphyromonas gingivalis*

In healthy conditions, periodontal and peri-implant tissues share a similar bacterial population, comprised mainly of Gram-positive facultative cocci (Donlan, 2002; Elter et al., 2008). In periodontitis and PI, the microbiota has similar features with increased proportions of Gram-negative obligate anaerobes, most commonly; *P. gingivalis, P. intermedia, P. nigrescens, F. nucleatum, T. forsythia, T. denticol*a and, *Aggregatibacter actinomycetemcomitans* (Lamont et al., 2018; Leonhardt et al., 1999; Mombelli, 2002). However, *in vivo* studies have shown considerable variation in microbiomes community between individuals with periodontitis and, in fact, between sites in the same individual (Diaz, 2012; Nowicki et al., 2018).

F. nucleatum is a common obligately anaerobic Gram-negative bacteria of the oral cavity that plays a crucial role and acts as a bridge between early and late bacterial colonizers (Lee & Wang, 2010; Socranskyet al., 1998). *F. nucleatum* carries an outer adhesin-rich membrane that enables its adhesion to salivary proteins, host tissue, and other microorganisms (Coppenhagen-Glazer et al., 2015; Guo et al., 2017). In addition, *F. nucleatum* plays a crucial role in balancing the formation and subsequent maturation of oral biofilm as a remarkable decrease in the biofilm bacterial count is observed in the absence of *F. nucleatum* (Thurnheer et al., 1999). Zhuang et al. (2016) compared the prevalence of peri-implant and periodontal pathogens in patients with various clinical conditions. Higher levels of *F. nucleatum* have been detected around periodontitis sites compared to healthy periodontal sites.

The primary virulence of *F. nucleatum* is attributed to its ability to adhere to other bacteria and host cells through various adhesins and adhesion proteins located on their outer membranes, such as FadA and RadD. Surface proteins FadA has been identified for its role in binding to various Gram-positive bacterial species, whereas RadD surface protein is known for binding to *P. gingivalis* (Coppenhagen-Glazer et al., 2015; Kaplan et al., 2009). Additionally, *F. nucleatum* has an outer membrane protein known as familial adenomatous polyposis 2 (Fap2), which can bind to and interacts with natural killer cells and lymphocytes and thus suppress their cytotoxic

effect (Coppenhagen-Glazer et al., 2015; Gur et al., 2015). RadD and Fap2 are autotransporter proteins known for their role in cell adhesion, coaggregation, and biofilm formation (Kaplan et al., 2009; Sherlock et al., 2004). Additionally, *F. nucleatum* has the ability to enhance hemolytic activity and produce hydrogen sulfide (H_2S), which are regarded as critical virulence traits employed by *F. nucleatum* (Okamoto et al., 2000; Yoshida et al., 2009).

P. gingivalis is a Gram-negative strictly anaerobic red-complex bacterium, strongly associated with the initiation and progression of PI (Casado et al., 2011; Tabanella et al., 2009). It is considered one of the most important bacterial pathogens actively engaged in periodontal and peri-implant diseases (Casado et al., 2011; Hajishengallis et al., 2012; Tabanella et al., 2009). *P. gingivalis* has been identified in subgingival plaque samples in 87.75 % of patients with chronic periodontitis (Datta et al., 2008) and 60 % with PI (Leonhardt et al., 1999) compared to patients with healthy periodontal and peri-implant tissues. Also, high serum antibody levels of *P. gingivalis* have been reported for patients with chronic periodontal diseases (Casarin et al., 2010; Mahanonda et al., 1991). However, Pussinen et al. (2011) demonstrated that the serum antibody levels elevation is strongly associated with the carriage of periodontal pathogens such as *P. gingivalis* instead of periodontal infection. The virulence of *P. gingivalis* is attributed to many factors, including fimbriae, capsules, lipopolysaccharide (LPS), and cysteine. Fimbriae are major and minor, hair-like projections emerging from the outer cell surface that enable bacterial adherence and colonization. Major fimbriae facilitate the bacterial binding to itself and other bacteria, whereas minor fimbriae play a role in biofilm formation (Amano, 2003; Bostanci & Belibasakis, 2012; Inaba et al., 2008; Zenobia & Hajishengallis, 2015). Encapsulated *P. gingivalis* are highly invasive strains that resist phagocytosis and can release vesicles from their outer membrane loaded with LPS and proteases (Irshad et al., 2012; Vernal et al., 2009).

2.6 Bioactive glasses

Bioactive glasses (BAG) are a group of biomaterials first introduced in 1969 by L Hench and his co-workers. The original BAG composition is based on Na_2O–CaO–SiO_2–P_2O_5 system (Hench, 2006). This glass has been termed as 45S5 and bioglass® with nominal composition; 45 wt.% SiO_2, 24.5 wt.% Na_2O, 24.5 wt.% CaO and 6 wt.% P_2O_5 (Hench, 2006). The properties of BAGs are controlled by their compositions, production techniques, and ionic dissolution rate.

After the BAG is in contact with simulated body fluid (SBF), the glass is immediately subjected to ionic dissolution and degradation by exchanging hydrogen (H^+) ions in the SBF and sodium (Na) and calcium (Ca^{2+}) ions from the glass network. This ion exchange gives rise to the hydrolysis of the silica (Si) group and

thus the formation of silanol group (Si-O-H) (Hench, 2006). An increased hydroxide (OH^-) concentration will increase the alkaline local environment and, therefore, increase the pH. As the pH rises, the silica network further increases, causing the formation of orthosilicic acid gel on the surface with a negative charge that acts as a matrix for the formation of hydroxyapatite (Hench, 2006). Furthermore, the release of Si, Na, Ca^{2+}, and phosphate (PO_4^{3-}) ions from the BAG surface elevates the concentration of salts and consequently the osmotic pressure. The previous mechanisms are believed to be the rationale of the antibacterial properties of BAG (Allan et al., 2001; Stoor et al., 1998).

BAG 45S5 has been considered an osteoconductive material (Hench, 1998). The bone healing process can benefit from the dissolved Si, Ca^{2+}, and PO_4^{3-} ions (Hench & Polak, 2002). In addition, the ionic release from the BAGs has been reported to promote the expression of osteogenic markers, such as collagen type 1, alkaline phosphatase, and osteocalcin, which may explain the osteoinductive properties of BAGs (Foppiano et al., 2007; Varanasi et al., 2009).

2.6.1 Antibacterial properties of bioactive glasses

BAGs possess broad-spectrum antimicrobial and antibiofilm activities against wide varieties of clinically important microorganisms (Allan et al., 2001; Allan et al., 2002; Stoor et al., 1998). The antimicrobial and antibiofilm effects of 45S5 BAG are mainly due to the increased pH and osmotic pressure locally, making the environment unfavorable for the growth and adhesion of bacteria (Allan et al., 2001; Hu et al., 2009; Stoor et al., 1998). Allan et al. (2001) showed that 45S5 BAG particles have a substantial antibacterial property against certain supra- and sub-gingival oral bacterial species. Therefore, it can reduce bacterial colonization and biofilm formation (Allan et al., 2002).

Results from earlier studies showed that the high aqueous pH value is accountable for the antibacterial effect of BAGs due to the release of alkali ions such as Na^+ and Ca^{2+} from BAG particles after their immersion into an aqueous environment (Allan et al., 2001; Mortazavi et al., 2010). Although, Hu et al. (2009) showed that the adhesion of bacteria to 45S5 BAG particles is necessary for the inactivation of bacteria. Allan et al. (2001) indicated that direct contact between 45S5 BAG particles and the bacterial cells is unnecessary to yield an antibacterial effect. However, it is not known whether BAG air-abrasion can endow bioactivity and impart antibacterial properties to the titanium abraded surface.

BAG S53P4 consists of similar oxide compositions but in different ratios compared to the 45S5 BAG. Particulate S53P4 BAG has also been demonstrated a broad-spectrum antibacterial effect against several oral bacteria species and shown an apparent antibacterial impact on many aerobic and anaerobic bacterial species of

clinical importance (Lepparanta et al., 2008; Munukka et al., 2008; Stoor et al., 1998). Nevertheless, Vallittu et al., 2015 reported that particulate S53P4 BAG (300-500μm) has been shown to cause less pH elevation compared to 45S5 BAG.

2.6.2 Zinc containing bioactive glass

The original 45S5 BAG has been modified by the inclusion of small proportions of biologically active elements such as zinc (Zn), strontium (Sr), copper (Cu), and magnesium (Mg) to enhance therapeutic behavior and impart specific biological functionalities. Zn^{2+} ion is a crucial element for cell growth, proliferation, and differentiation. Additionally, it has been shown to stimulate the attachment and proliferation of osteoblast cells, hinder osteoclastic cell activity, and be involved in the bone maturation process (Collier et al., 1998; Ishikawa et al., 2002). Zn also has an essential role in DNA replication, expression of growth factors, and enzyme production (Zorrilla et al., 2006). Indeed, the slow release of Zn promotes bone formation in the vicinity of the implant and accelerates the healing process (MacDonald, 2000). Therefore, Zn has been incorporated in the BAG structure to enhance healing and decrease post-surgical infections (Kamitakahara et al., 2006).

The antimicrobial activity of ZnO doped BAG may be explained by several mechanisms. The Zn^{2+} ion released from the BAG can penetrate the cell membrane of bacteria and generate the toxic reactive oxygen species (ROS), leading to bacterial death (Sawai et al., 1998; Yamamoto, 2001). It can also cause an interruption in the protein synthesis and interferes with DNA replication of the bacterial cell (Mohd Bakhori et al., 2017). Sawai et al. (1998) demonstrated that the release of H_2O_2 has also been considered a primary factor contributing to the antibacterial activity of ZnO. H_2O_2 can also penetrate the bacteria's cell wall, leading to bacterial cell growth inhibition (Sawai et al., 1998). Besides, the ultrahigh crystallization temperature used for ZnO containing BAG production has been reported to inhibit the glass's bioactivity and results in slow BAG degradation (Sergi et al., 2019).

Sr has also been reported to possess an antibacterial effect against bacteria associated with peri-implant infection (Alshammari et al., 2021), enhances pre-osteoblastic cell replication, and stimulates bone formation (Bonnelye et al., 2008). Results from Kapoor et al. (2014) indicated that both ZnO and SrO doped BAG can still provide antimicrobial properties against a wide variety of bacteria in the absence of pH elevation.

2.6.3 Clinical applications of bioactive glasses in dentistry

BAGs are used in many dental applications, such as bone substitutes in periodontal regeneration, maxillofacial reconstruction, and implantation procedures (Lovelace et

al., 1998; Skallevold et al., 2019; Stoor et al., 2017). BAG 45S5 particles such as PerioGlas® are widely used in augmenting periodontal bone defects to stimulate bone regeneration (Lovelace et al., 1998; Profeta & Prucher, 2015; Profeta & Huppa, 2016). A meta-analysis by Sohrabi et al. (2012) demonstrated that intrabony defects therapy using BAGs resulted in a significant probing depth reduction along with clinical attachment level gain compared to open debridement alone.

The addition of BAG to titanium implant surfaces can make such implants surface-active, helping the implant bond with the bone and provide antimicrobial protection (Civantos et al., 2017). Several implant coating methods by BAG surface deposition have been investigated, such as sol-gel deposition, pulsed laser deposition, electrophoretic deposition, and RF magnetron sputtering (D'Alessio et al., 1999; Fu et al., 2017; Moritz et al., 2004; Stan et al., 2009; van Oirschot et al., 2016). The latest method seems promising since it yields a pure and superb coating even in a complex geometrical object (Šimek et al., 2019). However, it is not known whether BAG air-abrasion can endow the bioactivity of titanium surfaces.

BAGs are also incorporated with restorative materials such as composite to create a tight bond between the restorations and the teeth, thus increasing their longevity (Profeta, 2014). The addition of BAG particles to resin composite has inhibited bacterial growth such as *S. mutans* and inhibited secondary caries formation (Chatzistavrou et al., 2015). Also, tiny particles of silicate BAG are incorporated into the toothpaste for remineralization and to reduce dentine hypersensitivity (Gjorgievska & Nicholson, 2011). BAGs have also been used in air abrasive devices to remove surface stains, resulting in whiter teeth and less dentine hypersensitivity compared to the conventional sodium bicarbonate particles (Banerjee et al., 2010). The particles of BAGs can lead to the dentinal tubules' occlusion by binding to collagen fibers and the formation of hydroxyapatite (Gillam, 1997).

3 Aims

The research presented in this thesis was performed to study novel BAG formulae for use in an air-abrasion device to eliminate the bacterial biofilm from the infected titanium surfaces to be used in treatment of PI.

This research was based on the working hypothesis that the BAG air-abrasion will yield antibacterial properties to titanium surfaces, eliminate the bacterial biofilm on SA titanium surfaces and promote the proliferation of bone-forming cells.

The following specific experiments were set to test the working hypotheses:

1. Study the pH levels and ions released from BAG particles into simulated body fluid (Study **I**).

2. Evaluate the effect of BAG air particle abrasion of titanium surfaces on the viability, adhesion, and biofilm formation of *S. mutans* (Study **I**).

3. Investigate the effect of BAG air particle abrasion on *S. mutans* biofilm and *F. nucleatum* and *P. gingivalis* dual biofilm formed on SA titanium surfaces (Studies **II** and **IV**).

4. Examine the effect of BAG air particle abrasion of *S. mutans* infected SA titanium surfaces on blood coagulation (Study **II**).

5. Evaluate the effect of BAG air particle abrasion on hydrophilicity, surface free energy, and the attachment and proliferation of human osteoblast-like MC3T3-E1 cells on SA titanium surfaces (Study **III**).

4 Materials and Methods

4.1 Bioactive glass preparation

BAG 45S5 and the ZnO/SrO dopped BAGs were prepared according to the molar exchange of ZnO and SrO for CaO and SiO_2 in the original 45S5 BAG composition. In Zn4 BAG, 2 mol% of both CaO and SiO_2 were substituted by 4 mol% ZnO. In Zn6, the total proportion of ZnO was exchanged for SiO. In the Zn4Sr8, 2 mol% of SiO_2 and 8 mol% of CaO were replaced by 4 mol% ZnO and 8 mol% of SrO. The oxide composition and the network connectivity of the prepared glasses are shown in (Table 1).

Table 1. Composition (mol.%) of 45S5 and the Zinc and Strontium oxide dopped bioactive glasses. Network connectivity (NC) for the glasses was determined based on Hill and Brauer (2011). Modified from the original publication I.

	SiO_2	Na_2O	P_2O_5	CaO	ZnO	SrO	NC
45S5	46.1	24.3	2.6	26.9			2.12
Zn4	44.1	24.3	2.6	24.9	4.0		1.94
Zn6	40.1	24.3	2.6	26.9	6.0		1.54
Zn4Sr8	44.2	24.5	2.6	16.6	4.0	8.0	1.95

The 45S5 BAG and ZnO/SrO containing BAGs were melted in-house at Johan Candolin process chemistry center, Åbo Academy University, Turku, Finland. The following analytical grade chemical was used to produce 300 g bathes: Na_2CO_3, $CaHPO_4 \cdot 2H_2O$, $SrCO_3$ and ZnO (Sigma-Aldrich), $CaCO_3$ (Fluka), H_3BO_3(Merck), and SiO_2 (Belgian quartz sand). Glasses were melted in an uncovered platinum crucible at 1360 ºC in the air for 3 hours. Subsequently, the produced glass blocks were annealed at 520 ºC for 1 hour and then allowed to cool down slowly in the oven. Then the obtained glasses were crushed, followed by re-melting to ensure homogeneity. Afterward, the annealed glasses were transformed into powder to yield

glass particles on the scale of 25-120 µm, 45-120 µm, and 300-500 µm. E-glass (commercial alumino borosilicate glass) was used as inert control.

The morphology of the obtained glass particles was assessed with a scanning electron microscope (SEM) (Jeol-JSM 5500, Japan). The obtained glass particles were carefully cleaned in an ultrasonic bath containing acetone to eliminate possible remnants of fine powder attached to their surfaces.

In vitro dissolution experiments of the bioactive glasses (I)

The particle size range (300-500 µm) was utilized to evaluate the bioactivity of the prepared glasses *in vitro.*

The static dissolution test was performed by immersing the above-specified glass particles size in 100 mg/mL^{-1} SBF, which was prepared according to Kokubo protocol (Kokubo et al., 1990). The containers containing the glass samples were settled in a shaking incubator at 37 ºC for 48 hours. Then, the glass particles' reaction was ceased by separating from the SBF and then washing in acetone. The ionic products dissolved from the glasses into SBF were calculated utilizing an inductively coupled plasma-atomic emission spectrometer (ICP-OES, Optima 5300 DV, Perkin Elmer). Eventually, triplicate pH measurements of the solution were obtained at 37 ºC at 2, 10, 30, 60, and 120 minutes.

The dynamic dissolution tests were carried out utilizing continuous SBF fed at 0.2 mL/minute via a bed of glass particles in the size range specified above. A coupled plasma optical emission spectrometer (Optima 5300 DV, Perkin Elmer) was used for the calculations. The concentration of ions released from the BAG particles was calculated using ICP-OES for 50 hours.

4.2 Surface treatments of titanium discs

Grade-1 commercially pure titanium (study I) and Ti-6Al-4V ($\alpha + \beta$) titanium alloy (studies II, III, and IV) square-shaped discs (thickness 1mm and size 10x10 mm) were used as substrates.

4.2.1 Titanium discs polishing (I)

The titanium discs were first polished with silicon carbide papers with grit size ranges from 1200 to 4000. An ultrasonic bath containing acetone was used to eliminate the possible carbide paper residuals. Finally, the titanium discs were washed in distilled water and left to dry at room temperature for 1 hour.

4.2.2 Titanium discs sandblasting and acid-etching (II-IV)

The sandblasting and acid-etching surface treatment process was performed in-house. Ti-6Al-4V (α + β) titanium alloy sheets were cut to make square discs of 1 cm and a thickness of 1mm. The sandblasting process was carried out using large grit (250-500 µm) aluminum oxide particles utilizing 5 bar compressed air pressure. Each titanium disc was subjected to sandblasting at a 4 mm distance from the sandblaster nozzle for 20 seconds. After sandblasting, discs were acid-etched using an acid mixture containing HCl (60 %) and H_2SO_4 (70 %) in an oven at 60 °C for 1 hour. Afterward, the sandblasted and acid-etched (SA) titanium discs were cleaned in an ultrasonic bath containing deionized water to remove acid remnants. The discs were further cleaned in distilled water and returned to the oven to dry at 50 °C for 30 minutes (Figure 4).

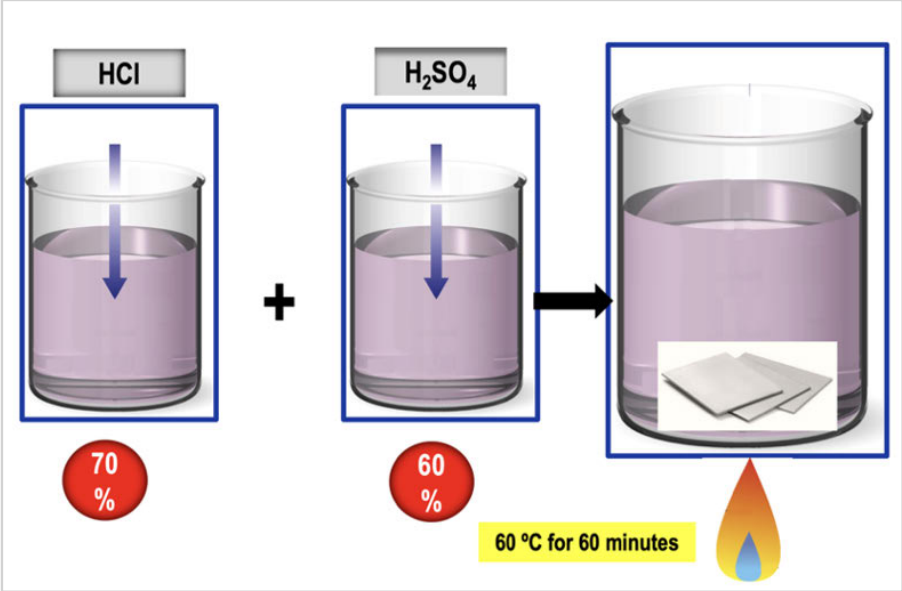

Figure 4. An illustration of the titanium discs acid-etching process

4.2.3 Air particle abrasion of titanium discs with bioactive glasses (I-IV)

The BAG air-abrasion of titanium discs (studies I and III) and the titanium discs with bacterial biofilm (studies II and IV) was executed using an air abrasive machine (LM ProPower, Parainen, Finland). In the first study (I), particle size used for air-abrasion was in the range of 25-120 µm, whereas 45-120 µm particle size was used for studies II-IV. For each disc, the air-abrasion procedure, utilizing the BAG/inert glass particle, was carried out using 4 bars air pressure, from a distance of 3 mm, at 90° angle, and for 20 seconds. The air-abrasion of titanium discs was carried out in a fume hood.

4.3 Surface characterization of titanium substrates

4.3.1 Scanning electron microscopy and Energy-dispersive X-ray spectroscopy (I-IV)

In order to evaluate the retention of abrasive glass particles on the abraded smooth titanium surface, the substrates were air-abraded using 45S5 BAG followed by cleaning in ultrasonic bathing containing water for 15 minutes. SEM- Energy-dispersive X-ray spectroscopy (EDS) (LEO Gemini 1530 with a Thermo Scientific UltraDry Silicon Drift Detector) was used to examine the matching spots on the substrate surfaces before and after ultrasonic bathing.

Before SEM imaging, the substrates were rinsed in deionized water 3 times and then fixed in 2.5 % glutaraldehyde overnight. Afterward, the substrates were dehydrated using graded ethanol series (50 %, 70 %, 85 %, 95 %, and 100 %). Subsequently, the SA substrates, with biofilm and after glasses air-abrasion, were sputter-coated with carbon utilizing Emscope TB 500 Temcarb (Thermo VG, Waltham, Massachusetts, USA). EDS analysis and SEM images were acquired using scanning electron microscopy (LEO Gemini 1530, Carl Zeiss, Hamburg, Germany).

4.3.2 Surface roughness test (III)

The surface roughness was estimated by calculating the Ra values of SA titanium substrates and after BAG or inert glass air-abrasion using a tester device (Leitz Wetzlar 601908, Wetzlar, Germany). The results were the mean of 5 measurements for each specimen.

4.3.3 Surface wettability test (III)

Contact angle measurements

The wettability of SA titanium disc surfaces and after air-abrasion using 45S5 BAG, Zn4 BAG, or inert glass was evaluated by the water CA method explained by de Jong et al. (1982). The surface CA was calculated using the sessile drop method with a contact angle meter (Theta, Biolin Scientific Oy, Espoo, Finland). In this procedure, a droplet of distilled water is placed on the studied surface, and then 120 images are recorded in 20 seconds. The CA measurements were expressed as the mean value of 120 contact angle calculations of 6 water drops on each substrate. The young-Laplace equation was used to define the contact angle and surface tension. The tests were performed with 5 replicates.

Surface free energy calculations

Owens-Wendt's (OW) approach was used to calculate the SFE of SA titanium discs before and after 45S5 BAG, Zn4 BAG, or inert glass air-abrasion. According to the OW method, the SFE (γ_S) of solid material is the total of a short-range polar (γ^P) and a long-range dispersion (γ^d) component. (γ^P) is a total of hydrogen, acidic/basic, and induction interactions, while (γ^d) determinates the strength of intermolecular interactions. Distilled ultrapure water, Diiodomethane >99 % purity, and Formamide pro analysis were utilized as a probe to determine the SFE of the titanium substrates using the sessile drop method. The tests were performed with 5 replicates.

The following equation is used:

$$1 + \cos\emptyset = 2\left(y_s^d\right)^{1/2}\left(\frac{\left(y_L^d\right)^{1/2}}{yL}\right) + 2\left(y_s^P\right)\left(\frac{\left(y_L^P\right)^{1/2}}{yL}\right)$$

∅ refers to the contact angle between the tested surface and the liquid, y_s is the SFE of the surface, and yL is the SFE the liquid. The tests were performed with 5 replicates.

4.4 Bacterial biofilm experiments on the titanium discs

4.4.1 *S. mutans* biofilm (I, II)

Antimicrobial activity test (I)

In this test, the capacity of titanium air-abraded substrates to prevent *S. mutans* growth was evaluated. The polished grade I titanium substrates were subjected to air-abrasion using 45S5, Zn4, Zn6, or Zn4Sr8 BAGs, and E-glass was used as a negative control. The air-abrasion procedure was performed using the method described earlier (chapter 4.2.3). The titanium substrates were disinfected by immersion in 70 % ethanol for 1 hour and then transferred to a 24-well cell culture plate. The formation of *S. mutans* biofilm on the titanium discs was performed by first coating the substrates with 1 ml pasteurized whole saliva diluted with (1:3) phosphate-buffered saline (PBS) at 37 °C for 30 minutes. Brain Heart Infusion (BHI) medium (Becton-Dickinson, Sparks, MD, USA) was used to grow the reference strain *S. mutans* Ingbritt. The bacterial cells were then centrifuged (5000 x g) for 10 minutes, followed by their suspension in a fresh BHI medium containing 0.03% sucrose to increase the glucan binding protein and thus glucosyltransferase of the

bacterial cells. Subsequently, 12 µl of the above *S. mutans* suspension was pipetted on the substrates in a 24-well cell culture plate. The wells containing the substrates were incubated in an anaerobic atmosphere at 37 °C for 4 hours (Don Whitley Scientific Ltd., Shipley, UK). Then, the biofilm-covered titanium substrates were transferred to wells containing 1 ml PBS. Afterward, the viable *S. mutans* cells on the substrate surfaces were collected using micro brushes (Quick-Stick, Dentsolv AB, Saltsjö-Boo, Sweden) and dispersed with mild sonication. The suspensions containing *S. mutans* cells were diluted and plated on Mitis Salivarius Agar (Becton-Dickinson and Company) then grown in an anaerobic chamber at 37 °C for 3 days. A stereomicroscope was used to count the bacterial colonies (CFU). The tests were performed with 4 replicates.

Biofilm experiment (I)

This test was conducted to evaluate the ability of BAG abraded titanium substrates to prevent *S. mutans* biofilm formation on titanium substrates after air-abrasion using 45S5 BAG, Zn4 BAG, Zn6 BAG, Zn4Sr8 BAG, or E-glass. *S. mutans* Ingbritt was grown in BHI as described earlier and then washed and suspended in BHI containing 1% sucrose. The resultant bacterial suspension was additionally diluted 1:50, 2 ml was then applied onto the glass abraded substrate in 24-well cell culture plates. The substrates were then incubated at 37 °C in an anaerobic incubator for 24 hours. The biofilm collection and bacterial cell culturing were conducted, as explained earlier. The tests were performed with 4 replicates.

Adhesion test (I)

This test was conducted to examine the adhesion of *S. mutans* cells to titanium substrates after being subjected to air-abrasion using 45S5 BAG, Zn4 BAG, Zn6 BAG, Zn4Sr8 BAG, or E-glass. The *S. mutans* Ingbritt was grown overnight in BHI, washed, and then suspended in PBS, A550 = 0.35. The BAG abraded substrates were rolled in the bacterial suspensions for 30 minutes. Afterward, the substrates were washed 3 times in PBS, and then the bacterial cells were collected from their surfaces using brush applicators. The applicator ends used to scrape the cells were cut and then transferred into a 0.5 ml Tryptic Soy Broth (TSB; Sigma Chemical). Culturing the suspension was performed as described earlier. The test was performed with 5 replicates.

Air-abrasion of *S. mutans* biofilm formed on SA titanium surface (II)

This test was performed to investigate the effect of BAG air-abrasion on *S. mutans* biofilm formed on SA titanium surfaces. The SA titanium substrates were covered with *S. mutans* biofilm as described earlier and incubated for 21 hours. After incubation, the substrates were immersed in 1 ml PBS and then subjected to air-abrasion using 45S5 BAG, Zn4 BAG, or inert glass by the method described earlier (chapter 4.2.3). The substrates were then transferred to cell culture plates containing 2 ml fresh BHI and incubated at 37 °C for 5 hours. Following incubation, bacterial cells were scraped from the surfaces of the substrates as described earlier and then cultured in anaerobic conditions at 37 °C for 3 days. A stereomicroscope was used to count the bacterial colonies (CFU). The test was performed with 5 replicates.

4.4.2 *F. nucleatum* and *P. gingivalis* dual biofilm (IV)

In this dual biofilm experiment, the pathogenic bacterial strains *F. nucleatum* type strain (ATCC 25586; American Type Culture Collection) and clinical strain of *P. gingivalis* (AHN 24155; the Finnish Institute for Health and Welfare) were used. The microorganisms were transferred to TSB (Sigma Chemical) enriched with hemin (5 mg/l) and menadione (5 mg/l). The bacteria were then cultured in an anaerobic environment overnight at 37 °C (10 % H_2, 5 % CO_2, and 85 % N_2); (Whitley A35 Anaerobic Workstation; Don Whitley Scientific).

Following incubations, the bacterial suspensions were adjusted to the optical density (OD) 0.5 at 490 nm equivalent to $4x10^7$ CFU/ml for *F. nucleatum* and $1.4x10^7$ CFU/ml for *P. gingivalis*. The SA titanium substrates were placed in 24-well culture plates and then coated with 1:3 PBS diluted pasteurized saliva at 37 °C for 30 minutes. After coatings, the substrates were washed with PBS and placed in new wells. Equivalent amounts (2×10^7 CFU/ml) of the bacterial suspension were pipetted on the substrates and then incubated in an anaerobic atmosphere at 37 °C for 70 hours. After incubation, the titanium substrates were rinsed with PBS to remove non-adherent cells.

Then, the titanium substrates covered with *F. nucleatum* and *P. gingivalis* biofilm were subjected to air-abrasion using 45S5 BAG, Zn4 BAG, or inert glass, as described earlier (chapter 4.2.3). Following the air-abrasion, the substrates were immediately placed in cell culture plates containing 2 ml of fresh TSB enriched with hemin (5 mg/ml) and menadione (5 mg/ml). The substrates were then incubated at 37°C for 23 hours under anaerobic conditions. After the incubation, the titanium substrates were washed in PBS, and the biofilm was collected using 4 micro brushes by the method described earlier. The tips of the brushes per substrate were placed into a sterile Ebbendorf tube containing 500 µl of TSB enriched with hemin (5 mg/l) and menadione (5 mg/l). The obtained suspensions were sonicated and serially

diluted to 10 folds. The suspensions were then cultured on enriched Brucella agar plates and incubated in an anaerobic environment at 37 °C for 7 days. Following incubation, the *F. nucleatum* and *P. gingivalis* count on the Brucella agar plates were calculated using a light microscope (Leica Microsystems, Wetzlar, Germany). The test was performed with 5 replicates.

4.5 Thrombogenicity and blood response (II)

Blood clotting measurement

In this test, SA titanium substrates with *S. mutans* biofilms were air-abraded using 45S5 BAG, Zn4 BAG, or inert glass by the method described earlier (chapter 4.2.3). Then, the titanium substrates' thrombogenic properties were assessed using fresh human whole blood by the kinetic clotting time method (Abdulmajeed et al., 2014; Imai & Nose, 1972). Disposable syringes were used to withdraw fresh blood from a healthy female volunteer. The first 3 ml of the drawn blood was discarded to avoid possible thromboplastin contamination due to needle puncture. The titanium substrates were placed in 12-well cell culture plates, and 0.1 ml of blood was pipetted on each substrate's surface. After a preplanned time of 10, 20, 30, 40, and 60 minutes, 3 ml of distilled water was gently pipetted into each well.

After 5 minutes of adding the distilled water, three samples were obtained from each well and then pipetted to a 96-well plate. The free hemoglobin concentration lysed from the red blood cells to the distilled water was measured colorimetrically using a spectrophotometer at 570 nm absorbance. The test was performed with 5 replicates.

4.6 Osteoblast cell cultures (III)

In this test, pre-osteoblastic MC3TC-E1 cells (subclone IV, ATCC. LCG Promochem, Manassas, Virginia) were used to study the effect of BAG/inert glass air-abrasion on their viability and proliferation. The cells were cultured in alpha Minimum Essential Medium (α-MEM) (Corning, New York, USA) containing 10 % fetal bovine serum (FBS) (Biowest, Nuaillé, France), 1 % penicillin/streptomycin, and 1 % l-glutamine (Gibco, Waltham, Massachusetts, USA). Passaging the cells was performed on an alternate day. The cells were then detached with 0.5 % trypsin-EDTA (Gibco, Waltham, Massachusetts, USA). SA titanium substrates without BAG air-abrasion and after BAG (45S5 and Zn4) or inert glass air-abrasion were used in this test. After their disinfection, the substrates were placed in well-culture plates and MC3TC-E1 cells were seeded at a density of 5×10^3 cells/ml per well.

Cover glasses were used as controls. The experiments were performed with 4 replicates.

4.6.1 Cell proliferation and viability test

In this test, the viability and proliferation of the pre-osteoblast cells on the surfaces of the substrates were determined by counting the cells at 1, 3, and 6 days after culturing. An MTT (3-(4,5-dimethylthiazol-2-yl)-2,5 diphenyltetrazolium bromide) assay was used. The substrates were transferred to a new medium containing 0.1 mg/ml MTT and then incubated at 37 °C for 3 hours. An absorbance value of 550 nm was quantified using a plate reader (Victor 2, PerkinElmer Life Science/Wallac, Turku, Finland). Then the result was background-corrected by measuring the absorbance at 650 nm due to the Phenol Red, which is included as a pH indicator in colored culture media.

4.6.2 Preparation of the cell culture substratess for microscopy

For preparing the substrates for fluorescence microscopy, the pre-osteoblast cells were cultured on titanium substrates for 2, 24, and 48 hours. After culturing, the cells were fixed in a 3 % paraformaldehyde (PFA) solution at room temperature for 10 minutes. Afterward, the cells were permeabilized utilizing 0.1% TritonX-100 in PBS (10 minutes on ice) and blocked with 0.2 % bovine serum albumin at room temperature for 30 minutes. Then, the substrates were washed with PBS, and the cells' actin cytoskeleton was stained using 1:200 diluted TRITC-phalloidin (Sigma) at 37 °C for 3 hours. The nuclei of cells were stained using 1:800 diluted Hoechst at room temperature for 10 minutes. The images were captured by a confocal laser scanning microscope (CLSM) (Zeiss LSM 750 Meta Oberkochen, Germany) using a 63x objective.

For preparing the substrates for Field Emission-Scanning electron microscopy (FE-SEM), the titanium substrates were fixed in 2.5 % glutaraldehyde for 15 minutes. After ethanol dehydration, the substrates were coated with 5 nm of platinum (Q150T ES, Quorum Technologies, UK) and then visualized in Σigma HD VP SEM (GmbH, Oberkochen, Germany).

4.6.3 Cell shape aspect ratio

Image-J 1.52 software (Fiji collection) was used to analyze the cells; number, surface area, and shape at 14x magnification (6144x4608 pixels). Cell counter plugin was

used to calculate 5.55 mm^2 ROI. Shape descriptors plugin was utilized to analyze the cell area and aspect ratio after the cell parameters were manually traced.

4.7 Statistical analysis

Statistical Package Software (SPSS. Inc., Chicago, II, USA) versions 23.0 and 25.0. were used for the statistical analysis.

The statistical significance between the experimental groups was analysed using ANOVA followed by Tukey's post-hoc test. If the distribution of the parameters were skewed, logarithmically transformed values were used. Differences were considered significant at 95 %, 99 % and 99.9 % confidence levels, with p-values below 0.05 ($p < 0.05$, $p < 0.01$, and $p < 0.001$ respectively).

5 Results

5.1 *In vitro* bioactive glasses dissolution results (I)

The ion concentrations released into SBF were evaluated in continuous and static flow conditions. In the continuous condition, maximum values of ions released into SBF were observed during the first 30-60 minutes of immersion. BAG 45S5 demonstrated ions concentrations of 41 mg/L for Si and 126 mg/L for Ca^{2+}. At 48 hours, the concentration of Si and Ca^{2+} decreased to 16 mg/L and 66 mg/L, respectively. The concentration of ions released from the experimental ZnO-containing glasses was considerably less. Their ranges were 5-10 mg/L for Si, 60-100 mg/L for Ca, and 0.01-0.2 mg/L for Zn. The concentrations were steady to relatively constant levels (Table 2).

In the static condition, the concentration of Si was higher (58 mg/mL) for 45S5 BAG compared to 30 mg/mL, 33 mg/mL and 37 mg/ml for Zn4, Zn6 and Zn4Sr8 BAGs respectively. Similarly, the Ca^{2+} concentration was 200 mg/mL for 45S5BAG in comparison with 149 mg/mL, 152 mg/mL and 130 mg/mL for Zn4, Zn6 and Zn4Sr8 BAGs respectively. The Zn^{2+} concentrations were relatively low at 48 hours, whereas comparatively high Sr^{2+} was seen for Zn4Sr8 (Table 2).

Table 2. The ion concentration (mg/L) released from 45S5 BAG and the Zn-containing BAG into simulated body fluid (SBF) in static and continuous flow conditions. The relative ± SD of the concentrations is around 5 %. (C = continuous flow condition; S = static flow condition). Modified from the original publication I.

Glass	Si (mg/L)			Ca (mg/L)			Zn (mg/L)			Sr (mg/L)		
Code	C		S	C		S	C		S	C		S
Time (h)	2	48	48	2	48	48	2	48	48	2	48	48
45S5	41	16	58	126	66	200	-	-	-	-	-	-
Zn4	5	6	30	83	70	149	0.2	0.2	0.04	-	-	-
Zn6	5	6	33	85	94	152	0.01	0.05	0.06	-	-	-
Zn4Sr8	9	6	37	82	67	130	0.01	0.05	0.01	7	5	68

The change in the SBF pH following immersion of BAG particles was assessed in static dissolution conditions at specific time points (Figure 5). BAGs 45S5 and Zn6 showed the highest rise in the pH ($p<0.001$) during the first 2 minutes of immersion. Subsequently, the 45S5 BAG displayed a linear elevation in the pH and demonstrated a value close to 9 at 120 minutes. BAG 45S5 showed a significantly higher increase in the pH than the other investigated BAGs ($p<0.001$). The pH for all Zn/Sr-containing BAGs remained on the same level following the initial increase at 2 minutes; however, Zn6 showed significantly higher pH at all time points than the other investigated experimental BAGs ($p<0.001$).

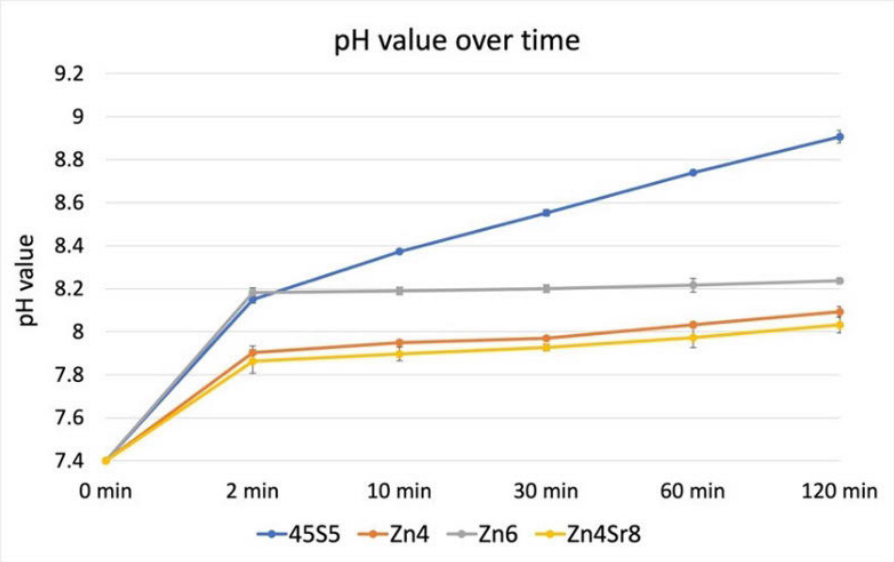

Figure 5. Mean (±SD) of the simulated body fluid (SBF) pH values following BAG particles immersion measured at six time points over 120 minutes. Statistical analysis was performed by means of ANOVA. At the first 2 minutes of immersion, 45S5 and Zn6 BAGs showed the highest pH increase ($p<0.001$). Afterward, at 120 minutes, 45S5 BAG demonstrated a significantly higher pH value than the Zn-containing glasses ($p<0.001$). The pH level was relatively similar for the three Zn-containing glasses, yet Zn6 BAG demonstrated a significantly higher pH value than Zn4 and Zn4Sr8 BAGs ($p<0.001$). Modified from the original publication I.

5.2 Surface characterization of titanium substrates

5.2.1 Scanning electron microscopy and Energy-dispersive X-ray spectroscopy (I, III)

SEM-EDS analysis of smooth surface titanium substrates after BAG particle air-abrasion showed that glass particles were firmly attached to the substrate surfaces. Placing the BAG air-abraded substrates in the ultrasonic bath for 15 minutes did not affect the retention of glass particles fixed to their surfaces (Figure 6). Figure 7 also demonstrated the presence of glass particles used for air-abrasion on the abraded surfaces. The particles remained embedded inside the SA surface pores, as confirmed by EDS analysis (Figure 7).

Figure 8 shows SEM images of SA titanium substrate before and after air-abrasion using BAG/inert glass. The sandblasting and the acid-etching process of titanium substrates resulted in evident surface irregularities at macro-and micro-scale levels (Figure 8A). After BAG/inert glass air particle abrasion, the SA surface topography altered and demonstrated smoother surface topography (Figure 8B-D).

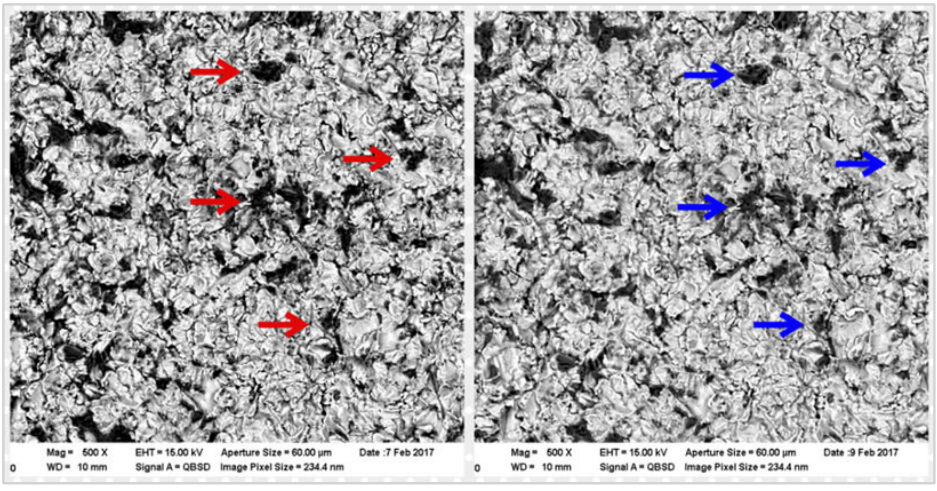

Figure 6. SEM image illustrating the retention of 45S5 bioactive glass particles to the disc surface. Red arrows indicate randomly selected glass particles before ultrasonic bathing.; blue arrows indicate the identical particles after 15 minutes of ultrasonic bathing. Image magnification: 600x Modified from the original publication I.

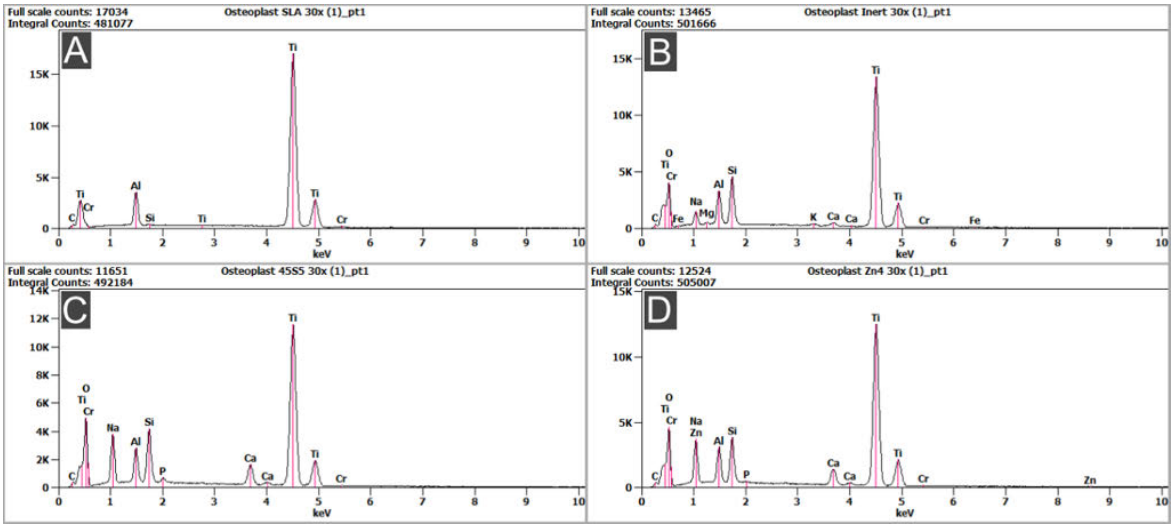

Figure 7. Energy dispersive X-ray spectroscopy (EDS) analysis of sandblasted and acid-etched (SA) substrates (**A**), after their air-abrasion utilizing inert glass (**B**), 45S5 BAG (**C**), and Zn4 BAG (**D**). Modified from the original publication III.

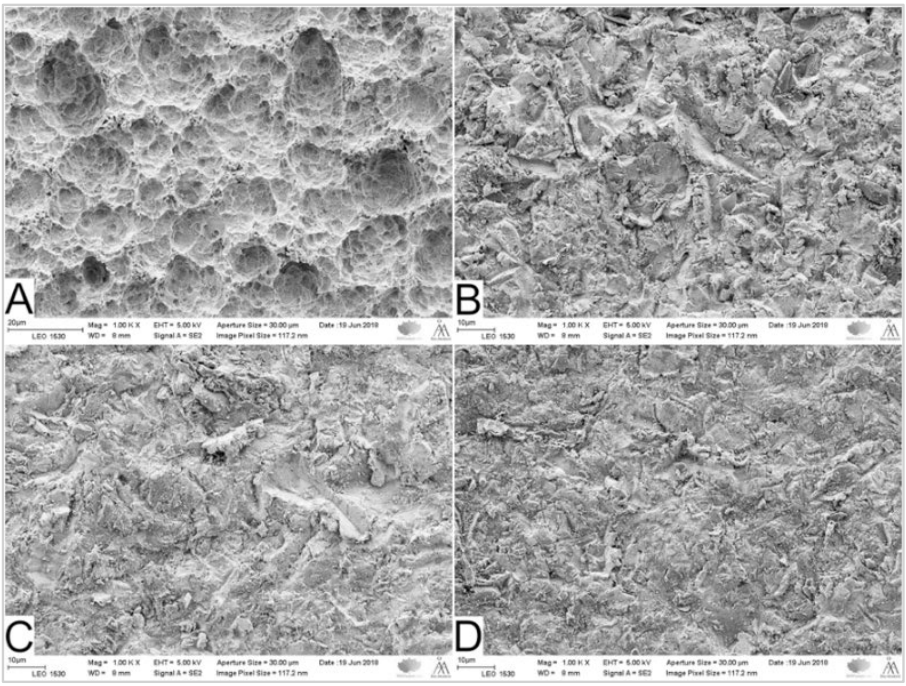

Figure 8. SEM images of the in house produced sandblasted and acid-etched (SA) titanium substrate (**A**). After air-abrasion utilizing inert glass (**B**), 45S5 BAG (**C**), and Zn4 BAG (**D**). Magnification: 1KX. Modified from the original publication III.

5.2.2 Surface roughness assessment (III)

The results of the surface roughness test demonstrated that the air-abrasion using either BAG or inert glass yielded a significant reduction in the SA surface roughness ($p<0.001$). However, no significant differences were observed in surface roughness values between the air-abraded substrates (Figure 9).

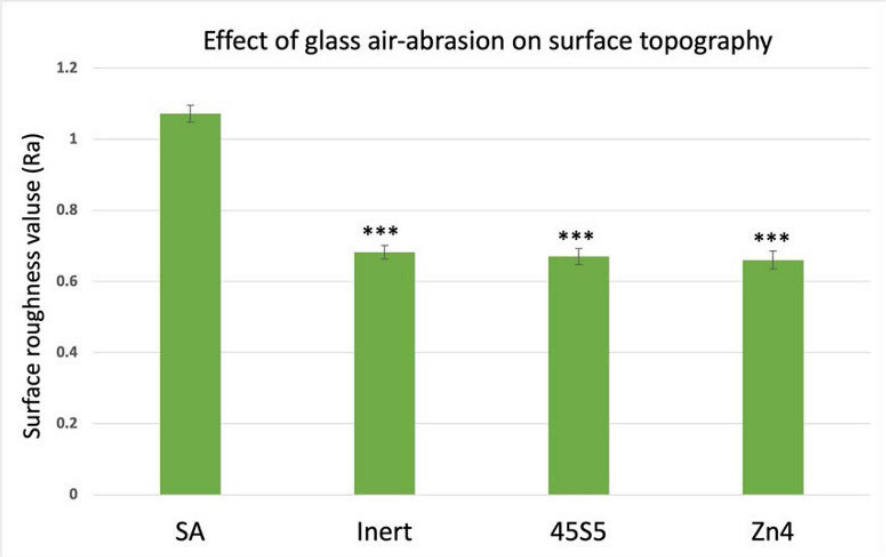

Figure 9. Mean (±SD) of surface roughness of sandblasted and acid-etched (SA) titanium discs, before and after air-abrasion with inert glass, 45S5 BAG or Zn4 BAG. Statistical analysis was performed with ANOVA, ***$p < 0.001$. Modified from the original publication III.

5.2.3 Surface wettability (III)

Contact angle measurements

Figure 10 shows the values of CA measurement for the SA titanium substrates before and after BAG/inert glass air-abrasion. A significantly higher water CA value (113.4°) was observed for the non-abraded SA substrates than the other groups. Glass particle air-abrasion of the SA discs significantly lowered the surfaces' CA, which resulted in hydrophilic surfaces ($p<0.001$). Zn4 BAG abraded discs had the lowest mean water CA (10.5°). The air-abrasion using 45S5 BAG or inert glass resulted in CA values of (14.7°) and (19.3°), respectively indicating less hydrophilicity.

Surface free energy calculations

Figure 11 illustrates the SFE values for SA titanium substrates and after BAG/inert glass air-abrasion. Significantly higher total (γ^{tot}) and polar (γ^{p}) SFE components

were observed for the glass air-abraded substrates compared to SA discs ($p<0.001$). However, the dispersive(γ^d) SFE component was not significantly different between substrates ($p = 0.413$).

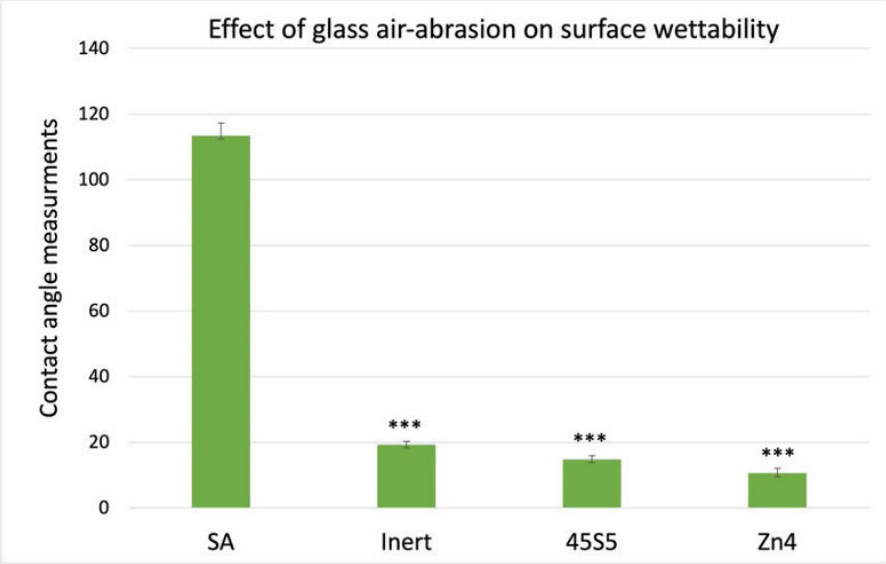

Figure 10. Mean (±SD) of water contact angle (CA) on sandblasted and acid-etched (SA) titanium substrates before and after air-abrasion with inert glass, 45S5 BAG or Zn4 BAG. Statistical analysis was performed with ANOVA, ***p<0.001. Modified from the original publication III.

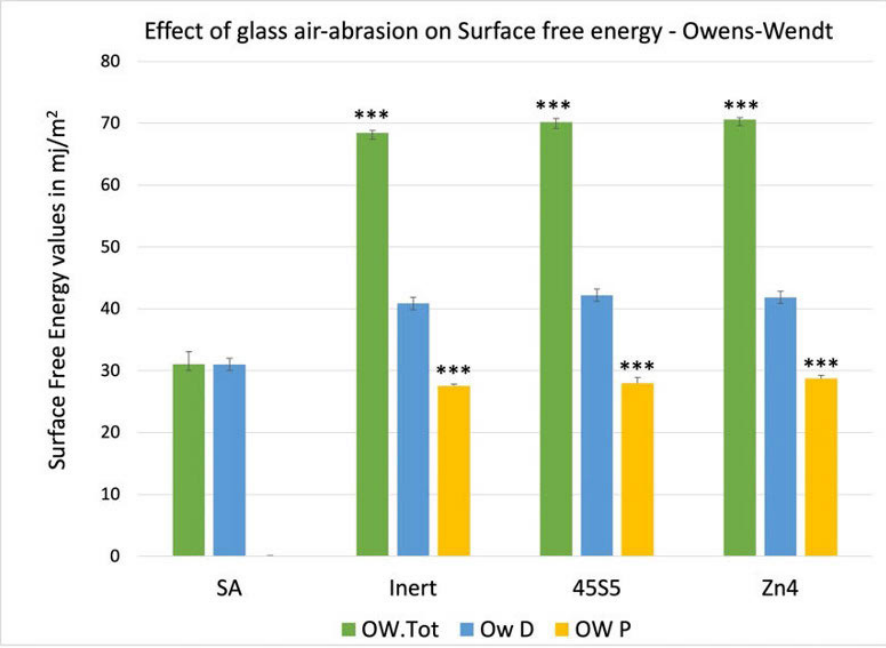

Figure 11. Mean (±SD) of total (OW.Tot), dispersive (OW.D) and polar (OW.P) surface free energy (SFE) on sandblasted and acid-etched (SA) titanium substrates before and after their air-abrasion with inert glass, 45S5 BAG or Zn4 BAG. Significantly higher OW.Tot and OW P was observed for the glass air abraded substrates. Statistical analysis was performed with ANOVA, ***p<0.001. Modified from the original publication III.

5.3 Biofilm eradication experiments (I, II, IV)

5.3.1 *S. mutans* biofilm results

Antimicrobial activity and biofilm (I)

A substantial decrease in the viable *S. mutans* cells was seen for titanium substrates subjected to air-abrasion with 45S5, Zn4, Zn6, and Zn4Sr8 BAGs than the control E-glass ($p<0.001$) (Figure 12). However, no significant differences were observed among the experimental BAGs. The number of viable S. *mutans* cells was the lowest for Zn4 BAG (18 ± 2), but the difference was not statically significant compared to Zn6 BAG (38 ± 18, $p = 0.748$), Zn4Sr8 BAG (58 ± 19, $P = 0.064$) and 45S5 BAG (28 ± 6, $p = 0.934$).

Furthermore, all investigated BAGs showed a significant reduction in biofilm formation on the surfaces of the substrates compared to E-glass ($p<0.01$; Fig. 13). Nevertheless, the *S. mutans* adhesion test demonstrated no differences in the bacterial adhesion between BAG and E-glass air-abraded substrates (Figure 14).

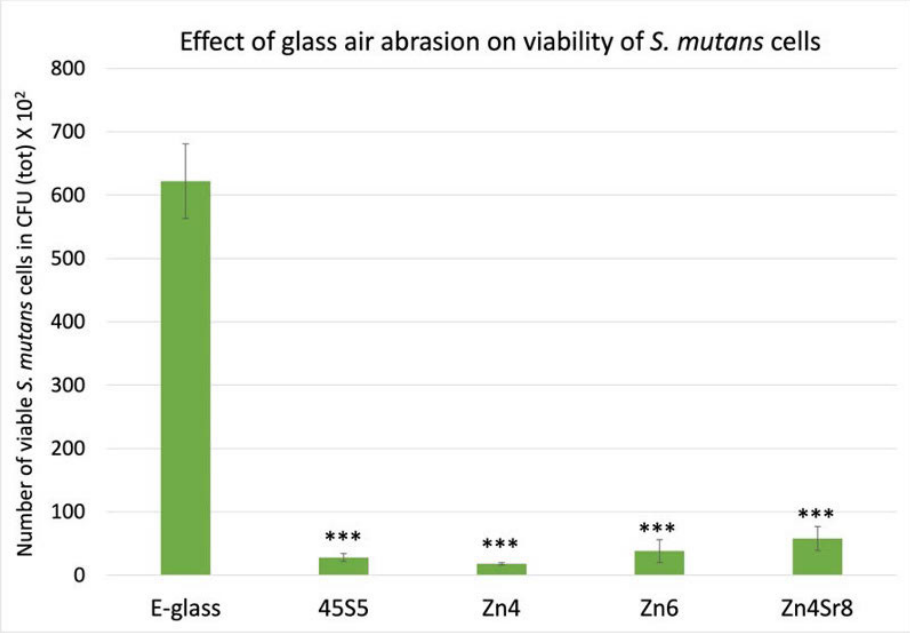

Figure 12. Mean (±SD) number of viable *S. mutans* cells on titanium substrates after E-glass or bioactive glasses (BAG) (45S5, Zn4, Zn6, Zn4Sr8) air-abrasion. Substrates were cultured for 4 hours and then subjected to air-abrasion, after which the cells were harvested from the substrate surfaces and cultured for 3 days. Significantly less viable *S. mutans* cells were found for substrates subjected to BAG air-abrasion compared to substrates air-abraded with E-glass. Statistical analysis was performed by means of ANOVA, ***$p<0.001$. Modified from the original publication I.

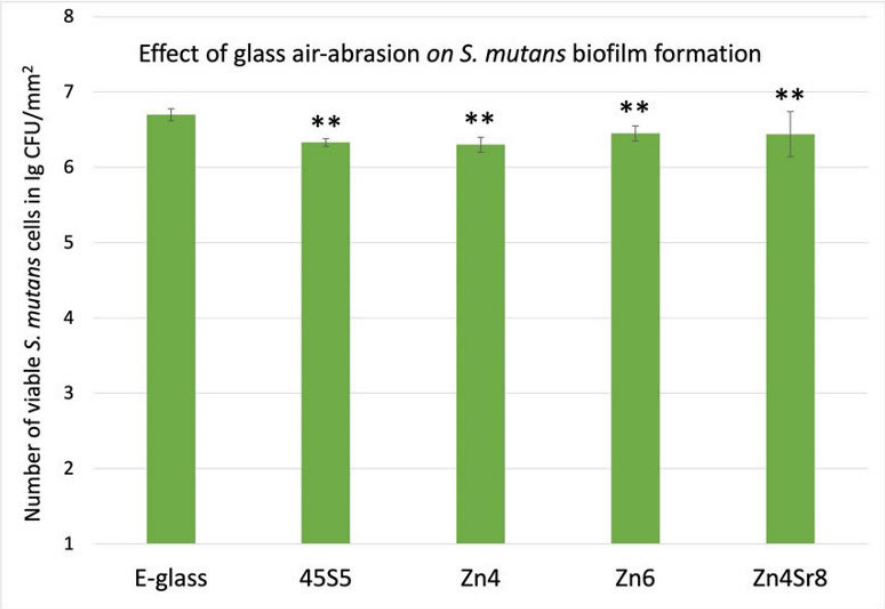

Figure 13. Mean (±SD) of *S. mutans* cells on E-glass or bioactive glasses (BAG) (45S5, Zn4, Zn6, Zn4Sr8) air-abraded substrates. Substrates were cultured for 24 hours and then cells were harvested from the substrate surfaces and cultured for 3 days. Significantly less *S. mutans* biofilm formed on substrates subjected to BAG air-abrasion compared to substrates air-abraded using E- glass. Statistical analysis was performed using ANOVA, **p<0.01. Modified from the original publication I.

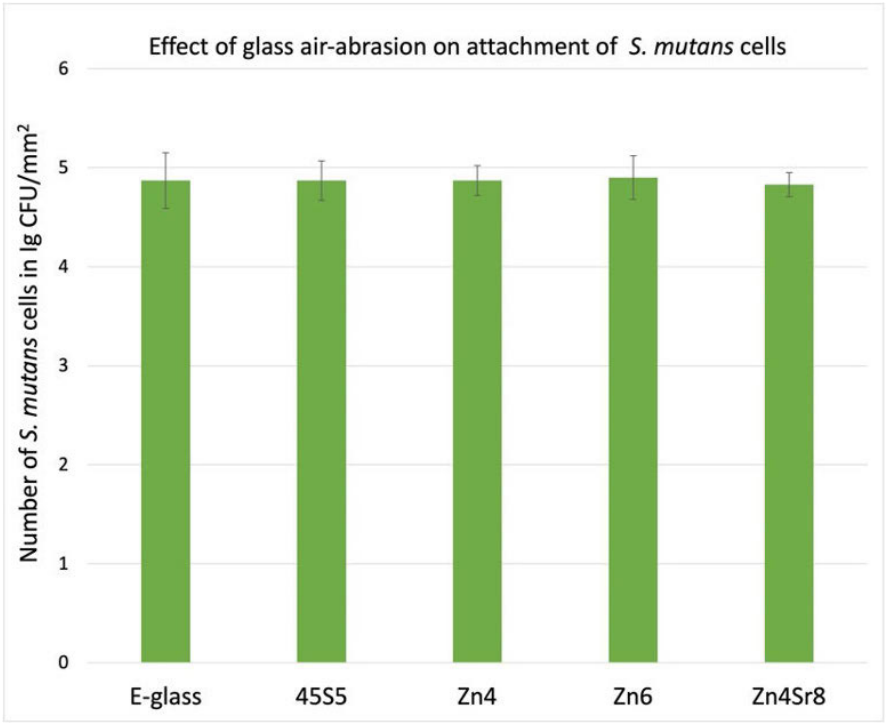

Figure 14. Mean (±SD) number of *S. mutans* cells adhered on E-glass or bioactive glasses (BAG) (45S5, Zn4, Zn6, Zn4Sr8) air-abraded substrates. Substrates were rolled in cell suspension for 30 minutes and then cells were harvested from the substrate surfaces and cultured for 3 days. Statistical analysis was performed using ANOVA. No statistically significant differences were observed among the tested groups. Modified from the original publication I.

Air-abrasion of *S. mutans* biofilm formed on SA titanium surface (II)

Air-abrasion of SA titanium substrates covered with *S. mutans* biofilm using 45S5 BAG, Zn4 BAG, or inert glass resulted in a significant decrease ($p<.001$) in the viable bacterial cells compared to non-abraded SA discs (intact biofilm). Furthermore, significantly less viable bacterial cells were observed on substrates subjected to Zn4 BAG and 45S5 BAG air-abrasion compared to inert glass air-abrasion (Figure 15). However, no bacterial cells could be detected from BAG or inert glass air-abraded substrates in the SEM image analysis. Images were captured at 5 random spots per sample. Figure (16-A) shows SA titanium substrate with *S. mutans* biofilm and (16-B-D) after BAG/inert glass air-abrasion.

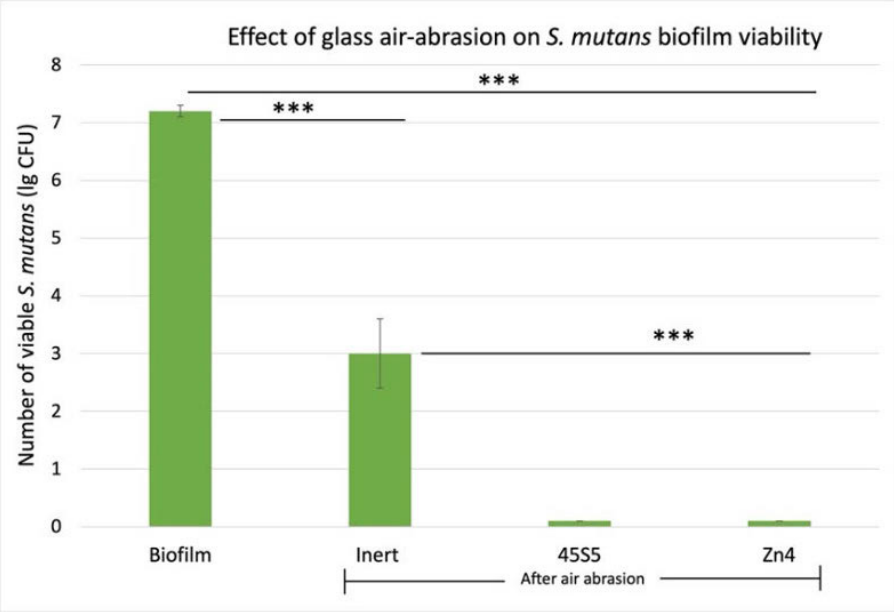

Figure 15. Mean (±SD) CFUs of viable *S. mutans* cells on BAG or inert glass air-abraded sandblasted and acid-etched titanium substrates. Substrates were cultured for 5 hours, and then cells were harvested from the substrate surfaces and cultured for 3 days. Significant reduction in the CFUs of viable *S. mutans* cells was observed for substrates subjected to glass air-abrasion. BAG air-abrasion resulted in a significant decrease in the CFUs of *S. mutans* cells compared to inert glass. Statistical analysis was performed using ANOVA, *** $p<.001$. Modified from the original publication II.

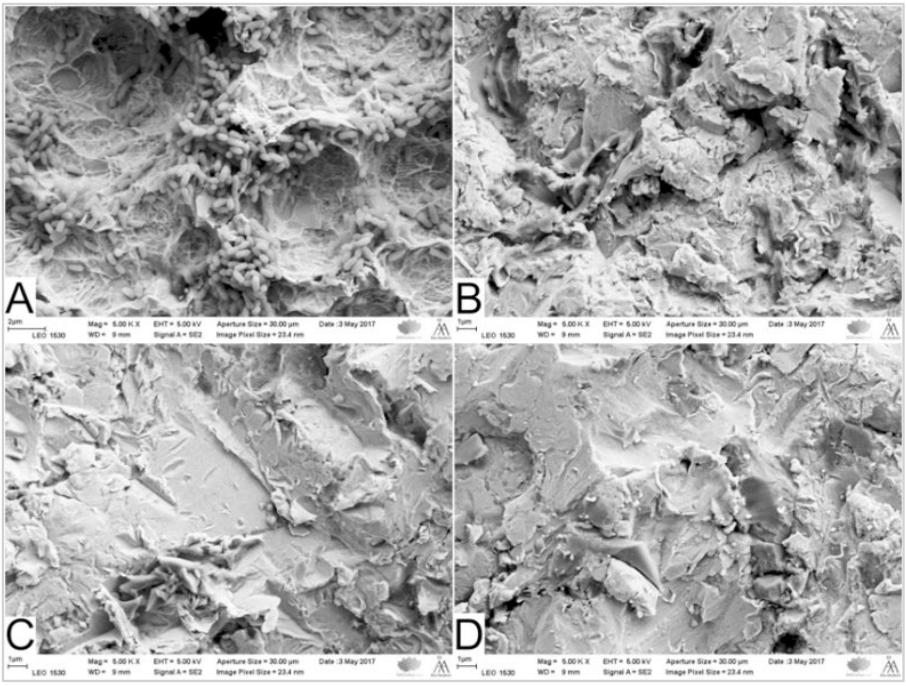

Figure 16. SEM images of sandblasted and acid-etched (SA) titanium substrates with *S. mutans* biofilm prior to air abrasion (**A**), and after air-abrasion utilizing inert glass (**B**), 45S5 BAG (**C**), and Zn4 BAG (**D**). Magnification: 5.0 KX. Modified from the original publication II.

5.3.2 *F. nucleatum* and *P. gingivalis* dual biofilm results (IV)

Air-abrasion of *F. nucleatum* and *P. gingivalis* dual *biofilm* formed on SA titanium surface

BAGs 45S5, Zn4, or inert glass air-abrasion resulted in a significantly lower total viable bacterial count (*F. nucleatum* and *P. gingivalis*; $p < 0.001$) compared to non-abraded biofilm (Figure 17). The air-abrasion using either 45S5 or Zn4 BAGs led to complete eradication of *P. gingivalis* compared with substrates subjected to air-abrasion with inert glass (Figure 18). Furthermore, inert glass air-abrasion resulted in a statistically significantly lower viable *P. gingivalis* count ($p < 0.001$) than observed for non-abraded substrates. Also, significantly lower viable *F. nucleatum* ($p = 0.011$) were seen for substrates exposed to BAG air-abrasion compared with those air-abraded using inert glass (Figure 19).

Figure 20 shows SEM images for the *F. nucleatum* and *P. gingivalis* biofilm after incubation for 70 hours (Fig 20A) and after 45S5 BAG, Zn4 BAG, or inert glass air-abrasion followed by culturing the substrates for 23 hours (Fig 20-BD). No *P. gingivalis* cells could be detected on substrates subjected to 45S5 or Zn4 BAGs air-abrasion from the SEM images examination, whereas *P. gingivalis* cells were present on substrates exposed to inert glass air-abrasion. The substrates' air-abrasion using either BAGs resulted in fewer *F. nucleatum* cells than in substrates subjected to inert glass air-abrasion.

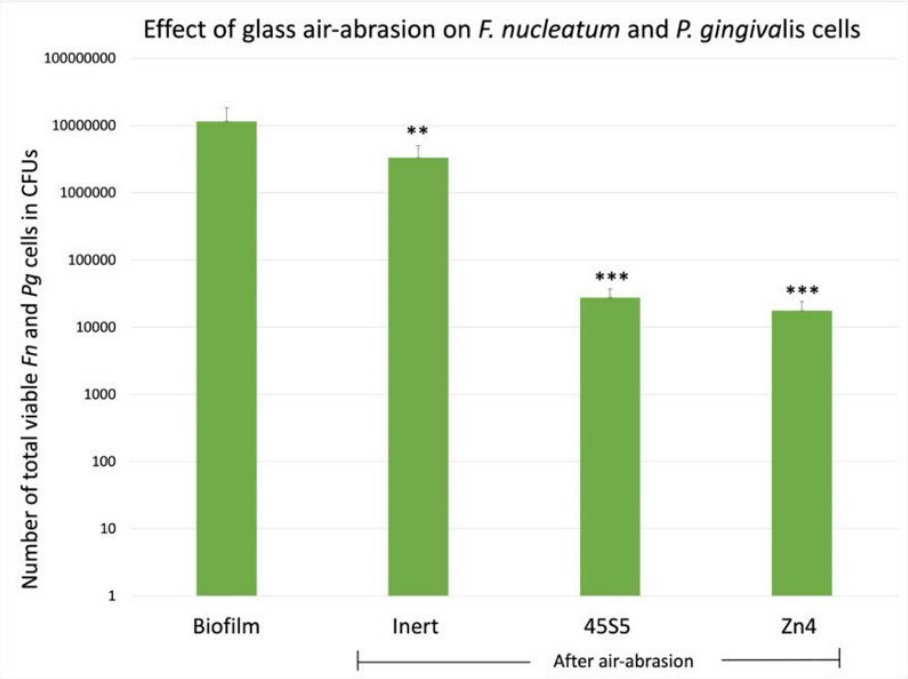

Figure 17. Mean(±SD) in colony forming units (CFUs) of total bacteria *F. nucleatum* (*Fn*) and *P. gingivalis* (*Pg*) on BAG or inert glass air-abraded titanium substrates compared to intact biofilm. Substrates were cultured for 23 hours and then cells were harvested from the substrate surfaces and cultured for 7 days. The y-axis is exhibited in logarithmic scale. Significant reduction in the viable *Fn and Pg* cells was observed for substrates subjected to glass air-abrasion. Statistical analysis was performed using ANOVA, **p<0.05, ***p<0.001. Modified from the original publication IV.

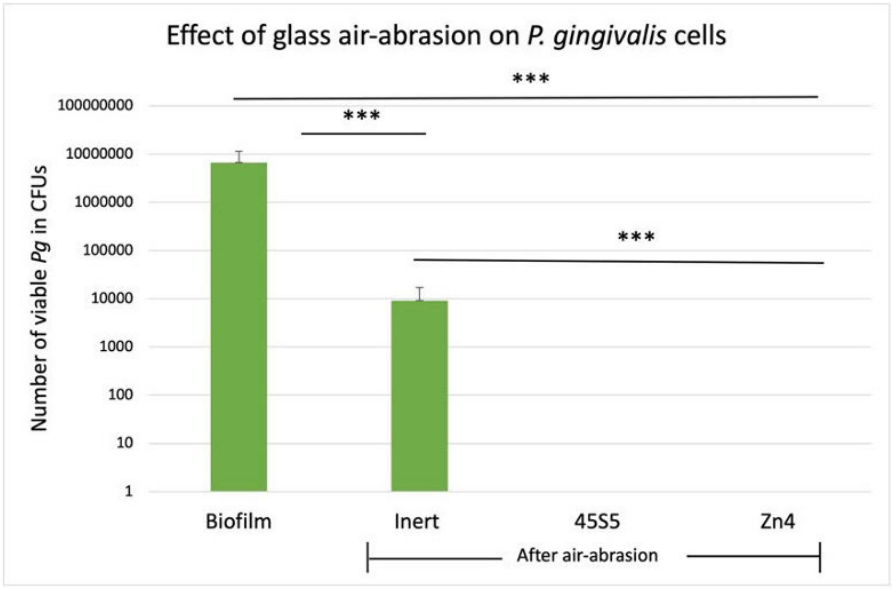

Figure 18. Mean (±SD) in colony forming units (CFUs) of *P. gingivalis* (*Pg*) on BAG or inert glass air-abraded titanium substrates compared to intact biofilm. Substrates were cultured for 23 hours and then cells were harvested from the substrate surfaces and cultured for 7 days. Significant reduction in the viable *Pg* cells was observed for substrates subjected to glass air-abrasion. The y-axis is exhibited in a logarithmic scale. Statistical analysis was performed using ANOVA, ***p<0.001. Modified from the original publication IV.

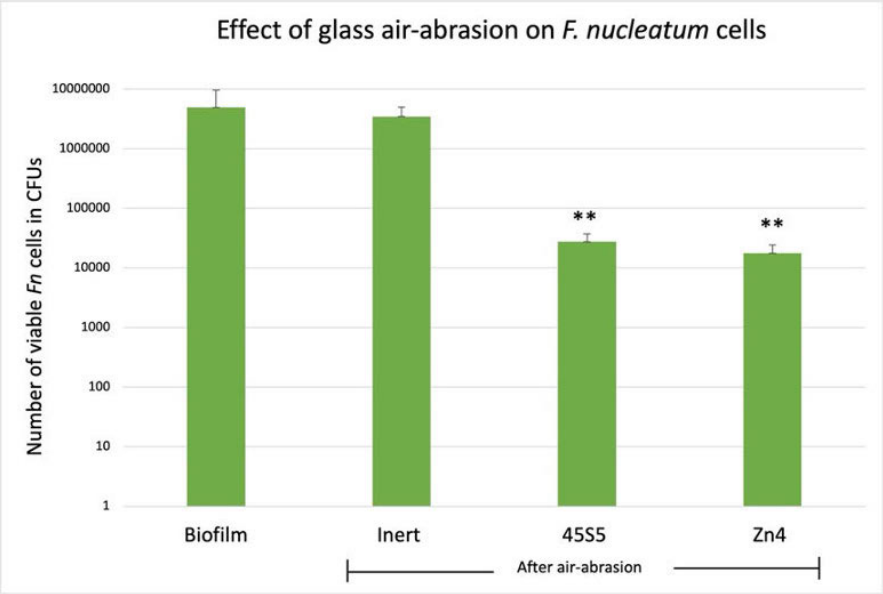

Figure 19. Mean (±SD) in colony forming units (CFUs) of total bacteria *F. nucleatum* (*Fn*) on BAG or inert glass air-abraded titanium substrates compared to intact biofilm. Substrates were cultured for 23 hours and then cells were harvested from the substrate surfaces and cultured for 7 days. Significant reduction in the viable *Fn* cells was observed for substrates subjected to BAG air-abrasion. The y-axis is exhibited in logarithmic scale. Statistical analysis was performed using ANOVA, **p<0.05. Modified from the original publication IV.

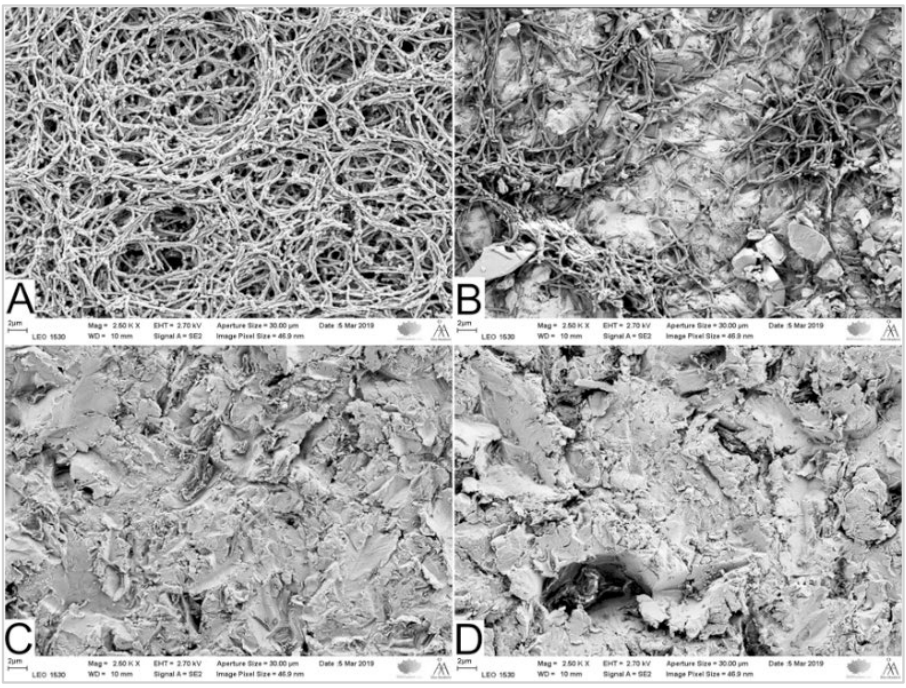

Figure 20. SEM images of sandblasted and acid-etched (SA) titanium substrates with a dual-species biofilm of *F. nucleatum* and *P. gingivalis*. Intact biofilm before air-abrasion (**A**), and after-air abrasion with inert glass (**B**), 45S5 BAG, 45S5 BAG (**C**), and Zn4 BAG (**D**). Magnification: 2.5 KX. Modified from the original publication IV.

5.4 Thrombogenicity and blood response (II)

Blood clotting

Figure 21 demonstrates the blood clotting profiles of the SA titanium substrates covered with *S. mutans* biofilm after their air-abrasion using 45S5 BAG, Zn4 BAG, or inert glass. The absorbance values of the hemolyzed hemoglobin in distilled water varied with time among groups. At 10 minutes, Zn4 BAG abraded substrates demonstrated significantly lower ($p<.001$) OD, indicating faster coagulation compared to 45S5 BAG or inert glass abraded substrates. Later, at 20 and 30 minutes, significantly lower OD was observed for inert glass abraded substrates than the BAG abraded substrates ($p<.001$). However, complete blood clotting was reached for all substrates in 40 minutes, at which OD value was > 0.1.

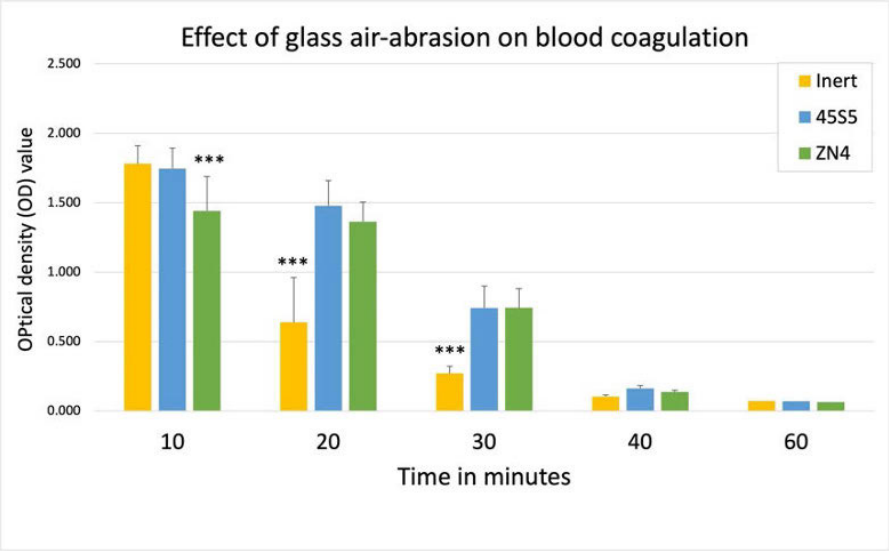

Figure 21. Mean (±SD) optical density (OD) vs time for SA titanium surface subjected to air-abrasion using Zn4 BAG, 45S5 BAG, or inert glass. Significantly faster blood coagulation was observed for Zn4 at minute 10. At minutes 20 and 30, inert glass demonstrated significantly faster blood coagulation. Statistical analysis was performed using ANOVA, ***p<0.001. Modified from the original publication II.

5.5 Cell culture results (III)

5.5.1 Osteoblast cells proliferation and viability

Figure 22 represents the proliferation of MC3T3-E1 cells cultured on SA titanium substrates before and after BAG/inert glass air-abrasion determined by MTT assay. The proliferation rate increased significantly on day 1 for 45S5 BAG and Zn4 BAG compared to SA and inert glass air-abraded substrates ($p<0.001$). However, when

the culture time extended to 3 or 6 days, no significant differences in the proliferation rate were observed among the groups.

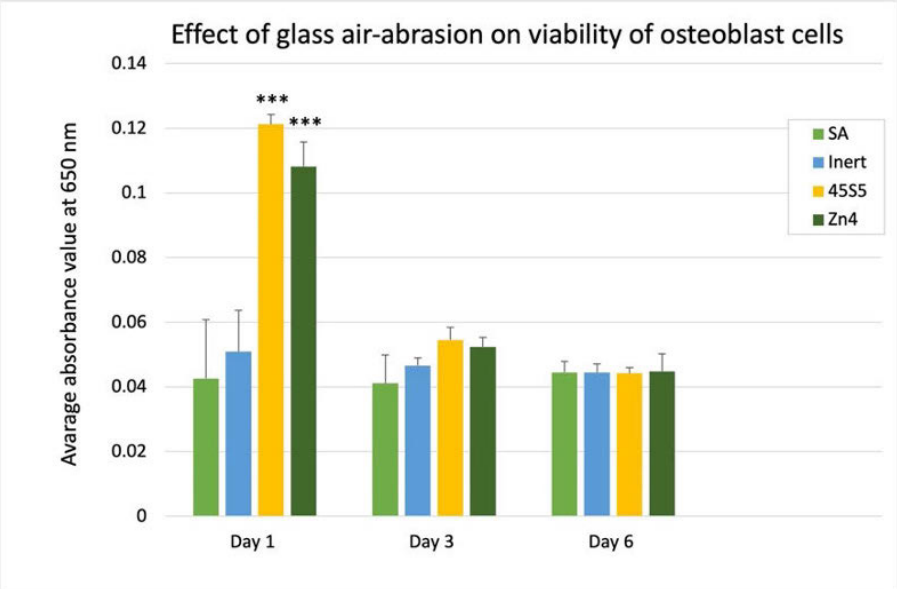

Figure 22. Mean (±SD) of viable osteoblast cells on the sandblasted and acid-etched (SA), and BAG or inert glass air-abraded substrates assessed by MTT assay. Measurements were calculated from the substrate surfaces after culture for 1 day, 3 days, and 6 days. Four replicate measurements at (650 nm) absorbance were obtained. A significant increase in the absorbance value was seen on day 1 for Zn4 and 45S5 BAG abraded substrates. Statistical analysis was performed using ANOVA, ***p<0.001. Modified from the original publication III.

5.5.2 Visualization and count of MC3T3-E1 pre-osteoblasts on titanium surfaces

MC3T3-E1 pre-osteoblast cells were visualized by confocal laser scanning microscope and SEM after culture for 2, 24, and 48 hours. The cells on the borosilicate coverslip displayed better spreading than on SA titanium substrates. The cells were firmly attached to the pores of the rough SA titanium surface. The BAG/inert glass air-abraded substrates showed that the optimum cell spread time appeared at a time period of 24-hour. When the culture time was extended to 48 hours, the morphology of the cells changed to a spindle-like shape. (Figure 23 and 24).

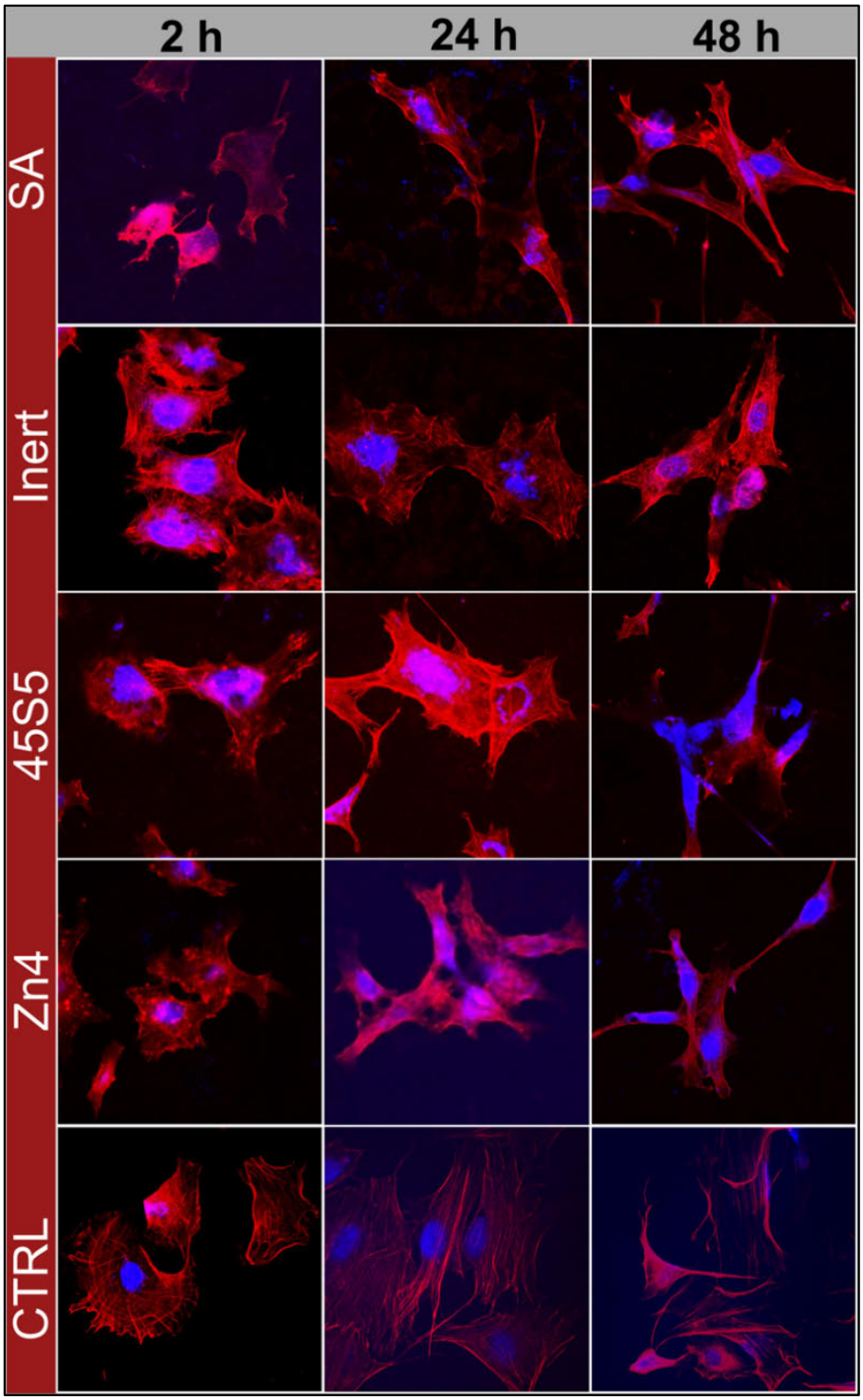

Figure 23. MC3T3-E1 osteoblasts cultured on sandblasted and acid-etched (SA) titanium substrates, BAG/inert, air-abraded substrates, or glass coverslips (CNTRL) for 2, 24, and 48 hours. The cells were stained with fluorescently labeled phalloidin for actin and Hoechst 33258 for nuclei. The confocal microscope images were acquired with 63x objective (frame size 143 x 143 µm). Modified from the original publication III.

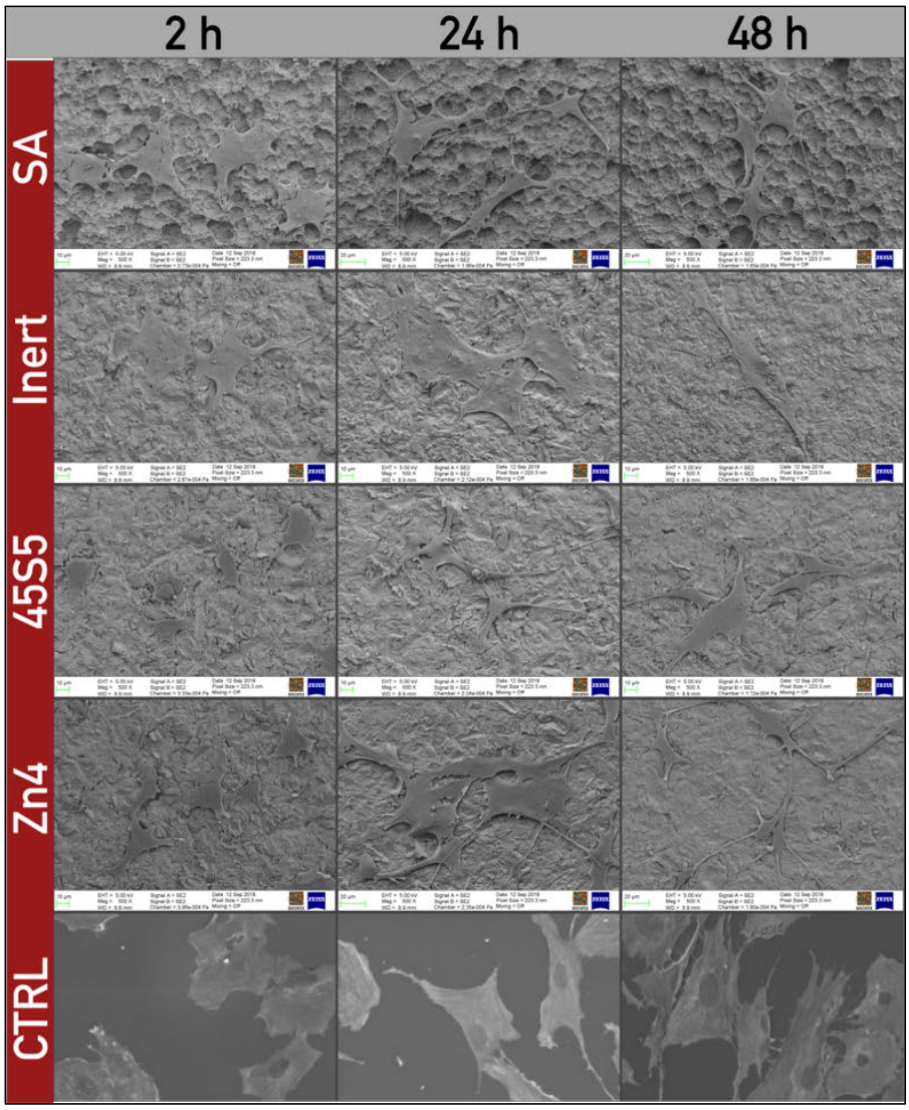

Figure 24. MC3T3-E1 osteoblasts cultured on sandblasted and acid-etched (SA) titanium substrates, BAG/inert air-abraded substrates, or glass coverslips (CNTRL) for 2, 24, and 48 hours. The field emission-scanning electron microscope (FE-SEM) images were acquired with 500x magnification. Modified from the original publication III.

Figure 25 demonstrates the average cell counts per 5.55 mm^2 at 2, 24, and 48 hours. The number of osteoblast cells was higher on substrates subjected to Zn4 BAG air-abrasion and borosilicate coverslip controls compared to SA, or 45S5 BAG and inert glass abraded surfaces. Analysis of the cell spreading area suggests that the MC3T3-E1 cells displayed a more prominent coverage on borosilicate coverslip than on other tested substrates. The cell spread on the SA and BAG/inert glass air-abraded substrates were below 2000 cell/μm^2 at all time points (Figure 26). The cells on the 45S5 or Zn4 BAG abraded substrates were more elongated than SA or inert glass abraded substrates as the cell shape aspect ratio was higher (Figure 27).

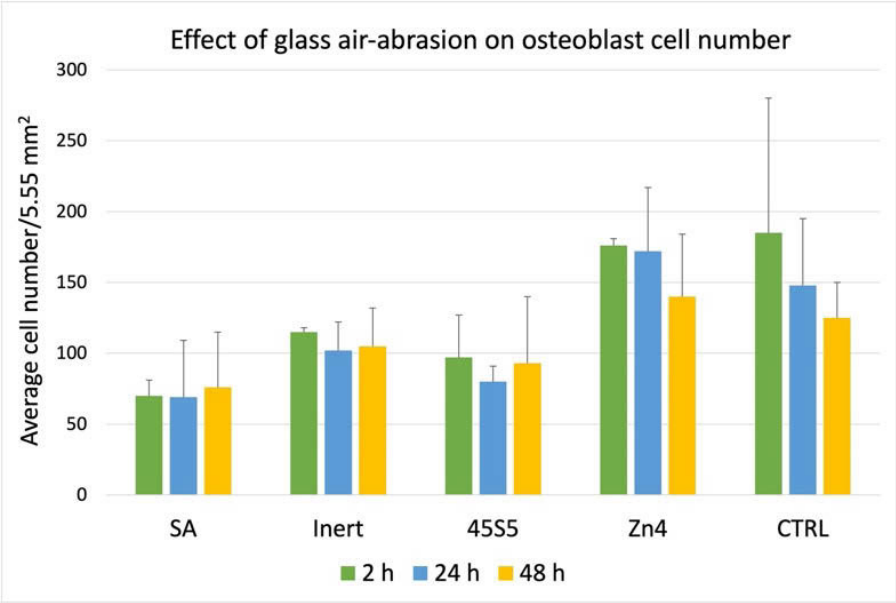

Figure 25. Cell number / 5.55 mm^2 ROI is an average of 3 similar randomly paced ROIs over the 100 mm^2 substrates at various time points. Modified from the original publication III.

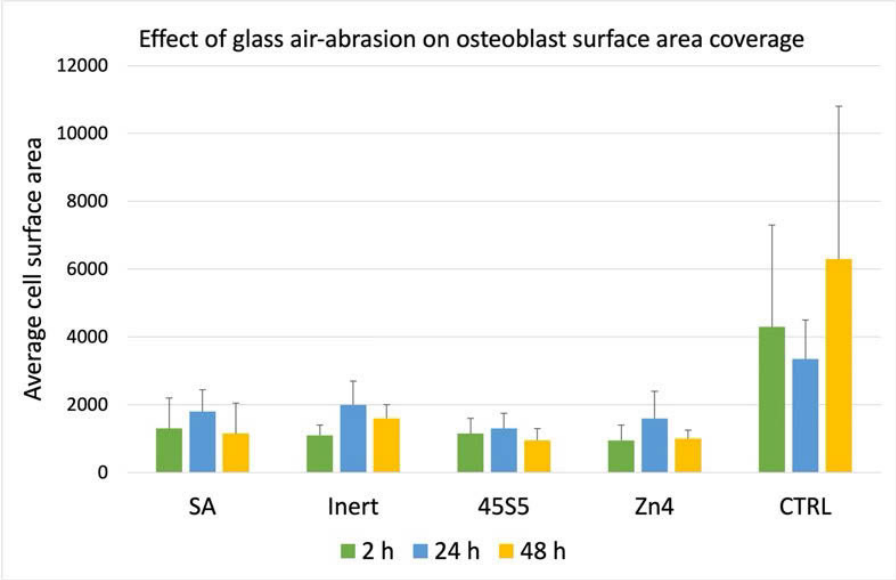

Figure 26. Average osteoblast cell surface area coverage on different substrates is expressed in μm^2. Modified from the original publication III.

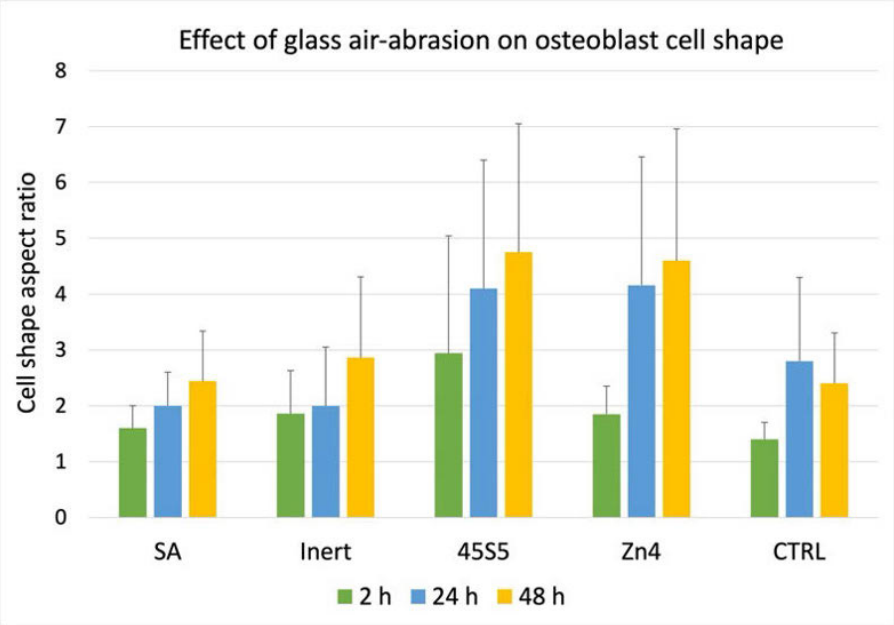

Figure 27. The aspect ratio of osteoblast cell shape on test substrates and control. The ratio is calculated as maximal cell diameter per minimal cell diameter. Modified from the original publication III.

6 Discussion

6.1 General discussion

These *in vitro* studies aimed to investigate novel zinc-containing BAG formulae for use in an air abrasive surface treatment. The ultimate goal is to develop bioactive glass powder for air particle abrasion to eliminate the bacterial biofilm from an infected implant surface and hinder further bacterial colonization. An additional goal is to promote bone formation and re-osseointegration of the exposed implant surfaces. There is a lack of knowledge about the bone-forming capacity and applicability of BAG air-abrasion to decontaminate the exposed implant surfaces in PI defects.

Study I was designed to assess the antibacterial activities and the potential ability of titanium substrates subjected to BAG particles' air-abrasion to inhibit biofilm formation. The ionic dissolution from BAG and the effect on the pH of the SBF were also evaluated in study I. Furthermore, studies II and IV were performed to assess the capacity of BAG particle air-abrasion to eliminate the bacterial biofilms on SA titanium surfaces. Study III investigated the effect of BAG/inert air-abrasion on the surface characteristics of SA titanium substrates. In addition, the behavior of the osteoblast cells on the treated surfaces was also studied. Besides, in study II, the blood clotting properties of the abraded SA titanium substrates were evaluated.

The biological reaction of BAG depends mainly on its composition and surface area. The smaller the particle size, the grater is the surface area, and thus the faster the rate of dissolution. The glass particle size used in the dissolution experiments was in the range of 300-500 μm. However, for the air-abrasion process, different BAG particle sizes were tested. The particle size ranges of 25-120 μm (study I) and 45-120 μm (studies II-IV) was found to be compatible with the air-abrasion device and demonstrated a consistent particle flow through the abrasion unit. Smaller abrasive particles of less than 20 μm can cause the formation of agglomerates. This will affect the flow of the abrasion materials and resulted in uneven surface consistency (Koller et al., 2007).

The first study evaluated the antibacterial properties of three novel BAG formulae, namely, Zn4, Zn6, and Zn4Sr8. Based on the Zn^{2+} ion dissolution results and the observation of the antibacterial effect, Zn4 BAG was chosen to be further

investigated in studies II-IV. Zn4 BAG demonstrated the higher and the most consistent Zn^{2+} ion concentration release than Zn6 and Zn4Sr8 BAGs. Besides, study I results showed that Zn4 has a relatively higher antimicrobial effect than the other investigated BAGs. Ning et al. (2015) showed that the Zn^{2+} demonstrated a minimum inhibitory concentration (MIC) of 10^{-7} M (0.0065 mg/L), and its optimal concentration that showed antimicrobial effect without cell cytotoxicity has been in the range of 10^{-4} – 10^{-6} M (6.53 - 0.065 mg/L) (Ning et al., 2015). Ion dissolution results from study I showed that Zn4 demonstrated higher Zn^{2+} ion release of 0.2 mg/L in both 2 and 48 hours than the other investigated experimental BAG (0.01-0.05 mg/L). According to Ning et al. (2015), Zn^{2+} ion released from Zn4 BAG was within the optimal concentration range, while Zn6 and Zn4Sr8 BAGs were within the MIC range.

Observations from SEM-EDS analysis showed that placing a titanium disc exposed to 45S5 BAG air-abrasion in an ultrasonic bath for 15 minutes did not affect the retention of the abrasive glass particles. These findings are in agreement with Koller et al. (2007). Their study also evaluated the retention of glass particles on titanium surfaces after 45S5 BAG air-abrasion. They showed that the glass particles remained firmly attached to the surface despite the thorough cleaning of substrates (Koller et al., 2007). It is hypothesized that the abrasion procedure resulted in the retention of glass particles on the surface; therefore, the residual BAG particles on the titanium surface will yield extended antibacterial activities. Besides, the BAG particles have the potential to produce a biologically active hydroxycarbonate apatite layer, as demonstrated in an earlier study (Hench & Wilson 1993). However, the potential effect of this air-abrasion treatment alone depends crucially on the shape and size of the peri-implant bone defect, and augmentation should be considered in most cases.

6.2 Surface characteristics (III)

Sandblasting and acid-etching is a universally used surface treatment technique to produce a moderately rough titanium surface. Ra is a classical parameter used to estimate the surface roughness value. It can be measured by an algorithm that calculates the average length between peaks and valleys and means line deviation on the whole surface within the sampling length (Wennerberg et al. 1998). In the reviews by Albrektsson and Wennerberg (2004a, 2004b) it is described that moderately rough titanium surfaces such as SLA (Straumann implant, Basel, Switzerland) or TiOblast™ (Astra Tech implants, Dentsply Sirona, Charlotte, USA) have average Ra values between 1.0 and 2.0 µm. The Ra values for the SA titanium substrates used in studies II-IV were within the previously reported range, with a mean Ra surface roughness value of 1.07 µm.

Glasses used for air-abrasion in studies II-IV have somewhat different densities (inert glass-2.5 g/cm^3; 45S5 BAG-2.7 g/cm^3; and Zn4 BAG- 2.8 g/cm^3) that may affect their impact on the substrate's surface. However, based on the Ra roughness values, their effect on the SA titanium surface topography was insignificant. The exposure of SA titanium substrates to air-abrasion with either BAGs or inert glass resulted in smoother surface topography, lower CA, and higher SFE values compared with SA surfaces without air-abrasion.

The CA and SFE of implant surfaces are essential parameters that play a vital role in initial protein conditioning as well as cell adhesion on the implant surfaces (Zhao et al., 2007). The wettability behavior of SA titanium substrates before and after BAG/inert glass air-abrasion was evaluated in study III by calculating the surface CA and SFE. The water CA on surfaces ranges from 0° to 180°, suggesting that the drop of the wetting liquid is either spreading or beading on the surfaces. Results from study III indicate that SA surface demonstrated a strong hydrophobic behavior with mean water CA value of 113°. These results are in agreement with the values reported in previous experimental studies (Rupp et al., 2014; Żenkiewicz, 2007). The hydrophobic characteristics of the SA surface may be explained by the fact that the micro-roughness produced by the sandblasting process is initially filled with water. In contrast, nano-roughness created by the acid-etching procedure is not. The exposure of SA titanium substrates to BAG/inert glass air-abrasion modified their surface roughness values, consequently affecting their wetting behavior and resulted in hydrophilic surfaces with lower CA values. The change in the wetting behavior of SA surfaces may be attributed to the glass particles used for the air-abrasion that got trapped within the surface pores, resulting in a smoother surface microtopography.

SFE is categorized into polar components and non-polar components. A high polar component of a surface reflects low CA and higher wettability and thus superior interaction to the surrounding biological environment (Ostrovskaya et al., 2002; Schrader, 1982; Zhao et al., 2005). Results from study III showed a significant increase in the total and polar SFE components after BAG/inert glass air-abrasion compared to SA substrates. Yet, SA substrates demonstrated zero polar value component, which indicates high CA and lower surface wettability. However, the dispersive component of SFE was somehow similar for all tested substrates. *In vivo* studies have shown that hydrophilic surfaces enhance the proliferation and differentiation of bone-forming cells (Bornstein et al., 2008; Eriksson et al., 2004), thus potentially enhancing the rate of OI.

6.3 Bacterial biofilms (I, II, IV)

Single species *S. mutans* biofilm was used in studies I and II. *S. mutans* cells were well grown on the smooth and SA titanium substrates with a cell count mean value of more than 700 x 10^2 CFU per substrate after 4 hours of incubation. *S. mutans* was chosen for our studies because it is one of the early bacterial colonizers which is believed to ease the colonization of the secondary bacterial colonizers leading to the formation of Gram-negative anaerobic biofilm (Shibli et al., 2007; Shibli et al., 2008). Furthermore, *S. mutans* is a very virulent bacteria that is recognized to has many efficient adhesion methods to different surfaces. It can produce an insoluble polymer matrix that has a high affinity for solid surfaces. Moreover, *S. mutans* can survive at low pH values that many other bacterial species cannot tolerate (Hamada & Slade, 1980; Koo et al., 2013; Tamura et al., 2009). In addition, *S. mutans* is reported at a higher level around infected implant sites in contrast to healthy implant sites (Kumar et al., 2012). Thus, *S. mutans* may has a role in the process, leading to the implant's failure (Nakazato et al., 1989).

In study IV, dual anaerobic bacterial biofilm was chosen, namely, *F nucleatum* and *P. gingivalis. F. nucleatum* has been shown to adhere to *P. gingivalis* through their surface RadD adhesin protein present on their outer surfaces (Coppenhagen-Glazer et al., 2015; Guo et al., 2017). Besides, *P. gingivalis* is actively involved in the progression of peri-implant infection and has also demonstrated significantly higher levels around infected implant sites than their healthy counterparts (Al-Ahmad et al., 2018; Lafaurie et al., 2017). The pathogenic role of *P. gingivalis* in the disease advancement depends, for the most part, on its ability to adhere to host cells and coaggregate with other bacterial species such as *F. nucleatum.*

Dual biofilm formed on SA titanium substrates was sufficiently grown and showed a cell count mean value of more than 8 x 10^6 CFU and 6 x 10^6 CFU *F. nucleatum* and *P. gingivalis,* respectively. After BAG/inert glass air-abrasion and 23-hour culturing, no *P. gingivalis* cells could be detected on BAG abraded substrates using either SEM images or culturing method. In contrast, approximately 2000-5000 CFU of viable *F. nucleatum* cells were counted on the same substrates. This may be explained by the finding presented by Diaz et al. (2002) that *F. nucleatum* could support the growth of *P. gingivalis* in an unfavorable environment that the latter bacteria could not tolerate alone.

6.4 Antimicrobial activity of bioactive glass (I, II, IV)

In study I, the capability of BAG abraded titanium substrates to prevent *S. mutans* growth was evaluated. The efficiency of BAG air-abrasion in eliminating the *S. mutans* biofilm on SA titanium surfaces was evaluated in study II. Study IV was designed to investigate BAG air-abrasion potential eliminating *F. nucleatum* and *P.*

gingivalis dual biofilm formed on the SA titanium substrates. A dramatic decrease in the viability of *S. mutans* and significant inhibition of the ability of the bacteria to form a biofilm were seen for substrates subjected to air-abrasion using BAGs compared to using E-glass. Studies II and IV demonstrated that the BAG air-abrasion successfully eradicated bacterial biofilms formed on the SA titanium surface compared to biofilms exposed to inert glass air-abrasion. Significant decrease in the total *S. mutans* count (study II) and *F. nucleatum* and *P. gingivalis* count (study IV) were seen for BAG abraded substrates compared to inert glass abraded substrates or intact biofilm.

In study I, three novel ZnO/SrO doped BAG formulae were compared to the known 45S4 BAG. The pH evaluation results indicated that 45S5 BAG demonstrated the highest increase in the pH compared with the other investigated BAGs. The increase in the pH and the non-physiological concentrations of Si, Na, and Ca^{2+} ions dissolved from the glass are believed to be the primary mechanism behind the 45S5 BAG antibacterial action (Allan et al., 2001; Stoor et al., 1998). Allan et al. (2001) showed that exposure of certain bacteria, including the bacterial species investigated in our studies, to 45S5 BAG, resulted in 91.2 % - 95.0 % of the bacterial loss of viability. Their study showed that the direct contact between the BAG particles and the bacterial cells is unnecessary to yield an antibacterial effect. Additionally, Stoor et al. (1998) showed that exposure of specific bacteria, including *S. mutans* planktonic cells, to S53P4 BAG powder for 10 minutes resulted in almost total bacterial cell inactivation.

However, the mechanism behind the antibacterial effect of the three investigated Zn-containing BAGs may not be related to the pH increase since they demonstrated only slight pH elevation. The Si concentration for 45S5 BAG is significantly higher in the static condition than observed for the zinc-containing glasses, explaining its high pH value. For the ZnO containing BAG, the Zn salts precipitation may explain the low pH values of SBF in static conditions. The lower network connectivity of Zn6 compared to Zn4 or Zn4Sr8 may explain its slightly higher release of Si, Ca^{2+}, and other ions. In the dynamic condition, the steady release of Zn^{2+} for Zn4 BAG composition proposes that the Zn^{2+} ion concentration is relatively high in the interfacial solution before any precipitation.

The dissolving Zn^{2+} ions from the zinc-containing BAGs were apparently involved in their antibacterial activity. Zinc ions are among the most potent antibacterial elements demonstrated to provoke an antibacterial effect. These ions have been shown to inhibit bacteria actively associated with dental plaque formation, including *S. mutans, F. nucleatum,* and *P. gingivalis* (Suzuki et al., 2018). Several mechanisms have been suggested to explain the antimicrobial activity of the zinc element. Yamamato (2001) demonstrated that Zn^{2+} ions could cause bacterial cell death by penetrating their cell membrane and generating toxic ROS, leading to DNA

and cell membrane damage. Also, Zn^{2+} ions can cause impairment to the acid production during the glycolysis process via an alteration to the enzymatic activity of the bacterial cell membranes. Other studies indicate that ZnO powder can produce antibacterial activity due to the generation of H_2O_2 from their surfaces (He et al., 2002; Phan et al., 2004; Yamamoto, 2001).

6.5 Thrombogenicity and blood response (II)

Blood clot serves as a connection between the implant surface and the surrounding tissues; therefore, the blood clotting ability of implant surface has been considered of absolute importance to determine the implant success (Davies, 2003; Hong et al., 1999; Park & Davies, 2000). The rapidly formed blood clot around the dental implant surfaces serves as a barrier against possible bacterial infection. Also, the formation of a blood clot on a moderately rough titanium surface can encourage cell recruitment and stimulate the process of wound healing (Park & Davies, 2000). Earlier studies have demonstrated that osteoblast cells can attach to implant surfaces covered with fibrin and platelets. Therefore, blood clots forming on the implant surfaces are critical factors in fibrin retention and may significantly influence cell behavior and osteogenesis and consequently affect bone healing (Naik et al., 2013; Yang et al., 2016).

In study II, the effect of BAG/inert glass air-abrasion on the blood clotting formation on the SA titanium substrates was evaluated using fresh human whole blood by the kinetic clotting time method. One donor approach was used to avoid individual variations. The spectrophotometric method was chosen to evaluate the OD, which indicates the hemoglobin concentration in the solution after blood is applied on substrate surfaces. A lower OD value indicates lower hemoglobin concentration in the solution, suggesting a faster clot formation on the substrate surfaces (Abdulmajeed et al., 2014; Sharma, 1984). Complete blood clotting is achieved when the OD value is 0.1. The reason for faster initial blood clot formation for substrates air-abraded using Zn4 BAG compared to the other air-abraded substrates is unknown. However, at a later time, inert glass abraded substrates demonstrated faster coagulation between 20-30 minutes. The ion dissolution from BAG might have affected the coagulation rate by decreasing the coagulation rate at later time points. Nevertheless, complete blood clotting was achieved for all substrates at 40 minutes. Inversely, Ostomel et al. (2006) evaluated the hemostasis effect of BAG *in vitro.* Findings from their study suggested that BAG is an ideal material to enhance hemostasis due to the release of Ca^{2+} ions, which is known to support the clotting cascade.

6.6 Osteoblast cell response (III)

Study III evaluated the attachment and proliferation of human osteoblast-like MC3T3-E1 cells on SA titanium substrate exposed to 45S5, Zn4 BAGs, or inert glass air-abrasion using MTT assay. An absorbance value of 550 nm was used and then corrected by its calculation at 650 nm. The correction of the absorbance value was to avoid the red color caused by the presence of Phenol Red in the culture media, which can affect the MTT assay. MC3T3-E1 cells were chosen due to their higher levels of osteogenic differentiation. They also exhibit similar behavior to primary osteoblasts, making them widely used cells in *in vitro* experiments (Maeda & Maeda, 2004). Both investigated BAG formulae (45S5 and Zn4) demonstrated an initial higher increase in the MC3T3-E1 cells proliferation rate. Improved surface wettability and increased SFE for the abraded substrates seem to be the reason for increased osteoblast viability. Indeed, it is well known that surface roughness and hydrophilicity are two critical factors that affect osteoblast behavior (Alfarsi et al., 2014). Previous research indicated that early-stage osteoblast cell adhesion and proliferation are significantly enhanced on hydrophilic compared to on hydrophobic surfaces (Bornstein et al., 2008; Eriksson et al., 2004). Study III showed that modification of SA surfaces via air-abrasion with BAG/inert glass resulted in lower CA value and higher SFE. Earlier studies report that modified-SA surfaces demonstrated lower CA value, higher SFE, enhancement in the osteogenic cell attachment, and higher bone apposition during early healing than unmodified-SA surfaces (Bornstein et al., 2008; Lai et al., 2010; Lee et al., 2015).

BAG particles were used in study III to modify the SA titanium substrates and endow bioactivity on the surfaces. The BAG particles have good potential to generate bioactivity to the SA surface, as SEM-EDS analysis demonstrated the presence of the BAG particles on the abraded surfaces. Ion released from BAG particles, such as Ca^{2+} and PO_4^{3-}, would directly improve surface bioactivity, resulting in superior cell proliferation and viability (Foppiano et al., 2007; Varanasi et al., 2009). This was also noticed in study III, but as the culture time extended to 3 or 6 days, the difference in the proliferation rates between groups vanished in our study. The ionic products released from BAG dissolution, such as Si and Ca^{2+} ions, generate a favorable environment for osteoblast cell proliferation and differentiation *in vitro* (Xynos et al., 2000) and have been shown to increase the insulin-like growth factor II (IGF-II) and stimulate osteoblast cell proliferation. IGF-II is an anabolic insulin peptide and comprises the bone's most abundant growth factor (Bautista & Bautista, 1991; Hench, 2009). However, the rapid elevation of pH due to ionic dissolution may be unfavorable for cellular metabolism. BAG 45S5 dopped with zinc oxide (ZnO) effectively controlled the chemical durability and bioactivity, resulting in minimal pH elevation, as demonstrated in the study (I). Additionally, Zn^{+2} plays a crucial role in stimulating osteoblast cell proliferation *in vitro* (Ishikawa

et al., 2002; Max, 2015). Furthermore, Yamaguchi & Weitzmann (2011) showed that zinc stimulates cell proliferation and differentiation and protein synthesis in MC3T3-E1 cells. However, the exact mechanism through which zinc stimulates osteoblast cells is not clearly understood.

Previous studies indicate that the morphology of cells on surfaces is closely correlated to cell function (Chen et al., 1997; Zheng et al., 2012). In general, an elongated cell with decreased circularity and an increased aspect ratio indicate that the cell is well spread and viable. In contrast, a round cell shape is typically inactive (Chen et al., 1997; Zheng et al., 2012). The pre-osteoblastic MC3TC-E1 cells seeded on BAG air-abraded substrates demonstrated a longer shape and increased aspect ratio indicating the cells are active and viable. Furthermore, the number of cells on Zn4 BAG abraded substrates was higher than on substrates exposed to 45S5 BAG or inert glass air-abrasion. The increased cell number on Zn4 abraded substrates may be explained by the zinc ion released from the residual glass particles. Zinc ion has been known to encourage attachment and proliferation of osteoblast (Collier et al., 1998; Ishikawa et al., 2002). However, the average cell surface area was similar for all investigated substrates compared to cells on control coverslips.

6.7 Limitations

These study series are *in vitro* experiments that are considered a static environment compared to *in vivo* studies. Results presented are valid for smooth and SA titanium surfaces making their external validity limited. Nevertheless, the SA titanium surface is a widely used surface modification method in oral implants.

Biofilm formation on dental implant surfaces is a dynamic, complex multistage and multispecies process that involves a wide variety of bacterial species (Dhir, 2013; Kumar et al., 2012; Shibli et al., 2008). In this study series, the capability of the BAG antibacterial effect was evaluated for three bacterial species, namely, *S. mutans* biofilm and *F. nucleatum* and *P. gingivalis* dual biofilm. However, *S. mutans* is a very virulent bacteria, can form a highly adhesive biofilm, and is believed to participate in the peri-implantitis process (Koo et al., 2013; Stoor et al., 1998). Moreover, *F. nucleatum* is an essential bacterium in regulating the biofilm as it serves as a bridge connecting the primary bacteria colonizers with the late colonizers (Coppenhagen-Glazer et al., 2015; Guo et al., 2017). Additionally, *P. gingivalis* is considered among the most important red-complex pathogens strongly associated with periodontal and peri-implant diseases (Casado et al., 2011; Hajishengallis et al., 2012).

Another limitation is that the air-abrasion of the anaerobic dual biofilm was carried out in an aerobic environment that would possibly compromise the viability of the bacterial cells. However, according to our preliminary findings (data not

shown), *F. nucleatum* and *P. gingivalis* biofilm could survive in a growth media at the aerobic environment for the time required to conduct the air-abrasion when they were in the stationary phase. The air-abrasion was performed for six samples at one time and lasted for a maximum of 10 minutes. Moreover, the air-abrasion experiment was repeated more than twice in similar laboratory conditions. Thus, the intra-laboratory reproducibility was validated.

A blood response experiment was conducted with a single donor approach, limiting the possibility of generalizing the results on BAG's effect on surface thrombogenicity.

All the studies were performed in cell culture conditions which cannot mimic true clinical conditions. This is an obvious limitation. However, the results on the effects of especially Zn4 BAG powder in air particle abrasion are promising, which merits the studies in more complex *in vivo* settings.

6.8 Future prospective

The potential use of BAG air-abrasion in treating PI needs to be investigated further before any definitive conclusion can be made. The effects of BAG air-abrasion on the surface properties and bacterial eradication need to be evaluated with various commercially available implant surfaces. Also, the potential of the BAG abraded implant surface to form a hydroxyapatite layer due to the retention of glass particles on the surface calls for future investigations. *In vivo* animal experiment needs to be conducted to investigate the decontamination effect and osteopromotive capacity of ZnO-containing BAG powders in experimentally-induced bone defects.

Currently, an *in vivo* study on the rat model evaluating the effect of BAG air-abrasion on *F. nucleatum* and *P. gingivalis* dual biofilm formed on SA implant surfaces is in progress. In this study implants were placed in the maxillary first molar region with a circumferential bone defect resembling PI lesion.

Finally, clinical studies to evaluate the true potential of ZnO containing BAG in air particle abrasion treatment of various PI defects will be required.

7 Conclusions

Based on the results included in this thesis, the conclusions can be summarized as follows:

1. ZnO/SrO doped BAGs have a lower ion dissolution rate than commercially available BAG 45S5. ZnO/SrO doped BAGs do not increase the pH level in simulated body fluid like 45S5 BAG.

2. Titanium substrates air-abraded with 45S5 or ZnO/SrO doped BAGs have a strong antibacterial effect against *S. mutans*. Additionally, BAG air-abrasion suppresses *S. mutans* biofilm formation on titanium substrates.

3. Air-abrasion with 45S5 or Zn4 BAGs successfully eradicates *S. mutans* biofilm and *F. nucleatum* and *P. gingivalis* dual biofilm formed on SA titanium surfaces.

4. Bioactive or inert glass air-abrasion does not affect the speed of blood coagulation.

5. Bioactive or inert glass air-abrasion enhances the surface wettability and increases the surface free energy of SA titanium surfaces. Besides, 45S5 or ZnO containing BAG air-abrasion enhances the viability and proliferation of pre-osteoblastic MC3T3-E1 cells on SA surfaces.

From the above, it can be concluded that air particle abrasion with BAG has good potential to be used for the treatment of PI. However, the true potential of using BAGs needs to be evaluated in *in vivo* experiments before any definitive conclusion can be made.

Acknowledgments

First and foremost, praises and thanks be to Almighty God. He has granted me countless blessings and knowledge so that I can finally accomplish my thesis. His mercy was with me throughout my life and ever more during this research.

This thesis was carried out at the Department of Prosthetic Dentistry and Stomatognathic physiology, Institute of Dentistry, and Turku Clinical Biomaterial Centre (TCBC), University of Turku, Finland. In collaboration with the Department of inorganic chemistry, Åbo Akademi University, and Research Unit for Cancer and Translational Medicine, University of Oulu. I gratefully acknowledge the Libyan Ministry of Education's scholarship support. In addition, I would like to thank the Finnish Doctoral Program in Oral Science (FINDOS) for the financial support received towards my PhD work. Without their support, this work would not have been possible. Thank you so much. I also wish to extend my thanks to LM Dental Oy for their continuous help and support whenever needed.

Undertaking this PhD has been a truly life-changing experience for me. It would not have been possible without the support and guidance that I received from many people. I would like to express my most profound appreciation and sincere gratitude to my supervisor Prof. ***Timo Närhi.*** Your support and encouragement were always important guiding lights towards my personal and professional development. I can't say thank you enough. Without your tremendous help and guidance, this thesis would not have materialized.

My sincere appreciation goes out to Professor ***Pekka Vallittu***, the dean of the Institute of Dentistry, University of Turku, as well as Dr. ***Lippo Lassila***, the head of TCBC, for their constant effort to create a supportive environment for researchers and research. I also extend my warm gratitude to Assistant Professor ***Ulvi Gürsoy*** (Chair of the board National FINDOS) for his constant support. I also extend my thanks to the Cheif Academic Officer of Doctoral training, ***Outi Irjala,*** for her support and guidance throughout the thesis preparation process.

I am grateful to Prof. ***Andreas Stavropoulos*** for accepting the invitation to be my dissertation opponent. I would also like to extend my sincere respect and thanks to the official pre- examiners, Docent ***Patricia Stoor*** and Docent ***Pirkko Pussinen***, for their excellent advice and detailed review during the preparation of this thesis.

A huge thanks to all co-authors who contributed to my scientific articles: ***LauraAalto-Setälä***, ***Johan Sangder,*** and ***Ilkka Miinalaine; your*** valuable work is highly appreciated. I'm deeply indebted to Prof. ***Leena Hupa*** for her help and the scientific support I received through our collaborative work. I also wish to faithfully thank Docents: ***Eva Söderling and Mervi Gürsoy*** for their valuable advice and immense knowledge. Special warm thanks to Pro. ***Juha Tuukkanen*** for his constant help and support whenever needed. It is an honor to have known you. Thank you so much.

To the skilful laboratory technicians: ***Katja Sampalahti***, ***Oona Hällfors***, for their technical assistance during the lab works involved in this thesis, as well as ***Mariia Valkama, Genevieve Alfont*** from TCBC laboratories for their generous help and guidance.

My sincere thanks to Dr. ***Ahmed Ballo,*** for introducing me to Prof. Timo Närhi and the University of Turku. I am grateful for your advice. Many thanks to my colleagues at the Institute of Dentistry (Dentalia), ***Khalil Shahramian***, ***Tarek Omran,*** and ***Anas Salim***; I feel blessed to have such great friends. I also wish to thank my friends in Turku, ***Mansour Almansori, Naser Buhmeida***, and ***Haitham Ballo,*** for their support and companionship. I would also like to extend my sincere gratitude to my batch fellow **A*hmed Ali Musrati***; I really feel fortunate to have you as a friend. A special thanks to my friend ***Sufyan Garoushi***; our friendship has always been a source of positive energy and support that encouraging me throughout my study. I also like to extend my exceptional acknowledgment to my role model and a person to learn from; Prof. ***Sanousi Taher***, the dean of Faculty of Dentistry, Libyan International Medical University, Benghazi, Libya. There are certain people who make the world a better place just by being in it. You are one of those people. I have been honored and blessed for having such a friend.

To my closest and dearest friend here in Turku, ***Ahmed Al-gahawi***. The beginning was as teaching fellows in the Department of Periodontology at the University of Benghazi, Libya. We decided to come to Turku and start this challenging journey together. Thank you for helping me in whatever way you could during this journey. I am blessed to have you as a true brother and a loyal friend. I am also greatly thankful to your wife, my true sister ***Samira Elmanfi*** for embracing my family and me with kindness and warmth.

My warm gratitude to my second family in Libya, my **parents-in-law**. Thank you for your love, support, and patience for these many years of hardship. To my respectful "**brothers and sisters-in-law**" and their lovely families. May God bless you with good health and lots of happiness.

I would also like to say a heartfelt thank you to my family, a circle of love, strength, and support. My fabulous and beloved **sisters** and **brothers** and their families always believed in me and encouraged me to follow my dreams.

To my **father** and **stepmother**; your love, prayers, sacrifice, and support have made this journey possible. May God bless you with long life, happiness, and good health.

To my late **mother**, although you are no longer in this world, yet your soul was always by my side, praying for me and gives me support, confidence, and help. I know you would have been proud of me. May Allah have mercy on your soul and grant you Al-Jannah. I dedicate this book to your pure soul.

I also dedicate this Ph.D. thesis to my loving children, ***Rahaf***, ***Roua***, ***Ahmed***, and ***Mohamed***; you are my inspiration to achieve greatness. Thank you for your unending support, care, and love.

Last but, of course, is not least to my beloved wife, ***Nagat***. Thank you for your endless love, encouragement, and support. Thank you for being my editor, proofreader, and sounding board. But most of all, thank you for being my best friend. I owe you everything. I am very fortunate to have you in my life.

Turku, September 15th, 2021
Faleh Abushahba

References

Abdulmajeed, A. A., Walboomers, X. F., Massera, J., Kokkari, A. K., Vallittu, P. K., & Närhi, T. O. (2014). Blood and fibroblast responses to thermoset BisGMA–TEGDMA/glass fiber-reinforced composite implants in vitro. *Clinical Oral Implants Research, 25*(7), 843-851.

Abrahamsson, I., Berglundh, T., Linder, E., Lang, N. P., & Lindhe, J. (2004). Early bone formation adjacent to rough and turned endosseous implant surfaces. an experimental study in the dog. *Clinical Oral Implants Research, 15*(4), 381-392.

Abrahamsson, L., Berglundh, T., & Lindhe, J. (1998). Soft tissue response to plaque formation at different implant systems. A comparative study in the dog. *Clinical Oral Implants Research, 9*(2), 73-79.

Abrahamsson, I., Berglundh, T., Wennstrom, J., & Lindhe, J. (1996). The peri-implant hard and soft tissues at different implant systems. A comparative study in the dog. *Clinical Oral Implants Research, 7*(3), 212-219.

Aghazadeh, A., Persson, R. G., & Renvert, S. (2020). Impact of bone defect morphology on the outcome of reconstructive treatment of peri-implantitis. *International Journal of Implant Dentistry, 6*(1), 33-35.

Al-Ahmad, A., Muzafferiy, F., Anderson, A. C., Wölber, J. P., Ratka-Krüger, P., Fretwurst, T., Nelson, K., Vach, K., & Hellwig, E. (2018). Shift of microbial composition of peri-implantitis-associated oral biofilm as revealed by 16S rRNA gene cloning. *Journal of Medical Microbiology, 67*(3), 332-340.

Albrektsson, T., & Sennerby, L. (1991). State of the art in oral implants. *Journal of Clinical Periodontology, 18*(6), 474-481.

Albrektsson, T., & Wennerberg, A. (2004a). Oral implant surfaces: Part 1--review focusing on topographic and chemical properties of different surfaces and in vivo responses to them. *The International Journal of Prosthodontics, 17*(5), 536-543.

Albrektsson, T. & Wennerberg, A. (2004b). Oral implant surfaces: Part 2 - review focusing on clinical knowledge of different surfaces. *Int J Prothodont* 17(5), 544-64.

Albrektsson, T., & Wennerberg, A. (2019). On osseointegration in relation to implant surfaces. *Clinical Implant Dentistry and Related Research, 21 Suppl 1*, 4-7.

Alfarsi, M. A., Hamlet, S. M., & Ivanovski, S. (2014). Titanium surface hydrophilicity modulates the human macrophage inflammatory cytokine response. *Journal of Biomedical Materials Research Part A, 102*(1), 60-67.

Allan, I., Newman, H., & Wilson, M. (2001). Antibacterial activity of particulate bioglass against supra- and subgingival bacteria. *Biomaterials, 22*(12), 1683-1687.

Allan, I., Newman, H., & Wilson, M. (2002). Particulate bioglass reduces the viability of bacterial biofilms formed on its surface in an in vitro model. *Clinical Oral Implants Research, 13*(1), 53-58.

Alshammari, H., Neilands, J., Svensater, G., & Stavropoulos, A. (2021). Antimicrobial potential of strontium hydroxide on bacteria associated with peri-implantitis. *Antibiotics (Basel, Switzerland), 10*(2), 10.3390/antibiotics10020150.

Amano, A. (2003). Molecular interaction of porphyromonas gingivalis with host cells: Implication for the microbial pathogenesis of periodontal disease. *Journal of Periodontology, 74*(1), 90-96.

Anselme, K., Bigerelle, M., Noel, B., Dufresne, E., Judas, D., Iost, A., & Hardouin, P. (2000). Qualitative and quantitative study of human osteoblast adhesion on materials with various surface roughnesses. *Journal of Biomedical Materials Research, 49*(2), 155-166.

Araujo, M. G., & Lindhe, J. (2018). Peri-implant health. *Journal of Periodontology, 89*(Suppl 1), 249-256.

Åstrand, P., Anzén, B., Karlsson, U., Sahlholm, S., Svärdström, P., & Hellem, S. (2000). Nonsubmerged implants in the treatment of the edentulous upper jaw: A prospective clinical and radiographic study of ITI Implants—Results after 1 year. *Clinical Implant Dentistry and Related Research, 2*(3), 166-174.

Atieh, M. A., Alsabeeha, N. H. M., Faggion Jr., C. M., & Duncan, W. J. (2013). The frequency of peri-implant diseases: A systematic review and meta-analysis. *Journal of Periodontology, 84*(11), 1586-1598.

Banerjee, A., Hajatdoost-Sani, M., Farrell, S., & Thompson, I. (2010). A clinical evaluation and comparison of bioactive glass and sodium bicarbonate air-polishing powders. *Journal of Dentistry, 38*(6), 475-479.

Bautista, & Bautista, C. (1991). Isolation of a novel insulin-like growth factor (IGF) binding protein from human bone: A potential candidate for fixing IGF-II in human bone. *Biochemical and Biophysical Research Communications, 176*(2), 756-763.

Becker, W., Becker, B. E., Ricci, A., Bahat, O., Rosenberg, E., Rose, L. F., Handelsman, M., & Israelson, H. (2000). A prospective multicenter clinical trial comparing one- and two-stage titanium screw-shaped fixtures with one-stage plasma-sprayed solid-screw fixtures. *Clinical Implant Dentistry and Related Research, 2*(3), 159-165.

Berglundh, T., Abrahamsson, I., Lang, N. P., & Lindhe, J. (2003). De novo alveolar bone formation adjacent to endosseous implants. *Clinical Oral Implants Research, 14*(3), 251-262.

Berglundh, T., Abrahamsson, I., Welander, M., Lang, N. P., & Lindhe, J. (2007). Morphogenesis of the peri-implant mucosa: An experimental study in dogs. *Clinical Oral Implants Research, 18*(1), 1-8.

Berglundh, T., Armitage, G., Araujo, M.G., Avila-Ortiz, G., Blanco, J., et al. (2018). Peri-implant diseases and conditions: Consensus report of workgroup 4 of the 2017 world workshop on the classification of periodontal and peri-implant diseases and conditions. *Journal of Clinical Periodontology, 45*(suppl 1), 286-291.

Berglundh, T., Gislason, Ö, Lekholm, U., Sennerby, L., & Lindhe, J. (2004). Histopathological observations of human periimplantitis lesions. *Journal of Clinical Periodontology, 31*(5), 341-347.

Berglundh, T., Lindhe, J., Ericsson, I., Marinello, C. P., Liljenberg, B., & Thornsen, P. (1991). The soft tissue barrier at implants and teeth. *Clinical Oral Implants Research, 2*(2), 81-90.

Berglundh, T., Zitzmann, N. U., & Donati, M. (2011). Are peri-implantitis lesions different from periodontitis lesions? *Journal of Clinical Periodontology, 38*, 188-202.

Bhardwaj, S., & Prabhuji, M. L. V. (2013). Comparative volumetric and clinical evaluation of peri-implant sulcular fluid and gingival crevicular fluid. *Journal of Periodontal & Implant Science, 43*(5), 233-242.

Blatt, S., Pabst, A. M., Schiegnitz, E., Hosang, M., Ziebart, T., Walter, C., Al-Nawas, B., & Klein, M. O. (2018). Early cell response of osteogenic cells on differently modified implant surfaces: Sequences of cell proliferation, adherence and differentiation. *Journal of Cranio-Maxillofacial Surgery, 46*(3), 453-460.

Bonnelye, E., Chabadel, A., Saltel, F., & Jurdic, P. (2008). Dual effect of strontium ranelate: Stimulation of osteoblast differentiation and inhibition of osteoclast formation and resorption in vitro. *Bone, 42*(1), 129-138.

Bornstein, M. M., Valderrama, P., Jones, A. A., Wilson, T. G., Seibl, R., & Cochran, D. L. (2008). Bone apposition around two different sandblasted and acid-etched titanium implant surfaces: A histomorphometric study in canine mandibles. *Clinical Oral Implants Research, 19*(3), 233-241.

Bostanci, N., & Belibasakis, G. N. (2012). Porphyromonas gingivalis: An invasive and evasive opportunistic oral pathogen. *FEMS Microbiology Letters, 333*(1), 1-9.

Brånemark, P. I., Adell, R., Albrektsson, T., Lekholm, U., Lundkvist, S., & Rockler, B. (1983). Osseointegrated titanium fixtures in the treatment of edentulousness. *Biomaterials, 4*(1), 25-28.

Branemark, P. I., Hansson, B. O., Adell, R., Breine, U., Lindstrom, J., Hallen, O., & Ohman, A. (1977). Osseointegrated implants in the treatment of the edentulous jaw. experience from a 10-year period. *Scandinavian Journal of Plastic and Reconstructive Surgery. Supplementum, 16*, 1-132.

Brett, P. M., Harle, J., Salih, V., Mihoc, R., Olsen, I., Jones, F. H., & Tonetti, M. (2004). Roughness response genes in osteoblasts. *Bone, 35*(1), 124-133.

Bullon, P., Fioroni, M., Goteri, G., Rubini, C., & Battino, M. (2004). Immunohistochemical analysis of soft tissues in implants with healthy and peri-implantitis condition, and aggressive periodontitis. *Clinical Oral Implants Research, 15*(5), 553-559.

Buser, D., Broggini, N., Wieland, M., Schenk, R.K., Denzer, A.J., Cochran, D.L., Hoffmann, B., Lussi, A. & Steinemann, S.G. (2004). Enhanced bone apposition to a chemically modified sla titanium surface. *J Den Res*, 83(7), 529–533.

Buser, D., Janner, S. F. M., Wittneben, J., Brägger, U., Ramseier, C. A., & Salvi, G. E. (2012). 10-year survival and success rates of 511 titanium implants with a sandblasted and acid-etched surface: A retrospective study in 303 partially edentulous patients. *Clinical Implant Dentistry and Related Research, 14*(6), 839-851.

Busscher, H. J., Rinastiti, M., Siswomihardjo, W., & van der Mei, H C. (2010). Biofilm formation on dental restorative and implant materials. *Journal of Dental Research, 89*(7), 657-665.

Carcuac, O., Abrahamsson, I., Albouy, J. P., Linder, E., Larsson, L., & Berglundh, T. (2013). Experimental periodontitis and peri-implantitis in dogs. *Clinical Oral Implants Research, 24*(4), 363-371.

Carcuac, O., & Berglundh, T. (2014). Composition of human peri-implantitis and periodontitis lesions. *J Den Res, 93*(11), 1083-1088.

Carlsson, L., Röstlund, T., Albrektsson, B., & Albrektsson, T. (1988). Implant fixation improved by close fit cylindrical implant – bone interface studied in rabbits. *Null, 59*(3), 272-275.

Casado, P. L., Otazu, I. B., Balduino, A., de Mello, W., Barboza, E. P., & Duarte, M. E. (2011). Identification of periodontal pathogens in healthy periimplant sites. *Implant Dentistry, 20*(3), 226-235.

Casarin, R. C. V., Del Peloso Ribeiro, É, Mariano, F. S., Nociti Jr, F. H., Casati, M. Z., & Gonçalves, R. B. (2010). Levels of aggregatibacter actinomycetemcomitans, porphyromonas gingivalis, inflammatory cytokines and species-specific immunoglobulin G in generalized aggressive and chronic periodontitis. *Journal of Periodontal Research, 45*(5), 635-642.

Chatzistavrou, X., Velamakanni, S., DiRenzo, K., Lefkelidou, A., Fenno, J. C., Kasuga, T., Boccaccini, AR., & Papagerakis, P. (2015). Designing dental composites with bioactive and bactericidal properties. *Mater Sci Eng.C, Mater Biol Appl, 52*, 267-272.

Chen, C. S., Mrksich, M., Huang, S., Whitesides, G. M., & Ingber, D. E. (1997). Geometric control of cell life and death. *Science, 276*(5317), 1425-8.

Civantos, A., Martinez-Campos, E., Ramos, V., Elvira, C., Gallardo, A., & Abarrategi, A. (2017). Titanium coatings and surface modifications: Toward clinically useful bioactive implants. *ACS Biomaterials Science & Engineering, 3*(7), 1245-1261.

Collier, F. M., Huang, W. H., Holloway, W. R., Hodge, J. M., Gillespie, M. T., Daniels, L. L., et al. Nicholson, G. C. (1998). Osteoclasts from human giant cell tumors of bone lack estrogen receptors. *Endocrinology, 139*(3), 1258-1267.

Coppenhagen-Glazer, S., Sol, A., Abed, J., Naor, R., Zhang, X., Han, Y. W., & Bachrach, G. (2015). Fap2 of fusobacterium nucleatum is a galactose-inhibitable adhesin involved in coaggregation, cell adhesion, and preterm birth. *Infection and Immunity, 83*(3), 1104-1113.

Dabdoub, S. M., Ganesan, S. M., & Kumar, P. S. (2016). Comparative metagenomics reveals taxonomically idiosyncratic yet functionally congruent communities in periodontitis. *Scientific Reports, 6*(1), 38993.

D'Alessio, L., Teghil, R., Zaccagnino, M., Zaccardo, I., Ferro, D., & Marotta, V. (1999). Pulsed laser ablation and deposition of bioactive glass as coating material for biomedical applications. *Applied Surface Science, 138-139*, 527-532.

Datta, H. K., Ng, W. F., Walker, J. A., Tuck, S. P., & Varanasi, S. S. (2008). The cell biology of bone metabolism. *Journal of Clinical Pathology, 61*(5), 577-587.

Davies, J. E. (2003). Understanding peri-implant endosseous healing. *Journal of Dental Education, 67*(8), 932-949.

de Jong, H. P., van Pelt, A. W. J., & Arends, J. (1982). Contact angle measurements on human enamel - an in vitro study of influence of pellicle and storage period. *J Dent Res, 61*(1), 11-13.

Decker, E., Dietrich, I., Klein, C., & von Ohle, C. (2011). Dynamic production of soluble extracellular polysaccharides by *streptococcus mutans*. *Int J Dent, 2011*, 435830.

Derks, J., & Tomasi, C. (2015). Peri-implant health and disease. A systematic review of current epidemiology. *Journal of Clinical Periodontology, 42*, S158-S171.

Dhir, S. (2013). Biofilm and dental implant: The microbial link. *Journal of Indian Society of Periodontology, 17*(1), 5-11.

Diaz, P. I. (2012). Microbial diversity and interactions in subgingival biofilm communities. *Frontiers of Oral Biology, 15*, 17-40.

Diaz, P. I., Chalmers, N. I., Rickard, A. H., Kong, C., Milburn, C. L., Palmer, R. J., & Kolenbrander, P. E. (2006). Molecular characterization of subject-specific oral microflora during initial colonization of enamel. *Applied and Environmental Microbiology, 72*(4), 2837-2848.

Diaz, P. I., Zilm, P. S., & Rogers, A. H. (2002). Fusobacterium nucleatum supports the growth of porphyromonas gingivalis in oxygenated and carbon-dioxide-depleted environments. *Microbiology (Reading, England), 148*(Pt 2), 467-472.

Dige, I., Nilsson, H., Kilian, M., & Nyvad, B. (2007). In situ identification of streptococci and other bacteria in initial dental biofilm by confocal laser scanning microscopy and fluorescence in situ hybridization. *European Journal of Oral Sciences, 115*(6), 459-467.

Dohan Ehrenfest, D. M., Coelho, P. G., Kang, B., Sul, Y., & Albrektsson, T. (2010). Classification of osseointegrated implant surfaces: Materials, chemistry and topography. *Trends in Biotechnology, 28*(4), 198-206.

Donlan, R. M. (2002). Biofilms: Microbial life on surfaces. *Emerging Infectious Diseases, 8*(9), 881-890.

Ellingsen, J. E., Thomsen, P., & Lyngstadaas, S. P. (2006). Advances in dental implant materials and tissue regeneration. *Periodontology 2000, 41*(1), 136-156.

Elter, C., Heuer, W., Demling, A., Hannig, M., Heidenblut, T., Bach, F. W., & Stiesch-Scholz, M. (2008). Supra- and subgingival biofilm formation on implant abutments with different surface characteristics. *The International Journal of Oral & Maxillofacial Implants*, 23(2), 327–334.

Eriksson, C., Nygren, H., & Ohlson, K. (2004). Implantation of hydrophilic and hydrophobic titanium discs in rat tibia: Cellular reactions on the surfaces during the first 3 weeks in bone. *Biomaterials, 25*(19), 4759-4766.

Esposito, M., Grusovin, M. G., & Worthington, H. V. (2012). Interventions for replacing missing teeth: Treatment of peri-implantitis. *Cochrane Database of Systematic Reviews,*18;1 (1) CD004970.

Estefanía-Fresco, R., García-de-la-Fuente, A. M., Egaña-Fernández-Valderrama, A., Bravo, M., & Aguirre-Zorzano, L. (2019). One-year results of a nonsurgical treatment protocol for peri-implantitis. A retrospective case series. *Clinical Oral Implants Research, 30*(7), 702-712.

Filiaggi, M. J., Coombs, N. A., & Pilliar, R. M. (1991). Characterization of the interface in the plasma-sprayed HA coating/ti-6Al-4V implant system. *Journal of Biomedical Materials Research, 25*(10), 1211-1229.

Fischer, K., & Stenberg, T. (2012). Prospective 10-year cohort study based on a randomized controlled trial (RCT) on implant-supported full-arch maxillary prostheses. part 1: Sandblasted and acid-etched implants and mucosal tissue. *Clinical Implant Dentistry and Related Research, 14*(6), 808-815.

Foppiano, S., Marshall, S. J., Marshall, G. W., Saiz, E., & Tomsia, A. P. (2007). Bioactive glass coatings affect the behavior of osteoblast-like cells. *Acta Biomaterialia, 3*(5), 765-771.

Forssten, S. D., Björklund, M., & Ouwehand, A. C. (2010). Streptococcus mutans, caries and simulation models. *Nutrients, 2*(3), 290-298.

Fouda, M., Nemat, A., Gawish, A., & Baiuomy, A. R. (2009). Does the coating of titanium implants by hydroxyapatite affect the elaboration of free radicals. An experimental study. Aust J Basic Appl Sci, 3(2), 1122-1129.

Froum, S. J., Froum, S. H., & Rosen, P. S. (2015). A regenerative approach to the successful treatment of peri-implantitis: A consecutive series of 170 implants in 100 patients with 2- to 10-year follow-up. *The International Journal of Periodontics & Restorative Dentistry, 35*(6), 857-863.

Froum, S. J., & Rosen, P. S. (2012). A proposed classification for peri-implantitis. *The International Journal of Periodontics & Restorative Dentistry, 32*(5), 533-540.

Fu, T., Alajmi, Z., Shen, Y., Wang, L., Yang, S., & Zhang, M. (2017). Sol-gel preparation and properties of ag-containing bioactive glass films on titanium. *International Journal of Applied Ceramic Technology, 14*(6), 1117-1124.

Fürst, M. M., Salvi, G. E., Lang, N. P., & Persson, G. R. (2007). Bacterial colonization immediately after installation on oral titanium implants. *Clinical Oral Implants Research, 18*(4), 501-508.

Ghassib, I., Chen, Z., Zhu, J., & Wang, H. L. (2019). Use of IL-1 beta, IL-6, TNF-alpha, and MMP-8 biomarkers to distinguish peri-implant diseases: A systematic review and meta-analysis. *Clinical Implant Dentistry and Related Research, 21*(1), 190-207.

Gillam, D. G. (1997). Clinical trial designs for testing of products for dentine hypersensitivity--a review. *The Journal of the Western Society of Periodontology/Periodontal Abstracts, 45*(2), 37-46.

Gittens, R. A., Olivares-Navarrete, R., Chenh, H., Anderson, D.M., McLachlan, T., et al. (2013). The roles of titanium surface micro/nanotopography and wettability on the differential response of human osteoblast lineage cells. *Acta Biomaterialia, 9*(4), 6268-6277.

Gjorgievska, E., & Nicholson, J. W. (2011). Prevention of enamel demineralization after tooth bleaching by bioactive glass incorporated into toothpaste. *Australian Dental Journal, 56*(2), 193-200.

Gottlander, M., Johansson, C. B., & Albrektsson, T. (1997). Short- and long-term animal studies with a plasma-sprayed calcium phosphate-coated implant. *Clinical Oral Implants Research, 8*(5), 345-351.

Gualini, F., & Berglundh, T. (2003). Immunohistochemical characteristics of inflammatory lesions at implants. *Journal of Clinical Periodontology, 30*(1), 14-18.

Gundoğar, H., & Uzunkaya, M. (2021). The effect of periodontal and peri-implanter health on IL-1² and TNF- α levels in gingival crevicular and peri-implanter sulcus fluid: A cross-sectional study. Odovtos International Journal of Dental Sciences, 23(1), 168-177.

Guo, L., Shokeen, B., He, X., Shi, W., & Lux, R. (2017). Streptococcus mutans SpaP binds to RadD of fusobacterium nucleatum ssp. polymorphum. *Molecular Oral Microbiology, 32*(5), 355-364.

Gupta, S., Dahiya, V., & Shukla, P. (2014). Surface topography of dental implants: A review. *Journal of Dental Implants, 4*(1), 66-71

Gur, C., Ibrahim, Y., Isaacson, B., Yamin, R., Abed, J., Gamliel, M., . . . Mandelboim, O. (2015). Binding of the Fap2 protein of fusobacterium nucleatum to human inhibitory receptor TIGIT protects tumors from immune cell attack. *Immunity, 42*(2), 344-355.

Hajishengallis, G. (2014). The inflammophilic character of the periodontitis-associated microbiota. *Molecular Oral Microbiology, 29*(6), 248-257.

Hajishengallis, G., Darveau, R. P., & Curtis, M. A. (2012). The keystone-pathogen hypothesis. *Nature Reviews.Microbiology, 10*(10), 717-725.

Hajishengallis, G., & Lamont, R. J. (2016). Dancing with the stars: How choreographed bacterial interactions dictate nososymbiocity and give rise to keystone pathogens, accessory pathogens, and pathobionts. *Trends in Microbiology, 24*(6), 477-489.

Hamada, S., & Slade, H. D. (1980). Biology, immunology, and cariogenicity of streptococcus mutans. *Microbiological Reviews, 44*(2), 331-384.

Hanada, N., & Kuramitsu, H. K. (1988). Isolation and characterization of the streptococcus mutans gtfC gene, coding for synthesis of both soluble and insoluble glucans. *Infection and Immunity, 56*(8), 1999-2005.

Hanada, N., & Kuramitsu, H. K. (1989). Isolation and characterization of the streptococcus mutans gtfD gene, coding for primer-dependent soluble glucan synthesis. *Infection and Immunity, 57*(7), 2079-2085.

He, G., Pearce, E. I. F., & Sissons, C. H. (2002). Inhibitory effect of ZnCl2 on glycolysis in human oral microbes. *Archives of Oral Biology, 47*(2), 117-129.

Heitz-Mayfield, L. J., & Mombelli, A. (2014). The therapy of peri-implantitis: A systematic review. *The International Journal of Oral & Maxillofacial Implants, 29 Suppl*, 325-345.

Heitz-Mayfield, L. J. A., & Salvi, G. E. (2018). Peri-implant mucositis. *Journal of Clinical Periodontology, 45 Suppl 20*, S237-S245.

Hench, L. L. (1998). Bioceramics. *Journal of the American Ceramic Society, 81*(7), 1705-1728.

Hench, L. L. (2006). The story of bioglass. *Journal of Materials Science.Materials in Medicine, 17*(11), 967-978.

Hench, L. L. (2009). *Genetic design of bioactive glass. J. Eur. Ceram. Soc.* 29(7), 1257-1265.

Hench, L. L., & Polak, J. M. (2002). Third-generation biomedical materials. *Science (New York, N.Y.), 295*(5557), 1014-1017.

Hench, L. L., & Wilson, J. (1993). An introduction to bioceramics. Singapore; River Edge, N.J.: World Scientific.

Hong, J., Andersson, J., Ekdahl, K. N., Elgue, G., Axen, N., Larsson, R., & Nilsson, B. (1999). Titanium is a highly thrombogenic biomaterial: Possible implications for osteogenesis. *Thrombosis and Haemostasis, 82*(1), 58-64.

Hu, S., Chang, J., Liu, M., & Ning, C. (2009). Study on antibacterial effect of 45S5 bioglass®. *Journal of Materials Science: Materials in Medicine, 20*(1), 281-286.

Hung, K., Lai, H., & Feng, H. (2017). Characteristics of RF-sputtered thin films of calcium phosphate on titanium dental implants. *Coatings, 7*, 126.

Imai, Y., & Nose, Y. (1972). A new method for evalution of antithrombogenicity of materials. *Journal of Biomedical Materials Research, 6*(3), 165-172.

Inaba, H., Nakano, K., Kato, T., Nomura, R., Kawai, S., Kuboniwa, M., Ishihara, K., Ooshima, T., & Amano, A. (2008). Heterogenic virulence and related factors among clinical isolates of porphyromonas gingivalis with type II fimbriae. *Oral Microbiology and Immunology, 23*(1), 29-35.

Irshad, M., van der Reijden, Wil A., Crielaard, W., & Laine, M. L. (2012). In vitro invasion and survival of porphyromonas gingivalis in gingival fibroblasts; role of the capsule. *Archivum Immunologiae Et Therapiae Experimentalis*, 60(6), 469–476.

Isehed, C., Holmlund, A., Renvert, S., Svenson, B., Johansson, I., & Lundberg, P. (2016). Effectiveness of enamel matrix derivative on the clinical and microbiological outcomes following surgical regenerative treatment of peri-implantitis. A randomized controlled trial. *Journal of Clinical Periodontology, 43*(10), 863-873.

Ishikawa, K., Miyamoto, Y., Yuasa, T., Ito, A., Nagayama, M., & Suzuki, K. (2002). Fabrication of zn containing apatite cement and its initial evaluation using human osteoblastic cells. *Biomaterials, 23*(2), 423-428.

Ivanovski, S., & Lee, R. (2018). Comparison of peri-implant and periodontal marginal soft tissues in health and disease. *Periodontology 2000, 76*(1), 116-130.

Jemat, A., Ghazali, M. J., Razali, M., & Otsuka, Y. (2015). Surface modifications and their effects on titanium dental implants. *BioMed Research International, 2015*, 791725.

Jepsen, S., & Jepsen. (2015). Primary prevention of peri-implantitis: Managing peri-implant mucositis. *Journal of Clinical Periodontology, 42*(S16), S152-S157.

Junker, R., Dimakis, A., Thoneick, M., & Jansen, J. (2009). Effects of implant surface coatings and composition on bone integration: A systematic review. *Clinical Oral Implants Research, 20 Suppl 4*, 185-206.

Kamitakahara, M., Ohtsuki, C., Inada, H., Tanihara, M., & Miyazaki, T. (2006). Effect of ZnO addition on bioactive CaO–SiO2–P2O5–CaF2 glass–ceramics containing apatite and wollastonite. *Acta Biomaterialia, 2*(4), 467-471.

Kaplan, C. W., Lux, R., Haake, S. K., & Shi, W. (2009). The fusobacterium nucleatum outer membrane protein RadD is an arginine-inhibitable adhesin required for inter-species adherence and the structured architecture of multispecies biofilm. *Molecular Microbiology, 71*(1), 35-47.

Kapoor, S., Goel, A., Tilocca, A., Dhuna, V., Bhatia, G., Dhuna, K., & Ferreira, J. M. F. (2014). Role of glass structure in defining the chemical dissolution behavior, bioactivity and antioxidant properties of zinc and strontium co-doped alkali-free phosphosilicate glasses. *Acta Biomaterialia, 10*(7), 3264-3278.

Keim, D., Nickles, K., Dannewitz, B., Ratka, C., Eickholz, P., & Petsos, H. (2019). In vitro efficacy of three different implant surface decontamination methods in three different defect configurations. *Clinical Oral Implants Research, 30*(6), 550-558.

Khoury, F., & Buchmann, R. (2001). Surgical therapy of peri-implant disease: A 3-year follow-up study of cases treated with 3 different techniques of bone regeneration. *Journal of Periodontology, 72*(11), 1498-1508.

Kogan, S., Sood, A., & Garnick, M. S. (2017). Zinc and wound healing: A review of zinc physiology and clinical applications. *Wounds : A Compendium of Clinical Research and Practice, 29*(4), 102-106.

Kokubo, T., Kushitani, H., Sakka, S., Kitsugi, T., & Yamamuro, T. (1990). Solutions able to reproduce in vivo surface-structure changes in bioactive glass-ceramic A-W. *Journal of Biomedical Materials Research, 24*(6), 721-734.

Koller, G., Cook, R. J., Thompson, I. D., Watson, T. F., & Di Silvio, L. (2007). Surface modification of titanium implants using bioactive glasses with air abrasion technologies. *J Mater Sci Mater Med*., 18(12), 2291-2296.

Koo, H., Falsetta, M. L., & Klein, M. I. (2013). The exopolysaccharide matrix: A virulence determinant of cariogenic biofilm. *Journal of Dental Research, 92*(12), 1065-1073.

Koo, H., Xiao, J., Klein, M. I., & Jeon, J. G. (2010). Exopolysaccharides produced by streptococcus mutans glucosyltransferases modulate the establishment of microcolonies within multispecies biofilms. *Journal of Bacteriology, 192*(12), 3024-3032.

Krzyściak, W., Jurczak, A., Kościelniak, D., Bystrowska, B., & Skalniak, A. (2014). The virulence of streptococcus mutans and the ability to form biofilms. *European Journal of Clinical Microbiology & Infectious Diseases, 33*(4), 499-515.

Kumar, P. S., Mason, M. R., Brooker, M. R., & O'Brien, K. (2012). Pyrosequencing reveals unique microbial signatures associated with healthy and failing dental implants. *Journal of Clinical Periodontology, 39*(5), 425-433.

Lacefield, W. R. (1999). Materials characteristics of uncoated/ceramic-coated implant materials. *Advances in Dental Research, 13*, 21-26.

Lafaurie, G. I., Sabogal, M. A., Castillo, D. M., Rincón, M. V., Gómez, L. A., Lesmes, Y. A., & Chambrone, L. (2017). Microbiome and microbial biofilm profiles of peri-implantitis: A systematic review. *Journal of Periodontology, 88*(10), 1066-1089.

Lai, H., Zhuang, L., Liu, X., Wieland, M., Zhang, Z., & Zhang, Z. (2010). The influence of surface energy on early adherent events of osteoblast on titanium substrates. *Journal of Biomedical Materials Research Part A, 93A*(1), 289-296.

Lamont, R. J., & Hajishengallis, G. (2015). Polymicrobial synergy and dysbiosis in inflammatory disease. *Trends in Molecular Medicine, 21*(3), 172-183.

Lamont, R. J., Koo, H., & Hajishengallis, G. (2018). The oral microbiota: Dynamic communities and host interactions. *Nature Reviews.Microbiology, 16*(12), 745-759.

Lang, N. P., Salvi, G. E., & Sculean, A. (2019). Nonsurgical therapy for teeth and implants—When and why? *Periodontology 2000, 79*(1), 15-21.

Larjava, H., Koivisto, L., Hakkinen, L., & Heino, J. (2011). Epithelial integrins with special reference to oral epithelia. *Journal of Dental Research, 90*(12), 1367-1376.

Larsson, L., Decker, A. M., Nibali, L., Pilipchuk, S. P., Berglundh, T., & Giannobile, W. V. (2016). Regenerative medicine for periodontal and peri-implant diseases. Journal of Dental Research, 95(3), 255-266.

Le Guéhennec, L., Soueidan, A., Layrolle, P., & Amouriq, Y. (2007). Surface treatments of titanium dental implants for rapid osseointegration. *Dental Materials, 23*(7), 844-854.

Lee, A., & Wang, H. (2010). Biofilm related to dental implants. *Implant Dentistry, 19*, 387-93.

Lee, C., Huang, Y., Zhu, L., & Weltman, R. (2017). Prevalences of peri-implantitis and peri-implant mucositis: Systematic review and meta-analysis. *Journal of Dentistry, 62*, 1-12.

Lee, H. J., Yang, I. H., Kim, S. K., Yeo, I. S., & Kwon, T. K. (2015). In vivo comparison between the effects of chemically modified hydrophilic and anodically oxidized titanium surfaces on initial bone healing. *Journal of Periodontal & Implant Science, 45*(3), 94-100.

Lemos, J. A., & Burne, R. A. (2008). A model of efficiency: Stress tolerance by streptococcus mutans. *Microbiology, 154*(11), 3247-3255.

Leonhardt, A., Renvert, S., & Dahlen, G. (1999). Microbial findings at failing implants. *Clinical Oral Implants Research, 10*(5), 339-345.

Lepparanta, O., Vaahtio, M., Peltola, T., Zhang, D., Hupa, L., Hupa, M., Ylänen, H., Salonen, J. I., Viljanen, M. K., & Eerola, E. (2008). Antibacterial effect of bioactive glasses on clinically important anaerobic bacteria in vitro. *Journal of Materials Science.Materials in Medicine, 19*(2), 547-551.

Li, D., Ferguson, S. J., Beutler, T., Cochran, D. L., Sittig, C., Hirt, H. P., & Buser, D. (2002). Biomechanical comparison of the sandblasted and acid-etched and the machined and acid-etched titanium surface for dental implants. *Journal of Biomedical Materials Research, 60*(2), 325-332.

Lindhe, J., Berglundh, T., Ericsson, I., Liljenberg, B., & Marinello, C. (1992). Experimental breakdown of peri-implant and periodontal tissues. A study in the beagle dog. *Clinical Oral Implants Research, 3*(1), 9-16.

Listgarten, M. A., Lang, N. P., Schroeder, H. E., & Schroeder, A. (1991). Periodontal tissues and their counterparts around endosseous implants. *Clinical Oral Implants Research, 2*(3), 1-19.

Liu, X., Chu, P. K., & Ding, C. (2004). Surface modification of titanium, titanium alloys, and related materials for biomedical applications. *Materials Science and Engineering: R: Reports, 47*(3), 49-121.

Liu, X., Poon, R. W. Y., Kwok, S. C. H., Chu, P. K., & Ding, C. (2004). Plasma surface modification of titanium for hard tissue replacements. *Surface and Coatings Technology, 186*(1), 227-233.

Lovelace, T. B., Mellonig, J. T., Meffert, R. M., Jones, A. A., Nummikoski, P. V., & Cochran, D. L. (1998). Clinical evaluation of bioactive glass in the treatment of periodontal osseous defects in humans. *Journal of Periodontology, 69*(9), 1027-1035.

MacDonald, R. S. (2000). The role of zinc in growth and cell proliferation. *The Journal of Nutrition, 130*(5), 1500-1508.

Maeda, T., & Maeda. (2004). Induction of osteoblast differentiation indices by statins in MC3T3-E1 cells. *Journal of Cellular Biochemistry, 92*(3), 458-471.

Mahanonda, R., Seymour, G. J., Powell, L. W., Good, M. F., & Halliday, J. W. (1991). Effect of initial treatment of chronic inflammatory periodontal disease on the frequency of peripheral blood T-lymphocytes specific to periodontopathic bacteria. *Oral Microbiology and Immunology, 6*(4), 221-227.

Marsh, P. (2005). Dental plaque: Biological significance of a biofilm and community life-style. *Journal of Clinical Periodontology, 32*(Suppl 6), 7-15.

Max, B. (2015). Influence of zinc and magnesium substitution on ion release from bioglass 45S5 at physiological and acidic pH. *Biomedical Glasses, 1*(1), 93-107.

Meirelles, L., Currie, F., Jacobsson, M., Albrektsson, T. & Wennerberg, A. (2008). The effect of chemical and nano topographical modifications on early stage of osseointegration. *Int J Oral Maxillofac Implants*. 23(4), 641–647.

Mohd Bakhori, S. K., Mahmud, S., Ling, C. A., Sirelkhatim, A. H., Hasan, H., Mohamad, D., Masudi, S. M., Seeni, A & Abd Rahman, R. (2017). In-vitro efficacy of different morphology zinc oxide nanopowders on streptococcus sobrinus and streptococcus mutans. *Materials Science and Engineering: C, 78*(1), 868-877.

Mombelli, A. (2002). Microbiology and antimicrobial therapy of peri-implantitis. *Periodontology 2000, 28*(1), 177-189.

Mortazavi, V., Nahrkhalaji, M. M., Fathi, M. H., Mousavi, S. B., & Esfahani, B. N. (2010). Antibacterial effects of sol-gel-derived bioactive glass nanoparticle on aerobic bacteria. *Journal of Biomedical Materials Research Part A, 94A*(1), 160-168.

Moritz, N., Rossi, S., Vedel, E., Tirri, T., Ylanen, H., Aro, H., & Närhi, T. (2004). Implants coated with bioactive glass by CO2-laser, an in vivo study. *Journal of Materials Science.Materials in Medicine, 15*(7), 795-802.

Munukka, E., Lepparanta, O., Korkeamäki, M., Vaahtio, M., Perltola, T., et al. (2008). Bactericidal effects of bioactive glasses on clinically important aerobic bacteria. *Journal of Materials Science.Materials in Medicine, 19*(1), 27-32.

Naik, B., Karunakar, P., Jayadev, M., & Marshal, V. R. (2013). Role of platelet rich fibrin in wound healing: A critical review. *Journal of Conservative Dentistry: JCD, 16*(4), 284-293.

Nakazato, G., Tsuchiya, H., Sato, M., & Yamauchi, M. (1989). In vivo plaque formation on implant materials. *The International Journal of Oral & Maxillofacial Implants, 4*(4), 321-326.

Nath, S. G., & Raveendran, R. (2013). Microbial dysbiosis in periodontitis. *Journal of Indian Society of Periodontology, 17*(4), 543-545.

Ning, C., Wang, X., Li, L., Zhu, Y., Li, M., et al. (2015). Concentration ranges of antibacterial cations for showing the highest antibacterial efficacy but the least cytotoxicity against mammalian cells: Implications for a new antibacterial mechanism. *Chemical Research in Toxicology, 28*(9), 1815-1822.

Nobbs, A. H., Lamont, R. J., & Jenkinson, H. F. (2009). Streptococcus adherence and colonization. *Microbiology and Molecular Biology Reviews: MMBR, 73*(3), 407-50, Table of Contents.

Nowicki, E. M., Shroff, R., Singleton, J. A., Renaud, D. E., Wallace, D., Drury, J., et al. (2018). Microbiota and metatranscriptome changes accompanying the onset of gingivitis. *mBio, 9*(2), e00575-18.

Okamoto, A. C., Gaetti-Jardim, E.,Jr, Cai, S., & Avila-Campos, M. J. (2000). Influence of antimicrobial subinhibitory concentrations on hemolytic activity and bacteriocin-like substances in oral fusobacterium nucleatum. *The New Microbiologica, 23*(2), 137-142.

Olivares-Navarrete, R., Hyzy, S., Hutton, D., Erdman, C., Wieland, M., Boyan, B., & Schwartz, Z. (2010). Direct and indirect effects of microstructured titanium substrates on the induction of mesenchymal stem cell differential towards the osteoblast lineage. *Biomaterials, 31*(10), 2728-35.

Ong, J. L., Carnes, D. L., & Bessho, K. (2004). Evaluation of titanium plasma-sprayed and plasma-sprayed hydroxyapatite implants in vivo. *Biomaterials, 25*(19), 4601-4606.

Ostomel, T., Shi, Q., Tsung, C., Liang, H., & Stucky, G. (2006). Spherical bioactive glass with enhanced rates of hydroxyapatite deposition and hemostatic activity. *Small, 2*(11), 1261-1265.

Ostrovskaya, L., Perevertailo, V., Ralchenko, V., Dementjev, A., & Loginova, O. (2002). Wettability and surface energy of oxidized and hydrogen plasma-treated diamond films. Diam. *Relat. Mater.*, 11 (3–6), 845-850

Pan, W., Wang, Q., & Chen, Q. (2019). The cytokine network involved in the host immune response to periodontitis. *International Journal of Oral Science, 11*(3), 30.

Park, J. Y., & Davies, J. E. (2000). Red blood cell and platelet interactions with titanium implant surfaces. *Clinical Oral Implants Research, 11*(6), 530-539.

Periodontitis. Current care recommendation. A working group set up by the Duodecim of the Finnish Medical Association and the Apollonia Association of the Finnish Dental Association. Helsinki: Finnish Medical Association Duodecim, 2019 (referenced December 11, 2019). Available on the Internet: www.kaypahoito.fi

Persson, G. R., & Renvert, S. (2014). Cluster of bacteria associated with peri-implantitis. *Clinical Implant Dentistry and Related Research, 16*(6), 783-793.

Phan, T., Buckner, T., Sheng, J., Baldeck, J. D., & Marquis, R. E. (2004). Physiologic actions of zinc related to inhibition of acid and alkali production by oral streptococci in suspensions and biofilms. *Oral Microbiology and Immunology, 19*(1), 31-38.

Ponsonnet, L., Reybier, K., Jaffrezic, N., Comte, V., Lagneau, C., Lissac, M., & Martelet, C. (2003). Relationship between surface properties (roughness, wettability) of titanium and titanium alloys and cell behaviour. *Materials Science and Engineering: C, 23*(4), 551-560.

Profeta, A. C. (2014). Dentine bonding agents comprising calcium-silicates to support proactive dental care: Origins, development and future. *Dental Materials Journal, 33*(4), 443-452.

Profeta, A. C., & Huppa, C. (2016). Bioactive-glass in oral and maxillofacial surgery. *Craniomaxillofacial Trauma & Reconstruction, 9*(1), 1-14.

Profeta, A. C., & Prucher, G. M. (2015). Bioactive-glass in periodontal surgery and implant dentistry. *Dental Materials Journal, 34*(5), 559-571.

Pussinen, P. J., Könönen, E., Paju, S., Hyvärinen, K., Gursoy, U. K., Huumonen, S., Knuuttila, M., Suominen, A. L. (2011). Periodontal pathogen carriage, rather than periodontitis, determines the serum antibody levels. *Journal of Clinical Periodontology, 38*(5), 405-411.

Ramanauskaite, A., Obreja, K., Sader, R., Khoury, F., Romanos, G., et al. (2019). Surgical treatment of periimplantitis with augmentative techniques. *Implant Dentistry, 28*(2), 187-209.

Renvert, S., & Persson, G. R. (2009). Periodontitis as a potential risk factor for peri-implantitis. *Journal of Clinical Periodontology, 36* (suppl 10), 9-14.

Renvert, S., Persson, G. R., Pirih, F. Q., & Camargo, P. M. (2018). Peri-implant health, peri-implant mucositis, and peri-implantitis: Case definitions and diagnostic considerations. *Journal of Clinical Periodontology, 45*(suppl 20), 278-285.

Renvert, S., Roos-Jansåker, A., & Claffey, N. (2008). Non-surgical treatment of peri-implant mucositis and peri-implantitis: A literature review. *Journal of Clinical Periodontology, 35*(suppl 8), 305–315.

Rompen, E., Domken, O., Degidi, M., Pontes, A. E., & Piattelli, A. (2006). The effect of material characteristics, of surface topography and of implant components and connections on soft tissue integration: a literature review. *Clinical Oral Implants Research*, 17(2), 55–67.

Rosales-Leal, J. I., Rodríguez-Valverde, M. A., Mazzaglia, P.J., Ramon-Torregrosa, L., Diaz-Rodriguez, O., et al. (2010). Effect of roughness, wettability and morphology of engineered titanium surfaces on osteoblast-like cell adhesion. *Colloids and Surfaces A: Physicochemical and Engineering Aspects, 365*(1), 222-229.

Rupp, F., Gittens, R. A., Scheideler, L., Marmur, A., Boyan, B. D., Schwartz, Z., & Geis-Gerstorfer, J. (2014). A review on the wettability of dental implant surfaces I: Theoretical and experimental aspects. *Acta Biomaterialia, 10*(7), 2894-2906.

Salvi, G. E., Cosgarea, R., & Sculean, A. (2017). Prevalence and mechanisms of peri-implant diseases. *Journal of Dental Research, 96*(1), 31-37.

Sawai, J., Shoji, S., Igarashi, H., Hashimoto, A., Kokugan, T., Shimizu, M., & Kojima, H. (1998). Hydrogen peroxide as an antibacterial factor in zinc oxide powder slurry. *J. Ferment. Bioeng*. 86 (5), 521-522.

Schenk, R. K., & Buser, D. (1998). Osseointegration: A reality. *Periodontology 2000, 17*(1), 22-35.

Schou, S., Holmstrup, P., Worthington, H. V., & Esposito, M. (2006). Outcome of implant therapy in patients with previous tooth loss due to periodontitis. *Clinical Oral Implants Research, 17*(suppl 2), 104-123.

Schrader, M. E. (1982). On adhesion of biological substances to low energy solid surfaces. *Journal of Colloid and Interface Science, 88*(1), 296-297.

Schwartz, Z., Lohmann, C., Vocke, A. K., Sylvia, V., Cochran, D., Dean, D., & Boyan, B. (2001). Osteoblast response to titanium surface roughness and 1alpha,25-(OH)(2)D(3) is mediated through the mitogen-activated protein kinase (MAPK) pathway. *Journal of Biomedical Materials Research, 56*(3), 417-426.

Schwartz, Z., Raz, P., Zhao, G., Barak, Y., Tauber, M., Yao, H., & Boyan, B. D. (2008). Effect of micrometer-scale roughness of the surface of Ti6Al4V pedicle screws in vitro and in vivo. *The Journal of Bone and Joint Surgery.American Volume, 90*(11), 2485-2498.

Schwarz, F., Derks, J., Monje, A., & Wang, H. (2018). Peri-implantitis. *Journal of Periodontology, 89*(1), 267-290.

Schwarz, F., Herten, M., Sager, M., Bieling, K., Sculean, A., & Becker, J. (2007). Comparison of naturally occurring and ligature-induced peri-implantitis bone defects in humans and dogs. *Clinical Oral Implants Research, 18*(2), 161-170.

Schwarz, F., Mihatovic, I., Golubovic, V., Bradu, S., Sager, M., & Becker, J. (2015). Impact of plaque accumulation on the osseointegration of titanium-zirconium alloy and titanium implants. A histological and immunohistochemical analysis. *Clinical Oral Implants Research, 26*(11), 1281-1287.

Schwarz, F., Sahm, N., Schwarz, K., & Becker, J. (2010). Impact of defect configuration on the clinical outcome following surgical regenerative therapy of peri-implantitis. *Journal of Clinical Periodontology, 37*(5), 449-455.

Sergi, R., Bellucci, D., Salvatori, R., Maisetta, G., Batoni, G., & Cannillo, V. (2019). Zinc containing bioactive glasses with ultra-high crystallization temperature, good biological performance and antibacterial effects. *Materials Science and Engineering: C, 104*, 109910.

Seymour, G. J., & Gemmell, E. (2001). Cytokines in periodontal disease: Where to from here? *Acta Odontologica Scandinavica, 59*(3), 167-173.

Shalabi, M. M., Gortemaker, A., Van't Hof, M. A., Jansen, J. A., & Creugers, N. H. (2006). Implant surface roughness and bone healing: A systematic review. *Journal of Dental Research, 85*(6), 496-500.

Sharma, C. P. (1984). Surface--interface energy contributions to blood compatibility. *Biomaterials, Medical Devices, and Artificial Organs, 12*(3-4), 197-213.

Sherlock, O., Schembri, M. A., Reisner, A., & Klemm, P. (2004). Novel roles for the AIDA adhesin from diarrheagenic escherichia coli: Cell aggregation and biofilm formation. *Journal of Bacteriology, 186*(23), 8058-8065.

Shibli, J. A., Melo, L., Ferrari, D. S., Figueiredo, L. C., Faveri, M., & Feres, M. (2008). Composition of supra- and subgingival biofilm of subjects with healthy and diseased implants. *Clinical Oral Implants Research, 19*(10), 975-982.

Shibli, J. A., Vitussi, T. R., Garcia, R. V., Zenobio, E. G., Ota-Tsuzuki, C., Cassoni, A., Piattelli, A., & d'Avila, S. (2007). Implant surface analysis and microbiologic evaluation of failed implants retrieved from smokers. *The Journal of Oral Implantology, 33*(4), 232-238.

Šimek, M., Černák, M., Kylián, O., Foest, R., Hegemann, D., & Martini, R. (2019). White paper on the future of plasma science for optics and glass. *Plasma Processes and Polymers, 16*(1), 1700250.

Skallevold, H. E., Rokaya, D., Khurshid, Z., & Zafar, M. S. (2019). Bioactive glass applications in dentistry. *Int. J. Mol.r Sci, 20*(23), 5960.

Smeets, R., Stadlinger, B., Schwartz, F., Beck-Broichsitter, B., Jung, O., et al. (2016). Impact of dental implant surface modifications on osseointegration. *BioMed Research International, 2016*, 6285620.

Socransky, S. S., Haffajee, A. D., Cugini, M. A., Smith, C., & Kent Jr., R. L. (1998). Microbial complexes in subgingival plaque. *Journal of Clinical Periodontology, 25*(2), 134-144.

Sohrabi, K., Saraiya, V., Laage, T. A., Harris, M., Blieden, M., & Karimbux, N. (2012). An evaluation of bioactive glass in the treatment of periodontal defects: A meta-analysis of randomized controlled clinical trials. *Journal of Periodontology, 83*(4), 453-464.

Stan, G. E., Morosanu, C. O., Marcov, D. A., Pasuk, I., Miculescu, F., & Reumont, G. (2009). Effect of annealing upon the structure and adhesion properties of sputtered bio-glass/titanium coatings. *Applied Surface Science, 255*(22), 9132-9138.

Stoor, P., Apajalahti, S., & Kontio, R. (2017). Regeneration of cystic bone cavities and bone defects with bioactive glass S53P4 in the upper and lower jaws. *J Craniofac Surg*. 28(5):1197-205.

Stoor, P., Söderling, E., & Salonen, J. I. (1998). Antibacterial effects of a bioactive glass paste on oral microorganisms. *Acta Odontologica Scandinavica, 56*(3), 161-165.

Suarez, F., Monje, A., Galindo-Moreno, P., & Wang, H. (2013). Implant surface detoxification: A comprehensive review. *Implant Dentistry, 22*(5), 465-473.

Subramani, K., Jung, R. E., Molenberg, A., & Hammerle, C. H. (2009). Biofilm on dental implants: A review of the literature. *The International Journal of Oral & Maxillofacial Implants, 24*(4), 616-626.

Surmenev, R. A., Surmeneva, M. A., Grubova, I. Y., Chernozem, R. V., Krause, B., Baumbach, T., Loza, K., & Epple, M. (2017). RF magnetron sputtering of a hydroxyapatite target: A comparison study on polytetrafluorethylene and titanium substrates. *Applied Surface Science, 414*, 335-344.

Suzuki, N., Nakano, Y., Watanabe, T., Yoneda, M., Hirofuji, T., & Hanioka, T. (2018). Two mechanisms of oral malodor inhibition by zinc ions. *Journal of Applied Oral Science: 18*(26), e20170161-0161.

Tabanella, G., Nowzari, H., & Slots, J. (2009). Clinical and microbiological determinants of ailing dental implants. *Clinical Implant Dentistry and Related Research, 11*(1), 24-36.

Tamura, S., Yonezawa, H., Motegi, M., Nakao, R., Yoneda, S., Watanabe, H., Yamazaki, T., & Senpuku, H. (2009). Inhibiting effects of streptococcus salivarius on competence-stimulating peptide-dependent biofilm formation by streptococcus mutans. *Oral Microbiology and Immunology, 24*(2), 152-161.

Teughels, W., Van Assche, N., Sliepen, I., & Quirynen, M. (2006). Effect of material characteristics and/or surface topography on biofilm development. *Clinical Oral Implants Research, 17*(suppl 2), 68-81.

Thurnheer, T., Guggenheim, B., Gruica, B., & Gmür, R. (1999). Infinite serovar and ribotype heterogeneity among oral fusobacterium nucleatum strains? *Anaerobe, 5*(2), 79-92.

Ting, M., Jefferies, S. R., Xia, W., Engqvist, H., & Suzuki, J. B. (2017). Classification and effects of implant surface modification on the bone: Human Cell–Based in vitro studies. *Journal of Oral Implantology, 43*(1), 58-83.

Valderrama, P., & Wilson,Thomas G.,,Jr. (2013). Detoxification of implant surfaces affected by peri-implant disease: An overview of surgical methods. *International Journal of Dentistry, 2013*, 740680.

Vallittu, P. K., Närhi, T. O., & Hupa, L. (2015). Fiber glass-bioactive glass composite for bone replacing and bone anchoring implants. *Dental Materials : Official Publication of the Academy of Dental Materials, 31*(4), 371-381.

van Oirschot, B. A., Meijer, G. J., Bronkhorst, E. M., Närhi, T., Jansen, J. A., & van den Beucken, J J. (2016). Comparison of different surface modifications for titanium implants installed into the goat iliac crest. *Clinical Oral Implants Research, 27*(2), 57.

Varanasi, V. G., Saiz, E., Loomer, P. M., Ancheta, B., Uritani, N., Ho, S. P., Tomsia, A. P., & Marshall, G. W. (2009). Enhanced osteocalcin expression by osteoblast-like cells (MC3T3-E1) exposed to bioactive coating glass (SiO2-CaO-P2O5-MgO-K2O-Na2O system) ions. *Acta Biomaterialia, 5*(9), 3536-3547.

Velasco-Ortega, E., Ortiz-Garcia, I., Jimenez-Guerra, A., Monsalve-Guil, L., Munoz-Guzon, F., Perez, R. A., & Gil, F. J. (2019). Comparison between sandblasted acid-etched and oxidized titanium dental implants: In vivo study. *International Journal of Molecular Sciences, 20*(13), 3267.

Vernal, R., León, R., Silva, A., Van Winkelhoff, A. J., Garcia-Sanz, J., & Sanz, M. (2009). Differential cytokine expression by human dendritic cells in response to different porphyromonas gingivalis capsular serotypes. *Journal of Clinical Periodontology, 36*(10), 823-829.

Vlacic-Zischke, J., Hamlet, S. M., Friis, T., Tonetti, M. S., & Ivanovski, S. (2011). The influence of surface microroughness and hydrophilicity of titanium on the up-regulation of TGFbeta/BMP signalling in osteoblasts. *Biomaterials, 32*(3), 665-671.

von Wilmowsky, C., Moest, T., Nkenke, E., Stelzle, F., & Schlegel, K. A. (2014). Implants in bone: Part II. research on implant osseointegration. *Oral and Maxillofacial Surgery, 18*(4), 355-372.

Wan, T., Aoki, H., Hikawa, J., & Lee, J. H. (2007). RF-magnetron sputtering technique for producing hydroxyapatite coating film on various substrates. *Bio-Medical Materials and Engineering, 17*(5), 291-297.

Wassmann, T., Kreis, S., Behr, M., & Buergers, R. (2017). The influence of surface texture and wettability on initial bacterial adhesion on titanium and zirconium oxide dental implants. *International Journal of Implant Dentistry, 3*(1), 32.

Wehner, C., Bertl, K., Durstberger, G., Arnhart, C., Rausch-Fan, X., & Stavropoulos, A. (2021). Characteristics and frequency distribution of bone defect configurations in peri-implantitis lesions—A series of 193 cases. *Clinical Implant Dentistry and Related Research, 23*(2), 178-188.

Wennerberg, A., & Albrektsson, T. (2009). Effects of titanium surface topography on bone integration: A systematic review. *Clinical Oral Implants Research, 20*(Suppl 4), 172-84.

Wennerberg, A., Albrektsson, T., & Andersson, B. (1996). Bone tissue response to commercially pure titanium implants blasted with fine and coarse particles of aluminum oxide. *The International Journal of Oral & Maxillofacial Implants, 11*(1), 38-45.

Wennerberg, A., Albrektsson, T., Andersson, B., & Krol, J. J. (1995). A histomorghometric study of screw-shaped and removal torque titanium implants with three different surface topographies. *Clinical Oral Implants Research, 6*(1), 24-30.

Wennerberg, A., Galli, S., & Albrektsson, T. (2011). Current knowledge about the hydrophilic and nanostructured SLActive surface. *Clinical, Cosmetic and Investigational Dentistry, 3*, 59-67.

Wennerberg, A., Hallgren, C., Johansson, C. & Danelli, S. (1998). A histomorphometric evaluation of screw-shaped implants, each prepared with two surface roughnesses. Clin Oral Impl Res 9(1), 11-19.

Wohlfahrt, J. C., Lyngstadaas, S. P., Rønold, H. J., Saxegaard, E., Ellingsen, J. E., Karlsson, S., & Aass, A. M. (2012). Porous titanium granules in the surgical treatment of peri-implant osseous defects: A randomized clinical trial. *The International Journal of Oral & Maxillofacial Implants, 27*(2), 401-410.

Wolke, J. G. C., De Groot, K., & Jansen, J. A. (1998). Dissolution and adhesion behaviour of radio-frequency magnetron-sputtered Ca–P coatings. *Journal of Materials Science, 33*(13), 3371-3376.

Wong, M., Eulenberger, J., Schenk, R., & Hunziker, E. (1995). Effect of surface topology on the osseointegration of implant materials in trabecular bone. *Journal of Biomedical Materials Research, 29*(12), 1567-1575.

Wright, C. J., Burns, L. H., Jack, A. A., Back, C. R., Dutton, L. C., Nobbs, A. H., et al. Jenkinson, H. F. (2013). Microbial interactions in building of communities. *Molecular Oral Microbiology, 28*(2), 83-101.

Xie, Y., Liu, X., Zheng, X., Ding, C., & Chu, P. K. (2006). Improved stability of plasma-sprayed dicalcium silicate/zirconia composite coating. *Thin Solid Films, 515*(3), 1214-1218.

Xynos, I. D., Hukkanen, M. V., Batten, J. J., Buttery, L. D., Hench, L. L., & Polak, J. M. (2000). Bioglass 45S5 stimulates osteoblast turnover and enhances bone formation in vitro: Implications and applications for bone tissue engineering. *Calcified Tissue International, 67*(4), 321-329.

Yamaguchi, M., & Weitzmann, M. N. (2011). Zinc stimulates osteoblastogenesis and suppresses osteoclastogenesis by antagonizing NF-kappaB activation. *Molecular and Cellular Biochemistry, 355*(1-2), 179-186.

Yamamoto, O. (2001). Influence of particle size on the antibacterial activity of zinc oxide. *International Journal of Inorganic Materials, 3*(7), 643-646.

Yang, J., Zhou, Y., Wei, F., & Xiao, Y. (2016). Blood clot formed on rough titanium surface induces early cell recruitment. *Clinical Oral Implants Research, 27*(8), 1031-1038.

Yoshida, A., Yoshimura, M., Ohara, N., Yoshimura, S., Nagashima, S., Takehara, T., & Nakayama, K. (2009). Hydrogen sulfide production from cysteine and homocysteine by periodontal and oral bacteria. *Journal of Periodontology, 80*(11), 1845-1851.

Young, T. (1805). III. an essay on the cohesion of fluids. *Philosophical Transactions of the Royal Society of London, 95*, 65-87.

Żenkiewicz, M. (2007). Methods for the calculation of surface free energy of solids. *Journal of Achievements in Materials and Manufacturing Engineering, 24, nr 1*, 137-145.

Zenobia, C., & Hajishengallis, G. (2015). Porphyromonas gingivalis virulence factors involved in subversion of leukocytes and microbial dysbiosis. *Virulence, 6*(3), 236-243.

Zhao, G., Raines, A. L., Wieland, M., Schwartz, Z., & Boyan, B. D. (2007). Requirement for both micron- and submicron scale structure for synergistic responses of osteoblasts to substrate surface energy and topography. *Biomaterials, 28*(18), 2821-2829.

Zhao, G., Schwartz, Z., Wieland, M., Rupp, F., Geis-Gerstorfer, J., Cochran, D. L., & Boyan, B. D. (2005). High surface energy enhances cell response to titanium substrate microstructure. *Journal of Biomedical Materials Research Part A, 74A*(1), 49-58.

Zheng, Y. et al., (2012). In vitro microvessels for the study of angiogenesis and thrombosis. *Proc Natl Acad Sci USA, 109*(24), 9342-7.

Zhuang, L. F., Watt, R. M., Mattheos, N., Si, M. S., Lai, H. C., & Lang, N. P. (2016). Periodontal and peri-implant microbiota in patients with healthy and inflamed periodontal and peri-implant tissues. *Clinical Oral Implants Research, 27*(1), 13-21.

Zitzmann, N. U., Berglundh, T., Ericsson, I., & Lindhe, J. (2004). Spontaneous progression of experimentally induced periimplantitis. *Journal of Clinical Periodontology, 31*(10), 845-849.

Zorrilla, P., Gómez, L. A., Salido, J. A., Silva, A., & López-Alonso, A. (2006). Low serum zinc level as a predictive factor of delayed wound healing in total hip replacement. *Wound Repair and Regeneration, 14*(2), 119-122.

TURUN
YLIOPISTO
UNIVERSITY
OF TURKU

ISBN 978-951-29-8613-2 (PRINT)
ISBN 978-951-29-8614-9 (PDF)
ISSN 0355-9483 (Print)
ISSN 2343-3213 (Online)

Painosalama, Turku, Finland 2021